The University of Nevada, Reno

Urbanization and freshwater salinity: Impacts on water quality, sediment, and microbial communities in semi-arid streams

A thesis submitted in partial fulfillment of the

requirements for the degree of Master of Science

in Natural Resources and Environmental Science

by

Keenan Seto

Dr. Joanna Blaszczak/ Thesis Advisor

December, 2022

THE GRADUATE SCHOOL

We recommend that the thesis
prepared under our supervision by

entitled

be accepted in partial fulfillment of the
requirements for the degree of

Advisor

Committee Member

Committee Member

Graduate School Representative

Markus Kemmelmeier, Ph.D., Dean
Graduate School

Abstract

Stream ecosystems can be sensitive to watershed urbanization, but less is known about how streams respond to urbanization in semi-arid cities. To characterize how urbanization and altered salinity regimes affect stream chemistry and microbial activity, I conducted (1) a mesocosm experiment to investigate how press versus pulse salinity regimes altered biogeochemical cycles in stream sediments and (2) a field survey of streams in Reno, Nevada. The mesocosm experiment results revealed that the press salinity regime caused the greatest fluxes in ammonium and potassium from exposed stream sediments, while microbial activity rates were not affected. Results from the field survey demonstrated that the heterogenous underlying lithology of Reno imparted a stronger signal on stream chemistry than watershed urbanization in paired sites. The results of this work characterize the wide temporal and spatial variability in how stream chemistry and microbial activity respond to urbanization and altered salinity regimes in a semi-arid city.

Acknowledgements

I would like to thank the U.S. Department of Agriculture for project funding and supporting my graduate career. Thank you to Dr. Joanna Blaszczak for her valuable insight on this project and everything relating to science. Her enthusiasm and positive attitude went a long way to help me understand the project, execute the data collection, and make it through grad school. Thank you to the Blaszczak lab members who have helped me throughout my time at UNR. I greatly appreciate being a part of a lab group who actively supports one another to be successful students and scientists. Helena Garrett-Paleda and Chloe Dodge provided invaluable help as project technicians and did amazing jobs during long field and lab days. Graduate students Kelly Loria and Meredith Brehob were two of the most supportive co-workers I've had, and I thank them for their emotional support, help during late lab nights, and being patient teachers to help me understand coding. I was new to coding when I came to UNR and I thank the lab Post-Doc, Dr. Heili Lowman for being a great resource.

Thank you to Kay Strain and the Hanan lab for allowing me to use their space as a second home during sample analysis. Thank you to Emily Carlson in the Chandra lab and Dr. Paul Verburg for allowing me to use their equipment for sample analysis. Thank you to Sarrah Dunham-Cheatham at the UNR Core Analytical Lab, Brooke Hassett at Duke University, and Julie Korak at CU-Boulder for their help with analyzing my samples.

Thank you to my committee members, Dr. Sudeep Chandra, Dr. Mae Gustin, and Dr. Erin Hanan for their project assistance and guidance.

Thank you to my parents, Courtney and Laurie for being amazing role models and always encouraging me to follow my passions.

Table of Contents

List of Tables

List of Figures

Chapter 1: Thesis introduction

1.1 Overview

Human activities have and are continuing to alter landscapes with consequences for water quality in the streams and rivers that drain affected areas (Grimm et al., 2008; Kaushal et al., 2017; Walsh et al., 2005). Land use such as urbanization, agriculture, mining, and road construction affect nutrient and contaminant mobilization and transport within landscapes, and therefore the concentrations of chemical stressors in downstream waters (Kaushal et al., 2018a; Meyer et al., 2005; Schuler & Relyea, 2018). Patterns in stream chemistry draining watersheds reflect the climactic, geologic, and biotic characteristics of the contributing watershed (Bormann & Likens, 1967). However, in cases of watersheds affected by human activities, patterns in stream chemistry can also reflect changes in watershed chemical loading and altered hydrologic regimes that concentrate or dilute stressors (Gallo et al., 2013; Paul & Meyer, 2001; Walsh et al., 2005; Figure 1).

This thesis explores how freshwater salinization and watershed urbanization lead to changes in freshwater biogeochemical cycling (i.e., microbial activity and solute fluxes), with this first chapter providing an introduction. In Chapter 2, entitled "Pulsed and pressed: Stream sediment biogeochemical responses to variable salinity regimes exposure in a laboratory mesocosm experiment", a laboratory mesocosm approach was used to test how surface water, sediment, and microbial activity in undeveloped and urban stream reaches respond to press and pulse salinity regimes. In Chapter 3, entitled "Water and sediment chemistry, and microbial activity in streams draining the semi-arid city of Reno, NV", a summer field survey was used to collect and analyze samples from stream sites in a paired

undeveloped and urban contributing watershed design with long-term stream chemistry data to contextualize this snapshot summer sampling.

1.2 Freshwater salinity regimes in the context of urban catchments

Freshwater ecosystems around the globe are experiencing higher salinity concentrations (Kaushal et al., 2021; Stets et al., 2018). Background stream salinity concentrations in all catchments are the result of what is known as primary salinization, or the natural weathering of rocks and groundwater inputs which can increase or dilute concentrations of salts in streams (Williams, 2001; Figure 1). Salinity caused by anthropogenic sources (e.g., agriculture, wastewater treatment plant (WWTP) effluent, road salt application, etc.) is known as secondary salinization and is the main cause of elevated stream salinity (Vengosh, 2013; Figure 1). Salinity concentrations are acutely increasing in many urban streams in the eastern United States, but patterns between downstream salinity and urban land cover are more variable in the western United States (Bolotin et al., 2022; Kaushal et al., 2018a, 2021). Although there are multiple contexts in which salinity in streams can be altered, my second chapter focuses on urban sources of salts and the direct and indirect effects of altered salinity regimes (i.e., characteristic temporal patterns) on stream biogeochemical patterns.

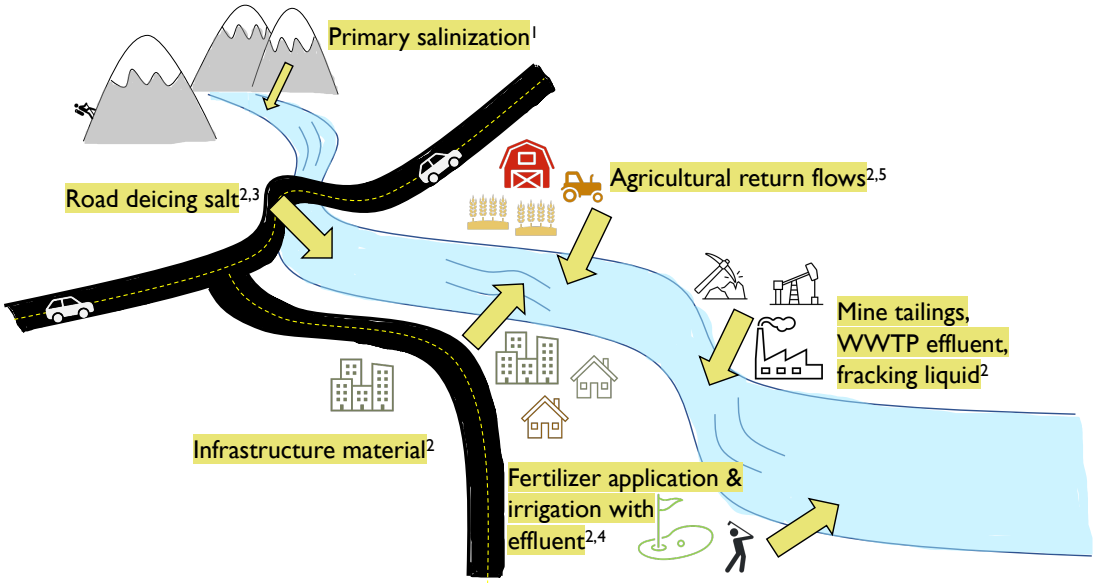

Figure 1. Conceptual figure showing sources of stream salinity ([1]Williams, 2001; [2]Kaushal, et al., 2018a; [3]Schuler & Relyea, 2018; [4]Bureau of Reclamation, 2006; [5]Vengosh, 2013).

1.2.1 Urban secondary salinization - road salt application

Road (and parking lot) deicing salt application is a leading cause of elevated salinity in rivers and streams around the world (Cañedo-Argüelles et al., 2013; Kaushal et al., 2005, 2018a, 2021). Over 90% of road salt application is sodium chloride, but magnesium chloride and calcium chloride are commonly used (Schuler & Relyea, 2018). In the United States, road salt application has dramatically increased from less than 1 million tons in 1950 to over 20 million tons in 2014 (Bolen, 2014). Road salt application is prevalent during the winter in northeastern and midwestern cities which have the highest freshwater salinity increases in the United States (Kaushal et al., 2018a). Streams in the semi-arid western cities of Denver, CO and Salt Lake City, UT have also been exposed to high salinity from road salts and certain urban streams exceed the EPA chronic and acute standards for chloride (Corsi et al., 2010). Due to warmer winter temperatures and less

snowfall than northeastern or midwestern cities, road salt impacts to streams in Reno are likely less pronounced, however, these salts can still make their way into local streams.

1.2.2 Urban secondary salinization – lawn irrigation, fertilization, and infrastructure

Lawn irrigation return flows and the weathering of urban infrastructure can affect salinity patterns in streams. Infrastructure material such as concrete is easily weathered and is a source of bases and carbonates that are components of salinity (Moore et al. 2017; Bird et al., 2018; Kaushal et al., 2018a). Fertilizers applied on residential lawns can contain salt sources such as potassium and calcium (Kaushal et al., 2018a) which can be leached by overwatering and carried via stormwater infrastructure to streams (Fillo et al., 2021). Golf courses in the semi-arid west are known to use WWTP effluent for irrigation, and effluent can contain high salinity concentrations (Bureau of Reclamation, 2006) that can contribute to downstream salinity concentrations in streams. Residential and commercial lawn irrigation flows to streams may convert previously non-perennial streams to perennial streams (Fillo et al., 2021), and increase the duration of baseflow mobilization of salts from the contributing watershed.

1.2.3 Indirect effects of secondary salinization - altered fluxes of bioreactive elements

Freshwater salinization can alter the flux of bioreactive elements from sediments and soils through direct and indirect chemical and biological mechanisms (Kaushal et al., 2018b, 2019). Elevated salinity alters the ion exchange and sorption capacity of sediments directly and changes the pH and sodium-induced dispersion indirectly through release of dissolved organic carbon (Duan & Kaushal, 2015). Deicing salts in urban areas have been

shown to mobilize metals (Schuler & Relyea, 2018). In my second thesis chapter, press and pulse salinity regimes were used to measure solute fluxes through time.

1.2.4 Temporal dynamics of stream salinity

The temporal dynamics of salinity in a stream are dependent on salt loading, hydrologic connectivity, and the precipitation regime in the contributing watershed. These chemical and hydrologic controls on salt delivery can result in pulse or press salinity regimes. A pulse can occur when road salts are carried by runoff to streams which results in a short period of high salinity (Blaszczak et al., 2019). A press can occur when salt from fertilizers or weathered infrastructure material accumulate in groundwater and are leached into streams, contributing to long-term elevated salinity (Kaushal et al., 2005; Lake, 2000; Paul & Meyer, 2001). Cities in warm, arid climates like Phoenix, AZ do not have road salt application but can have elevated baseflow salinity due to evapoconcentration of salts from urban sources such as sewage (Hale et al., 2016); whereas cold, humid cities like Baltimore, MD can have a strong salinity signal from road salts (Kaushal et al., 2005). Reno, NV is located at the edge of the Great Basin and has a comparable climate and topography to Salt Lake City, UT. Both cities have cold, snowy winters, and in Salt Lake City, road salt application has been shown to increase stream salinity in the winter and contribute to elevated baseflow salinity throughout the year due to long subsurface residence times (Gabor et al., 2017). The results in Salt Lake City suggest that the streams draining urbanized watersheds in Reno, NV may experience both pulse and press salinity regimes.

1.2.5 Downstream consequences of altered salinity regimes

Salinization alters freshwater biodiversity directly via toxicity and indirectly via altered species interactions which shifts the community composition of algal assemblages (Lind et al., 2018), macroinvertebrates (Cañedo-Argüelles et al., 2012; Clements & Kotalik, 2016), and fish (Cañedo-Argüelles et al., 2013) to be dominated by salt-tolerant species. Salinity-induced releases of nutrients can enhance the activity of some microorganisms while decreasing the activity of other microbes due to osmotic stress (Wang et al., 2014). Press and pulse salinity regimes cause decreases in bacterial density on biofilms, but once the salinity stressor is removed, the community can recover (Cochero et al., 2017). The results of previous freshwater salinity studies on aquatic biota indicate that sediment microbial community composition may shift with altered salinity regimes.

1.3 Urban area expansion

Urban areas are increasing in size faster than population growth, and by 2030, urban land cover is expected to nearly triple, relative to their physical extent in 2000 (Seto et al., 2012). Streams and rivers that drain these cities are becoming increasingly degraded from contaminant loading and hydrologic changes which limits their capacity to provide ecosystem services for humans and wildlife (McDonald et al., 2011; Paul & Meyer, 2001). My third thesis chapter provides a snapshot of watershed urbanization impacts to hydrology, stream chemistry, and microbial activity, and is contextualized with long-term stream chemistry data and the underlying lithology of Reno (Figure 2).

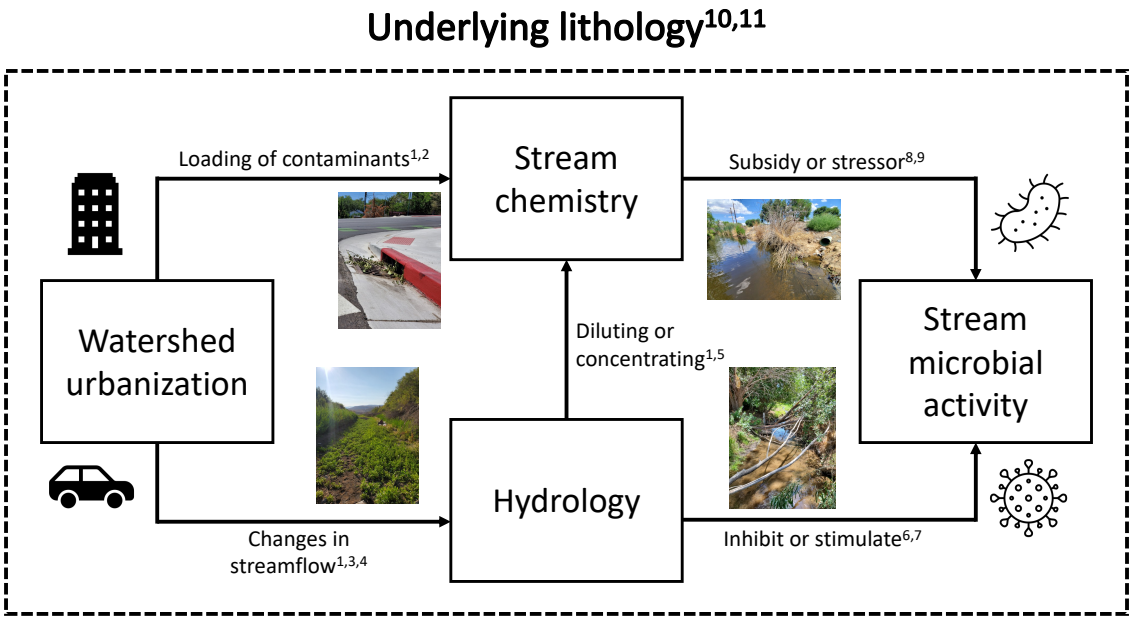

Figure 2. Conceptual diagram of watershed urbanization impacts on hydrology, stream chemistry, and microbial activity. Underlying lithology can mediate all of these relationships ([1]Walsh et al., 2005; [2]Kaushal et al., 2018a; [3]Fillo et al., 2021; [4]Bhaskar et al., 2016; [5]Gallo et al., 2013; [6]Amalfitano et al., 2008; [7]Schimel, 2018; [8]Allison & Vitousek, 2005; [9]Martin et al., 2021; [10]Blaszczak et al., 2019; [11]Nickolas et al., 2017).

1.3.1 Underlying lithology controls on stream hydrology, chemistry, and microbial activity

Underlying lithology plays an important role mediating the relationships between urbanization, hydrology, stream chemistry, and microbial activity (Figure 2). Varying lithology types can cause groundwater discharge to change throughout the year and result in heterogeneous streamflow patterns within watersheds (Nickolas et al., 2017). Stream chemistry can be influenced by underlying lithology directly through bedrock variation and weathering rates, and indirectly through the discharge rates of groundwater contaminants (Blaszczak et al., 2019; Gabor et al., 2017; Utz et al., 2016). Reno has a highly heterogeneous surface geology, as well as hydrothermal alterations which can impart a strong signal in stream solute concentrations (Ramelli et al., 2011; Romero-Mujalli et al.,

2022). Underlying lithology can influence microbial activity through detectable changes in stream hydrology (inhibit or stimulate) and chemistry (subsidy or stressor) (Amalfitano et al., 2008; Wang et al., 2014).

1.3.2 Urbanization effects on stream biogeochemistry - hydrology & stream chemistry

Impervious surfaces dominate urban areas and change storm flows because of the rapid routing of water to rivers and streams, bypassing vegetation and soils which can act as contaminant buffers (Hale et al., 2015; Hatt et al., 2004). In arid and semi-arid watersheds, urbanization increases baseflows because of lawn irrigation return flows (Fillo et al., 2021), leaking water delivery and sewer pipes (Bhaskar et al., 2016), and WWTP effluent (Paul & Meyer, 2001; Figure 2). For example, WWTP effluent has at times comprised 100% of discharge in the South Platte River downstream of the semi-arid city of Denver, CO (Dennehy et al., 1998). Urban stream baseflow can also decrease due to impervious surface cover, which prevents infiltration and groundwater recharge (Bhaskar et al., 2016). These changes in baseflow patterns alter the perenniality of urban streams in which previously non-perennial streams become perennial (Fillo et al., 2021; Paul & Meyer, 2001; Walsh et al., 2005; Figure 2). Reno most likely experiences enhanced perenniality of stream flow because of the semi-arid climate that results in dry streams in the area surrounding the city and the transport of Truckee River water upslope into catchments through drinking water infrastructure and canals (e.g., the Steamboat Ditch).

Watershed urbanization can change stream chemistry by increasing solute concentrations in downstream waters (Paul & Meyer, 2001; Walsh et al., 2005; Figure 2). Large urban catchments can have point source loading of solutes from wastewater

treatment plant (WWTP) effluent, but for smaller catchments, the predominant sources are non-point source (e.g., fertilizers, road salts, and infrastructure degradation, etc.) (Paul & Meyer, 2001, Gabor et al. 2017; Table 1). Patterns in non-point source nutrient and contaminant export from watersheds depends on the climate (Hale et al., 2016), age of a city (Grimm et al., 2000), stormwater infrastructure design (Hale et al., 2015), and underlying lithology (Blaszczak et al., 2019; Utz et al., 2016).

Table 1. Urban non-point sources of total phosphorus (TP), total nitrogen (TN), cations, and anions. Examples of studies in arid urban environments are given in the right column.

Solute	Urban non-point source	Arid urban studies
TP	- Fertilizers (Paul & Meyer, 2001) - Sewer leakage (Walsh et al., 2001, 2005) - Dog defecation (Hobbie et al., 2017)	- Victoria, Australia (Walsh et al., 2001) - Arizona (Grimm et al., 2000, 2005; Hale et al., 2015)
TN	- Fertilizers (Paul & Meyer, 2001) - Sewer leakage (Walsh et al., 2001, 2005) - Dog defecation (Hobbie et al., 2017)	- Victoria, Australia (Walsh et al., 2001) - Arizona (Grimm et al., 2000; Hale et al., 2015)
Na^+, K^+, Ca^{2+}, Mg^{2+}	- Fertilizers and concrete (Bird et al., 2018; Kaushal et al., 2018a; Moore et al., 2017) - Road salt (Kaushal et al., 2005)	- Nevada, Utah, Colorado, Arizona, New Mexico (Kaushal et al., 2018a)
Cl^-, SO_4^{2-}	- Sewer leakage (Blaszczak et al., 2019) - Road salt (Gabor et al., 2017; Kaushal et al., 2005) - WWTP effluent irrigation (Bureau of Reclamation, 2006) - Construction material (Moore et al., 2017)	- Nevada, Utah, Colorado (Stets et al., 2018) - Utah, Colorado (Corsi et al., 2010) - Utah (Gabor et al., 2017) - Arizona (Bureau of Reclamation, 2006)

1.3.3 Urban hydrologic changes influence stream chemistry

Changing hydrologic patterns because of urbanization can alter stream chemistry through dilution or concentration (Walsh et al., 2005; Figure 2). Urban stream solute concentrations can be diluted from summer runoff sources, such as lawn and agriculture return flows (Gallo et al., 2013), or concentrated from reduced baseflow which exacerbates water quality problems (Walsh et al., 2005). Storm peak flows cause stream channel

incision which lowers the streambed and causes a disconnection from the floodplain and riparian vegetation, both of which can buffer high contaminant concentrations when the channel is not incised (Groffman et al., 2003). Reduced infiltration from watershed impervious surface cover causes lower riparian groundwater levels and affects soil, plants, and microbial activity in the riparian zone of a stream (Groffman et al., 2003). These changes in hydrology and stream chemistry can vary between cities. Hot, arid cities (e.g., Phoenix) tend to experience flashy hydrologic regimes and low baseflows, whereas mesic, temperate cities (e.g., Baltimore) have a more uniform distribution of rain, runoff, and streamflow throughout the year (Grimm et al., 2000). Due to Reno's limited precipitation, we might expect low baseflows and limited stormflows. Precipitation events can cause a contaminant pulse or "first flush" when concentrations sharply rise then fall with dilution (Duncan et al., 2017; Kaushal & Belt, 2012). Contaminants can also have a press disturbance where concentrations are consistently elevated for long periods of time (Lake, 2000). Altered hydrologic regimes because of urbanization can impact stream water quality with potential consequences for stream and riparian biotic communities.

1.3.4 Urbanization effects on stream biogeochemistry - microbial responses

Changes in stream hydrology can affect microbial activity in stream sediments because of the inhibition or stimulation of activity under wet or dry conditions (Figure 2). Microbial activity in stream sediment decreases with desiccation, and soil microbes with a history of drying and rewetting are tolerant to moisture stress (Amalfitano et al., 2008; Fierer et al., 2003a). In semi-arid cities like Reno, precipitation events can stimulate microbial activity in dry streams by creating a replenishment pulse of nutrients and organic

matter (Schimel, 2018). As a non-perennial stream bed becomes increasingly dry, water retention in sediment can be an important refuge for microbes (Febria et al., 2015); however, riparian vegetation removal in urban areas increases heat and evaporation on streambeds and can cause faster sediment desiccation (Paul & Meyer, 2001).

Urbanization induced stream chemistry changes can alter microbial activity in multiple ways because elevated nutrients can subsidize microbial activity, while increased concentrations of contaminants can act as stressors to inhibit microbial activity (Figure 2). Seasonal periods of low baseflow create pools within stream channels which concentrate solutes and can change rates of microbial processes such as denitrification (Amalfitano et al., 2008; Febria et al., 2015; Wang et al., 2014). Microbial activity can be constrained by nutrient limitation as nutrients are needed for their growth and survival, however, microbes can produce extracellular enzymes to enhance their access to nutrients in the environment (Allison & Vitousek, 2005). Stressors associated with urbanization (e.g., salts and metals) can inhibit microbial activity and cause a shift in community composition to more stress-tolerant species (Martin et al., 2021). The combination of elevated concentrations of nutrients and contaminants in urban streams makes it difficult to predict whether rates of microbial functioning will increase or decrease with the chemical mixtures found in streams.

The composition of microbial communities and legacy of their exposure to stressors is hypothesized to determine their resilience to new disturbances (Blanck et al., 1988; McCann, 2000). The legacy hypothesis predicts that microbial communities previously exposed to stressful conditions should have a higher tolerance to new exposure as they are accustomed to stress (Wang et al., 2014). The insurance hypothesis predicts that microbial

communities with a high functional diversity are more likely to include microbial taxa that are tolerant to a particular stressor, and therefore whole community function is more resistant to new disturbances (Wang et al., 2014). In both chapters, the legacy hypothesis was tested by comparing potential microbial respiration and extracellular enzyme activity in streams with undeveloped (minimal exposure to stressors) and urban (high exposure to stressors) watersheds, as well as exposing the microbes to different regimes of a stressor (salt). The insurance hypothesis was tested by measuring the potential activity of seven extracellular enzymes to see if certain enzymes are more or less tolerant to stress.

The relative importance of hydrologic and chemical stressors on potential microbial respiration and extracellular enzyme activity is unclear. To answer this, 13 streams were sampled in the summer of 2021 to provide a snapshot on how microbial activity changes with varying nutrient availability and stressors (i.e., salt, urbanization, and desiccation). Microbial activity can change throughout the year based on nutrient availability, stressor delivery, and streamflow status (Allison & Vitousek, 2005; Amalfitano et al., 2008; Rocca et al., 2019); however, this study was conducted in the summer and not able to capture these seasonal changes.

1.4 Rational behind thesis

The overarching objective of this thesis is to investigate how watershed urbanization in the semi-arid city of Reno, Nevada has altered biogeochemical cycling in urban streams. First, a mesocosm study was conducted to address the knowledge gap of whether a pulse or press salinity regime results in a greater flux of solutes from sediments and decreased microbial activity. Second, a field observational study was conducted to

explore spatial patterns in solute concentrations and microbial activity to understand background variation within and among streams draining urbanized catchments.

The results from this thesis expand our knowledge on the direct and indirect effects of anthropogenic salt inputs and urbanization on stream ecosystem biogeochemical activity. The majority of work on salinization effects on stream biogeochemistry has focused on the effects of salinity along concentration gradients (Duan & Kaushal, 2015) or episodic pulses in eastern urban areas (Kaushal et al., 2019). Little work has been done to understand how different salinization regimes may alter the relative influence of salinity on coupled biogeochemical cycles. Reno is a fast-growing semi-arid city, and it is important to characterize how temporal dynamics and natural geologic variation affect local stream water quality.

Chapter 2: Pulsed and pressed: Stream sediment biogeochemical responses to variable salinity regimes exposure in a laboratory mesocosm experiment

2.1 Introduction

As environmental conditions in freshwater ecosystems are increasingly altered through land use change in their contributing watersheds, there is a growing need to understand how in-stream biotic communities and biogeochemical cycles might respond to these changes. Over the past few decades, wastewater discharge, road salt application, human-accelerated weathering, and groundwater irrigation has increased, which has led to the increased salinization of freshwater (Cañedo-Argüelles et al., 2016; Cochero et al., 2017; Duan & Kaushal, 2015). Salt inputs, like those released from irrigation return flows (Pillsbury, 1981) and road deicing salt application, mobilize nutrients and metals from river sediments into the water column with consequences for river ecology, agriculture, and drinking water sources (Duan & Kaushal, 2015; Schuler & Relyea, 2018). The timing and magnitude of salt inputs can lead to variable salinity regimes (i.e., characteristic annual temporal patterns) in streams with unclear consequences for biogeochemical cycles and aquatic biota in downstream aquatic ecosystems.

Impervious surface cover (e.g., buildings, roads, and parking lots) is increasing across the US as cities expand their footprints (Baker et al., 2019; Hopkins et al., 2015), and is a major source of nonpoint source pollution to streams (Blaszczak et al., 2019). The accelerating construction of these impervious surfaces leads to decreased groundwater infiltration and increased surface runoff of precipitation (Bhaskar et al., 2016; Jacobson,

2011; Walsh et al., 2005). The effects of impervious surface cover are compounded during storm events when stormwater runoff infrastructure (e.g., subsurface pipes) provides efficient avenues for water runoff and the delivery of contaminants to nearby waterways, bypassing soil and vegetation which can act as contaminant buffers (Groffman et al., 2003; Hatt et al., 2004; Hale et al., 2015). Road salts, used to prevent the buildup of ice on roads to reduce vehicle accidents, can be retained in the landscape, contaminate groundwater, and elevate baseflow salinity long after salt application (Gabor et al., 2017; Snodgrass et al., 2017). These patterns in the retention and release of salts from watersheds, are reflected in the temporal patterns of salts in the receiving streams. While stormwater may deliver a short-term "pulse" of salt, contaminated groundwater inflows can result in a long-term "press" of persistent elevated salinity relative to background concentrations, representing two different temporal patterns in the chemical disturbance of streams (Bolotin et al. 2022; Lake, 2000).

Increased river salinization from sources like road salt runoff has been shown to mobilize bioreactive elements (carbon, nitrogen, phosphorus, and sulfur) and trace metals in sediment increasing the relative flux of particular elements to the water column (Duan & Kaushal, 2015; Schuler & Relyea, 2018). Changes to the mobilization of elements is caused by increased ion exchange and altered sorption capacity of sediment (Duan & Kaushal, 2015). Globally, sodium chloride (NaCl) is the most common road salt applied (>90%) (Schuler & Relyea, 2018), and in the United States, NaCl application has increased from less than one million tons in 1950 to over 20 million tons in 2014 (Bolen, 2014). These road salts that are applied onto urban landscapes are transported to streams and may

be leading to changes in the rates of bioreactive element mobilization, which in turn, might depend on the magnitude and duration of elevated salinity concentrations in a stream.

Stream sediment microbial communities that drive nutrient and carbon cycling in streams are sensitive to anthropogenic disturbances, such as elevated salinity concentrations (Wang et al., 2011, 2014). Microbial communities produce extracellular enzymes, which are used to decompose and transform organic matter into smaller soluble molecules, make nutrients bioavailable to aquatic organisms, and improve water quality (Allison & Martiny, 2008; Bell et al., 2013). Elevated stream chloride concentrations can lead to osmotic stress-induced toxicity in freshwater organisms (Elphick et al., 2011), and the legacy of salinity exposure may shape the response of microbial communities and alter community composition to favor salt tolerant species (Chowdhury et al., 2011, Devilbiss et al. 2022). One hypothesis about the functional responses of sediment microbial communities to chemical disturbances is that previously undisturbed and diverse microbial communities are more resistant salt stressors because there are more taxa that have redundant functional capabilities, and therefore, even if some are eliminated through the stress exposure, the other taxa compensate for the loss ('insurance hypothesis') (Yachi & Loreau, 1999). An alternative hypothesis is the 'legacy hypothesis', which predicts that microbial communities which have been previously disturbed (i.e., exposed to chemical stressors) have more tolerant taxa (sensu pollution induced community tolerance (Blanck & Wängberg, 1988)) and are therefore more functionally tolerant of additional disturbances (Wang et al., 2014). The functional responses of sediment microbial communities to chemical disturbances may not only depend on their source, but also the duration and

magnitude of elevated salinity exposure which may determine the cumulative change of microbial communities and fluxes of elements from stream sediments.

Freshwater salinization can change the mobilization of bioreactive elements from sediments (Duan and Kaushal 2015), and change sediment microbial community composition and activity (DeVilbiss et al., 2022), yet there is still uncertainty regarding how different salinity regimes (i.e., a 'pulse' versus long-term 'press' of elevated salinity) result in different cumulative changes to sediment biogeochemical and microbial activity and how those changes might depend on legacies of chemical stressor exposure. A laboratory mesocosm experiment was conducted to investigate how different regimes of elevated salinity exposure to sediments from two different reaches from the same stream, one reach with no development upstream and another reach with urban development in the contributing watershed, impact microbial communities and the flux rates (release or retention) of nutrients and metals from sediment to the water column. Surface water and sediment were exposed to press and pulse salinity regimes to test three hypotheses: 1) the flux rates of nutrients and metals from stream sediments at the end of the experiment will be greater for a high press NaCl treatment over pulse and low press treatments, 2) sediment microbial communities will be resistant to a short-term pulse of salinity but low and high press salinity treatments will decrease microbes ability to respire and produce extracellular enzymes, and 3) microbes from the urban watershed will experience a lower response rate than microbes from the undeveloped watershed because the communities will be accustomed to chemical stressors.

2.2 Methods

2.2.1 Site description

Surface water and sediment were collected from two contrasting undeveloped and developed reaches along Thomas Creek in Reno, Nevada (Figure 3). We chose to sample in two locations along the same creek to retain a comparable underlying geology in the contributing watershed between the two locations given the high lithological heterogeneity among catchments in Reno, NV that imprints a chemical signal on the downstream waters. The headwaters of the Thomas Creek watershed are located in the Humboldt-Toiyabe National Forest in a nearly entirely undeveloped east-facing forested catchment draining primarily volcanic and sediment breccia (TUB) (Ramelli et al., 2011). Thomas Creek then flows into the developed valley dominated by glacial deposits (QOO) (Ramelli et al., 2011) where it alternates between buried and unburied reaches until its eventual confluence with Steamboat Creek, then the Truckee River.

Upstream watershed area was delineated in the NHDplusV2 Medium Resolution (1:100,000-scale) NHDFlowlines layer (Brakebill et al., 2019). Percent cover of different land cover types was estimated using the Model My Watershed Tool Version 1.33.7 (Stroud Water Research Center, 2021). The 2019 National Land Cover Database was used to characterize the area upland of the sites. Land use was grouped by four categories: urban, agriculture, undeveloped and open water, as well as the total upland watershed area. To make the four categories, similar land classifications were grouped together: urban (developed open space + developed high intensity + developed low intensity + developed medium intensity), agriculture (cultivated crops), undeveloped (pasture Hay + perennial

ice snow + barren Land + deciduous forest + evergreen forest + mixed forest + shrub scrub + grassland herbaceous) and open water (open water + woody wetlands + emergent herb wetlands).

To collect sediment and water from the relatively undisturbed reach, we sampled from a reach (N 39.39146, W -119.84274) upslope from urban development with <0.1% of NLCD classified urban land cover in the contributing catchment. This section of the creek was in a steep valley with abundant riparian vegetation (Figure 3B). For the previously disturbed reach, we sampled a comparable stream reach length approximately 10 km downstream of the undisturbed reach (N 39.44088, W -119.77050) with 15% of NLCD classified urban land cover in the contributing catchment. The effects of urbanization on downstream waters are commonly observed past as little as 5 and 10% impervious surface area (Booth & Jackson, 1997; Conway, 2007), and therefore the downstream reach represents a location that we would expect to have experienced changes to its hydrologic and chemical regimes. The downstream reach was channelized in a concrete ditch about 0.5 meters wide with limited riparian vegetation (Figure 3C). In-between the sites, Thomas Creek flowed through residential areas, a golf course, and across four disconnected ditches.

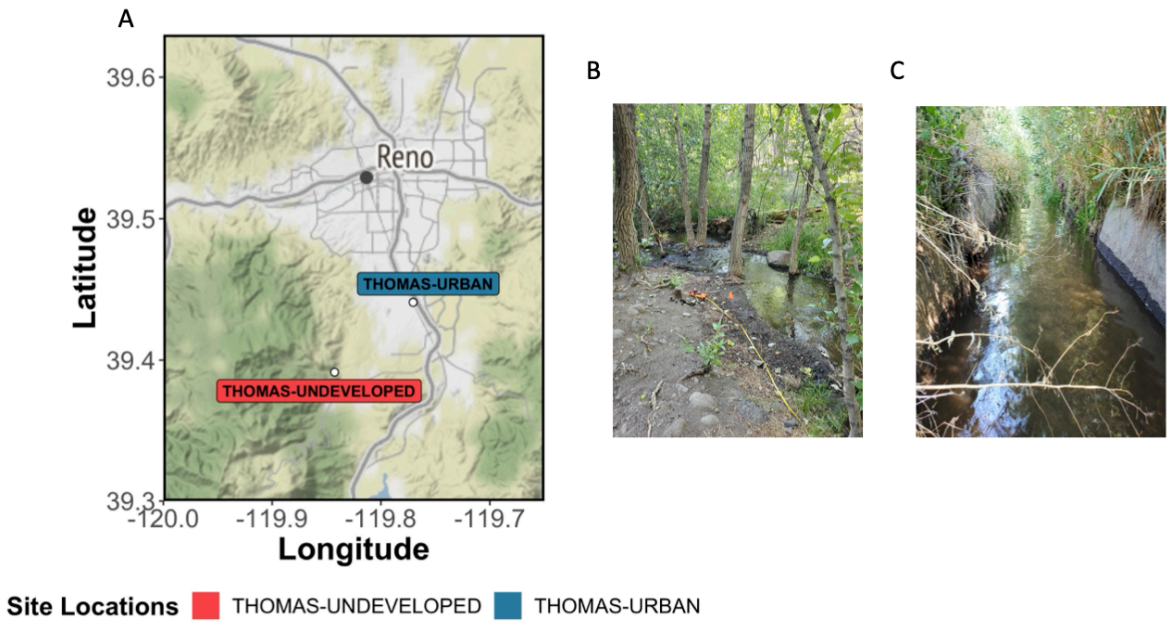

Figure 3. Map of the undeveloped (B) and urban (C) locations where water and sediment were collected for the mesocosm experiment. The Google Maps 2022 land cover base map was used. Urban development is indicated by grey shading.

2.2.2 Field sample collection

We sampled surface water and stream sediment from the upstream undeveloped reach on August 2nd and 9th, and surface water was collected every day for two days following each sediment sampling date to replenish mesocosms. We sampled surface water and stream sediments from the downstream urban reach on August 16th and 23rd, and continued to collect surface water daily over two days following the initial sediment collection. For the final downstream urban reach mesocosm experiment, Thomas Creek had no flowing surface water as a result of an unexpected diversion. There were no standing pools of water, and sediment in the reach was moist with little observed desiccation. Sediment was collected from the site, but water was collected approximately three kilometers upstream at the nearest public access point with flowing water in Thomas Creek.

The subsequent water replenishments for this week were collected from the new site (N 39.42969, W -119.78786).

We measured water quality parameters (pH, dissolved oxygen, temperature, and specific conductance) at each site using a multiparameter sonde (YSI, Yellow Springs, OH, USA) (Table S1 and S2). At each site, four transects were established perpendicular to the flow of water and spaced 10 meters apart in the stream for a total reach length of 40 m. A hand shovel was used to collect the top 5-10 cm of sediment at three locations on each transect (25%, 50%, and 75% of wetted width). Large rocks and woody debris were removed, and the remaining composite samples transported in Ziplock bags on ice to the lab, where they were sieved using a stainless steel #10 2 mm opening sieve (VWR, Radnor, PA, USA) and mixed to form a single composite sample from each site. Subsamples of sediment were measured into 50 mL acid-washed falcon tubes and stored at 4°C in the dark until analysis.

Triplicate unfiltered water samples were collected into 60 mL HDPE bottles for total suspended solids analysis. Water samples were filtered using acid-washed syringes through Whatman GF/F filters (Whatman, Piscataway, NJ, USA) into acid-washed 60 mL HDPE bottles for dissolved nutrients, cations, and anions analysis (Table S2). Water samples were held on ice and frozen once returned to the lab. Approximately 30 liters of unfiltered river water were collected daily in acid washed water jugs for the mesocosm experiment.

2.2.3 Mesocosm experiment design

A mesocosm experiment approach was used to quantify the fluxes of nutrients and metals, as well as changes in sediment potential extracellular enzyme activity (EEA) and potential microbial respiration rate in response to different salinity regime treatments and reach locations. Sediment collected from each reach was exposed to four different salt regimes during the experiment: (1) a pulse of high salinity, (2) a consistently elevated press of high salinity matching the peak of the pulse, (3) a consistently elevated press of salinity at a lower baseline, and (4) a control treatment only replenished with streamwater. The pulse regime was used to simulate the winter runoff of road salts, which equates to a few days of high salinity water entering streams via stormwater infrastructure or roads adjacent to streams (Blaszczak et al., 2019). This regime was also used to test the resilience of microbial communities (ability to return to their original composition following a disturbance). The high and low baseline regimes tested the resistance of microbial communities to disturbance to see if they remain unchanged and bracketed the pulse regime to compare whether the cumulative effects of a pulse of salinity were greater than either press exposure treatment.

Although originally intended to replicate the U.S. Environmental Protection Agency (USEPA) thresholds of acute and chronic stress chloride concentrations of 860 mg/L and 230 mg/L, respectively, the Cl concentrations added to the treatments were approximately 65% of those values because we added the compound NaCl instead. However, when measured as specific conductance (SpC) (μS/cm) the low and high baseline concentrations were in the 57th and 87th percentiles, respectively, of SpC observations in Great Basin streams. We determined these relative percentiles by using the

Water Quality Data Portal (Read et al. 2017) to compare SpC data from more than 232,000 observations in streams in the Great Basin. The portal was developed by the USEPA, U.S. Geological Survey, and National Water Quality Monitoring Council and is the largest publicly available water quality data set in the US (Read et al., 2017). At the end of the experiment, SpC in the low baseline treatment was 568 ± 17 μs/cm (undeveloped: 564 ± 22 μs/cm, urban: 572 ± 13 μs/cm) and 1769 ± 20 μS/cm in the high baseline treatment (undeveloped: 1772 ± 17 μs/cm, urban: 1766 ± 25 μs/cm).

The structure of the mesocosms was modeled after modified abrasion mills (Sklar & Dietrich, 2001; Figure 4). The entire mesocosm set up consisted of eight acid-washed 4 L glass cylinders (17 cm diameter x 18 cm tall) placed inside a plexiglass housing with a lid that mostly covered the top of each chamber (with a large opening for the propellers) to minimize water evaporation (Figure 4). Stainless steel propellers were submerged in the middle of the water column and set at 52 rounds per minute to circulate the water, but not create a vortex or vigorously stir the sediment. Each experiment was conducted primarily in the dark with overhead fluorescent lights turned on for ~3 hours daily during sample collection and water replenishment.

Given the restriction of eight total chambers, the experiment was repeated four times with two replicates per treatment in each round. The first two rounds used sediment and water from the upstream undeveloped reach in Thomas Creek and the last two rounds used sediment and water from the downstream urban reach. This experimental design achieved four replicates per treatment type per site. Treatment types were randomly distributed along the mesocosm setup (Figure 4).

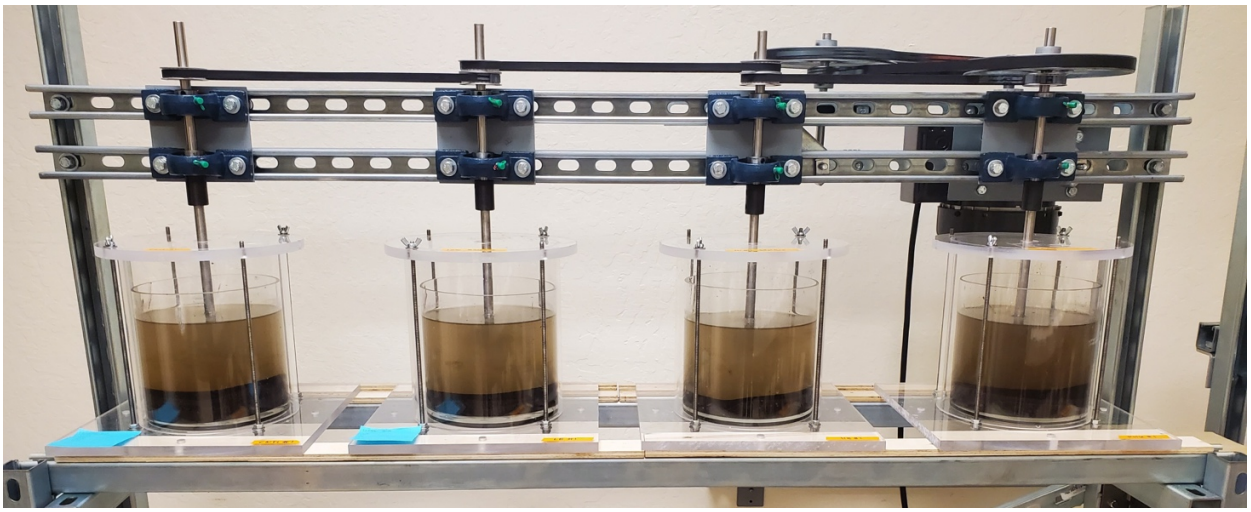

Figure 4. Mesocosm experimental set up.

At the start of each round of the mesocosm experiments, we added 2.5 L of unfiltered stream water and 500 mL of sieved, field moist sediment from the same site into each of the glass cylinders. Each experimental round lasted 66 hours with the initial 24 hours being an equilibration period where no salt was added to account for sampling disturbance and allow for the sediment and water to adjust to the experimental conditions (Figure 3). Following the equilibration period, there were three successive 14-hour incubation periods, totaling 42 hours (Figure 5). In each experimental round of eight, two mesocosm chambers were controls, with no NaCl additions; two were low baseline press treatments with 230 mg/L NaCl added for all 3 incubations; two were high baseline press treatments with 860 mg/L of NaCl added for all 3 incubations; and the final two were pulsed treatments with 860 mg/L NaCl added only for the second 14-hour incubation (Figure 5).

After the equilibration and each 14-hour incubation period, 2 L of water were siphoned out of the mesocosms into a graduated cylinder and replaced with 2 L of

unfiltered stream water from the same site, collected within the previous 24 hours and refrigerated at 4°C until use. The water was replaced to replenish nutrients and reduce experimental artifacts from the enclosed chamber design. We mixed all of the sediment in each chamber with stainless-steel spatulas after each incubation period to prevent sediment from becoming stratified. Despite this mixing, it is likely the sediments became anoxic contributing to the experimental artifacts that likely changed our results. To prevent the carryover of nutrients or metals between experiments, each glass cylinder and propeller was washed in 10% HCl acid and 10% HNO_3 acid solutions before the next experiment round.

Before water was siphoned, we collected 60 mL of unfiltered water and 60 mL of water filtered through Whatman GF/F filters into acid-washed HDPE bottles triple rinsed with filtered water from the water column of each chamber at four time points in the mesocosm experiment: post-equilibration, post-incubation #1, post-incubation #2 and post-incubation #3 (i.e., the end of the experiment; Figure 5; Table S2). The amount of unfiltered and filtered water removed from each mesocosm chamber was recorded and subtracted from 2 L. When water was siphoned, we used the subtracted amount for each chamber assuring that exactly 2 L of water was removed from each mesocosm chamber following each incubation period. We used the same multiparameter YSI sonde that we used in the field to measure pH (calibrated within the previous 24 hours), dissolved oxygen, temperature, and specific conductance immediately following surface water sample collection in the chamber. 50 mL of sediment was collected in 50 mL acid-washed falcon tubes after the water was siphoned out and the sediment completely mixed but only during the post-equilibration time point and end of the experiment (i.e., post-incubation #3) (Table

S2). Immediately following collection, we subsampled approximately 15 mL of sediment from the falcon tubes for organic matter, metal concentrations, and pH measurements. The remaining 35 mL of sediment in the falcon tubes was stored at 4°C within two hours of collection for sediment WSF constituent extraction within 24 hours and measurements of EEA and potential microbial respiration (described below).

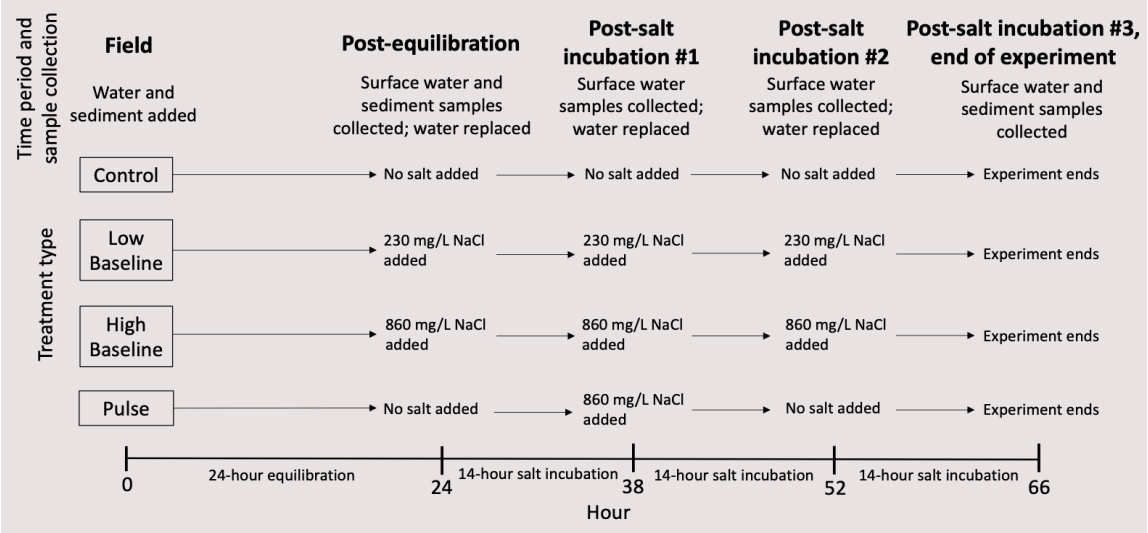

Figure 5. Mesocosm time periods and sample collection based on treatment type.

2.2.4 Sediment and water chemistry analysis

Filtered surface water and the water soluble fraction (WSF) of sediment were analyzed for nutrients, anions, and cations. WSF constituents were extracted by vortexing 2.5 ± 0.25 g of wet sediment with 25 mL of deionized water (i.e., Type 1 MilliQ ultrapure water) at 3400 RPM for 10 seconds every 30 minutes over four hours. After settling overnight at 4°C, the samples were centrifuged at 3400 RPM for 15 minutes and the supernatant filtered through Whatman GF/F filters.

A TOC analyzer with a TN module (TOC-V CPH; Shimadzu, Kyoto, Japan) was used to measure total dissolved carbon (TDC), dissolved organic carbon (DOC) and total dissolved nitrogen (TDN). Soluble reactive phosphorus (SRP) and ammonia (NH_3) were measured on an AQ400 discrete analyzer (SEAL Analytical, Mequon, WI, USA) based on US EPA methods 350.1 revision 2.0 and method 365.1 revision 2.0 (US EPA, 1993b, 1993a). Ammonium (NH_4^+) concentrations were calculated from NH_3 values, incorporating the influence of water pH and temperature (Emerson et al., 1975). Concentrations of anions: chloride (Cl^-), bromide (Br^-), nitrate (NO_3^-) and sulfate (SO_4^{2-}) and cations: sodium (Na^+), potassium (K^+), magnesium (Mg^{2+}) and calcium (Ca^{2+}) were measured on an ion chromatograph (ICS-2000) equipped with an AS18 anion column and KOH eluent generator (Dionex Corporation, Sunnyvale, CA, USA) at Duke University. All instruments for water analysis used standard calibration methods with calibration curves of $R^2 > 0.998$ (Table S3). Duplicate mesocosm and analytical samples were run on each instrument with percent difference <10%. Mid-analysis calibration checks were performed on each instrument with <5% deviation from the standard concentration on the AQ400 and ICS-2000, and <10% deviation on the Shimadzu for TDC and DOC. TDN was excluded from analysis because certain mid-analysis checks deviated >15% from the calibration standard concentration and certain duplicates had >20% difference between one another. Three Type 1 (i.e., MilliQ ultrapure water) water blanks were run on each instrument during the water analyses to measure container or laboratory instrument contamination.

To measure the total suspended solids (TSS), we combusted Whatman GF/F filters at 500°C for 4 hours, weighed each filter, and filtered a known volume (50 mL or less) of unfiltered water from a 60 mL HDPE bottle vortexed immediately prior to filtering. The

filters were then dried at 60°C for 48 hours, cooled in a desiccator, and re-weighed. We subtracted the post filtration weight from the filter weight and divided by the volume of the unfiltered water that was passed through the filter to determine TSS in units of mg/mL.

Sediment was analyzed for organic matter content, pH, potential microbial respiration, EEA, trace metals, and bulk density. 3 ± 0.25 g of wet sediment was dried at 60°C for 48 hours, weighed, and then combusted at 500°C for 4 hours to determine dry weight and ash free dry mass (AFDM), respectively. We calculated the percent of organic matter in the sample using the equation (dry weight – AFDM) / dry weight) x 100 = percent organic matter (% OM). Sediment pH was measured using 6g of air-dried sediment in 10 mL of 0.01 mol/L $CaCl_2$ (Carter & Gregorich, 1993). The sediment and solution were measured into an acid-washed falcon tube and vortexed for 30 seconds. After settling for 30 minutes, an Orion Star A211 pH meter (ThermoFisher Scientific, Waltham, MA, USA) was placed in the supernatant to get the pH reading. The pH meter was calibrated 30 minutes before use with a 3-point method of pH buffer solutions 4, 7, and 10. Three samples were run in triplicate with an average coefficient of variance of <1%. Sediment bulk density (g/mL) was determined by weighing 50 mL of homogenized wet sediment and was used to calculate the amount of organic matter in the sediment used for potential microbial respiration rates.

To measure trace metal concentrations, a ~3 g wet sediment subsample was dried (48 hours at 60°C), ground using a porcelain mortar and pestle, passed aggregate through a stainless steel #80 180 μm opening sieve (Method 3051A, US EPA 2007). A subsample of dried sediment (0.3 g) was measured into acid-washed glass scintillation vials and submitted for analysis to the UNR Analytical Core Lab. Samples were microwave digested

using a Multiwave 5000 (Anton Parr, Graz, AT) at a ratio of 0.3 g of sieved aggregate to 9 mL omnitrace nitric acid (HNO_3) and 3 mL omnitrace hydrochloric acid (HCl). Trace metal concentrations of aluminum (Al), cadmium (Cd), cobalt (Co), copper (Cu), lead (Pb), nickel (Ni), and zinc (Zn), and nutrient concentrations of Na^+, K^+, Mg^{2+}, and Ca^{2+} were analyzed using inductively coupled plasma-mass spectrophotometry (ICPMS-2000, Shimazdu Corp, Kyoto, JP). One sample was run in triplicate with an average coefficient of variance of 3 ± 1% (Table S4). Cadmium had a high standard deviation (78%) and was excluded from analysis. Six method blanks and three Type 1 water blanks were analyzed during the sediment analyses. Three replicates of a fresh water sediment certified reference material (CRM016, Sigma Aldrich, St. Louis, MO, USA) were used to calibrate the instrument. Recovery rates of all CRM elements except Ca^{2+} and Ni ranged from 85 to 126% (100 ± 12%; Table S4). Sediment Ca^{2+} and Ni had high recovery rates at 240% and 483%, respectively, and were therefore excluded from analyses. Samples that had concentrations below detection were reported as below detection.

Background nutrient and metal concentrations in the salt were measured by dissolving the salt used in the experiment in Type 1 (i.e., MilliQ) water at the low and high press baseline concentrations. The solutions were measured in triplicate using the same instruments as the water samples. The majority of analytes in the salt solutions were below the detection limit (TDC, DOC, TDN, SO_4^{2-}, K^+, Al, Cd, Co, Cu, Ni, Pb, Zn), however there were measured amounts of Br^- (low baseline (230 mg/L NaCl) (LB): 1.07 mg/L, high baseline (860 mg/L NaCl) (HB): 1.04 mg/L), Mg^{2+} (LB: 0.06 mg/L, HB: 0.26 mg/L) and Ca^{2+} (LB: below detection, HB: 0.28 mg/L) (Table S5).

2.2.5 Potential microbial respiration and extracellular enzyme activity

Potential microbial respiration rates were estimated using a modified version (Fierer et al., 2003b) of the substrate-induced respiration (SIR) method (West & Sparling, 1986). Triplicate wet sediment samples (10 ± 0.25 g) were mixed with an autolyzed yeast extract solution (20 mL) and sealed in 125-mL acid-washed glass jars with septa. Rates of CO_2 production were measured over 4 hours using a 500 μl gas-tight syringe and needle (7658-01, 7806-02; Hamilton Co, Reno, NV, USA) to extract gas (via the septa) and dispense into an infrared gas analyzer (LI-6265; LI-COR, Lincoln, Nebraska, USA) with N_2 as the carrier gas. The instrument was calibrated using a 6-point standard method with $r^2 > 0.995$ and CO_2 was measured as a proxy of microbial respiration at 2-hour intervals over 4 hours. In-between measurements, the glass jars were placed on a shaker table at low speed to prevent anoxic buildup in the sediment. Higher rates of CO_2 accumulation in each glass jar equated to higher potential rates of respiration.

Microbes produce extracellular enzymes that break down and make complex organic molecules bioavailable to microbes and plants (Allison & Vitousek, 2005). Potential extracellular enzyme activity was measured using a modified version of the potential soil extracellular enzyme activity method (Bell et al., 2013). 91 mL of a Tris buffer solution, titrated to sample pH, was blended with 2.75 g of homogenized wet sediment. Triplicates of each sample slurry (800 μl) were placed into deep well plates and the slurry was inoculated with a fluorescence facilitating substrate (200 μl) for each enzyme measured. The activity of seven enzymes were measured: three carbon (4-Methylumbelliferyl α-D-glucopyranoside (AG_C), 4-Methylumbelliferyl β-D-glucopyranoside (BG_C) and 4-Methylumbelliferyl β-D-cellobioside (CB_C)), two

nitrogen (L-Leucine-7-amido-4-methylcoumarin hydrochloride (LAP_N) and 4-Methylumbelliferyl N-acetyl-β-D-glucosaminide (NAG_N)), one phosphorus (4-Methylumbelliferyl phosphate (PHOS_P)), and one sulfur (4-Methylumbelliferyl sulfate potassium salt (AS_S)) degrading enzymes. 4-Methylumbelliferone (MUB) was the standard measurement for all enzymes, except LAP_N. 7-amino-4-methylcoumarin (MUC) was the standard measurement for LAP_N. After incubating in the dark for three hours at 25°C, the deep well plates were centrifuged for 3 minutes then 250 μl of supernatant was transferred into black well plates and stabilized with 5 μl of 10N NaOH. Sample fluorescence was read (365/450 nm) in analytical triplicate on an Infinite Pro 200 plate reader (Tecan Group, Männedorf, CH). The instrument was calibrated using a 7-point standard method with $R^2 > 0.995$. The samples were run at 5 below the optimal gain of the standards. This relationship was corrected in a second round of standards analysis using linear relationships with $R^2 > 0.999$ (Table S6a, b).

2.2.6 Data analysis

A generalized linear model was used to compare the differences between the control and the different salinity regime treatments at the end of the experiment in surface water and WSF constituent chemistry (anions, cations, nutrients, carbon), TSS, pH, SpC, DO, sediment % OM and metal concentrations, EEA, and potential microbial respiration. Post-equilibration values in the chambers were averaged then subtracted from individual mesocosm chamber values at the end of the experiment to only examine the cumulative effects of the different treatments relative to their post-equilibration values given the considerable differences between field conditions and the conditions within each

mesocosm chamber. We were unable to use models to evaluate the change in surface water, sediment, or sediment WSF constituent chemistry, or microbial activity after the intermediate first or second incubation periods because of a lack of sediment samples and limited surface water chemistry samples from each salt incubation (n=2).

Two-sample t-tests were used to assess how the experiment transformed TSS from the field to post-equilibration and how the controls at the end of each experiment (undeveloped and urban) compared to one another. Kendall rank correlation coefficient tests were performed to assess the relationship between sediment organic matter with microbial respiration and extracellular enzyme activity.

To test for normal distribution of data, we used a Shapiro-Wilk test (Shapiro & Wilk, 1965) and we used a Levene Test (Levene, 1960) to test for homogeneity of variance. A linear mixed effect model with an interaction of week as the random effect (1-4) was initially used however the model showed week had no clear effect so it was removed. Data that were non-normal or heterogeneous ($p < 0.05$) were log-transformed to meet assumptions of normality. If the log-transformed data still did not fall within normality or homogeneity, a Kruskal Wallis test with a Wilcoxon rank sum exact test for pairwise comparison were used. All models were analyzed using the 'lme4' package in R (Bates et al. 2015; R Core Team 2021).

2.3. Results

2.3.1 Mesocosm chamber salinity treatments

Surface water specific conductance (SpC) and Na^+ concentrations in the water column of the mesocosms increased relative to the control by experimental treatment matching the experiment design (Figure 6). The specific conductance as well as surface water and sediment WSF Na^+ and Cl^- in the end of experiment controls were not significantly different among the two experiments (Table 2). Patterns in chloride concentrations at the end of each incubation did not separate as clearly from the control as SpC and Na^+. At post-equilibration in the undeveloped experiment, SpC was 104 ± 2 μs/cm (mean ± standard deviation) (n = 6) and at the end of the experiment, SpC was 107 ± 3 μs/cm in the controls (n = 4), 564 ± 21 μs/cm in the low baselines (n = 4), 1773 ± 16 μs/cm in the high baselines (n = 4), and 411 ± 75 μs/cm in the pulsed treatments (n = 4) (Table 3). Mean surface water Na^+ and Cl^- concentrations at the end of experiment changed on similar magnitudes to SpC, with the high baseline having the highest concentrations and controls having the lowest (Figure 6; Table S7a, b). SpC, Na^+, and Cl^- concentrations in the urban experiment followed similar patterns as the undeveloped experiment (Figure 6; Table 3 and S7a, b).

Table 2. Specific conductance (SpC), and surface water (SW) and sediment WSF Cl^- and Na^+ in the controls at the end of each experiment (n = 4). Instrument level of detection (LOD) is given for Cl^- and Na^-.

Experiment	SpC (μs/cm)	Cl^- (mg/L): LOD 0.007 mg/L		Na^+ (mg/L): LOD 0.06 mg/L	
	SW	SW	WSF	SW	WSF
Urban	117 ± 13	64.7 ± 70.3	5.3 ± 4.7	11.5 ± 2.3	3.4 ± 1.8
Undeveloped	107 ± 3	88.7 ± 70.3	1.5 ± 0.2	8.7 ± 2.8	4.5 ± 0.3

Table 3. Mean specific conductance measurements across experiments, treatments, and time periods. Standard deviations are given when n > 2.

		Time period: SpC (μs/cm)				
Experiment	Treatment	Field	Post-eq	Post-incub 1	Post-incub 2	Post-incub 3
Undeveloped	Control	107	104 ± 3	115	109	107 ± 3
	Low Baseline	-	-	468	554	564 ± 21
	High Baseline	-	-	1466	1716	1773 ± 17
	Pulse	-	-	114	1488	411 ± 75
Urban	Control	129	121 ± 14	140	114	117 ± 13
	Low Baseline	-	-	476	534	572 ± 13
	High Baseline	-	-	1402	1645	1766 ± 25
	Pulse	-	-	124	1366	455 ± 23

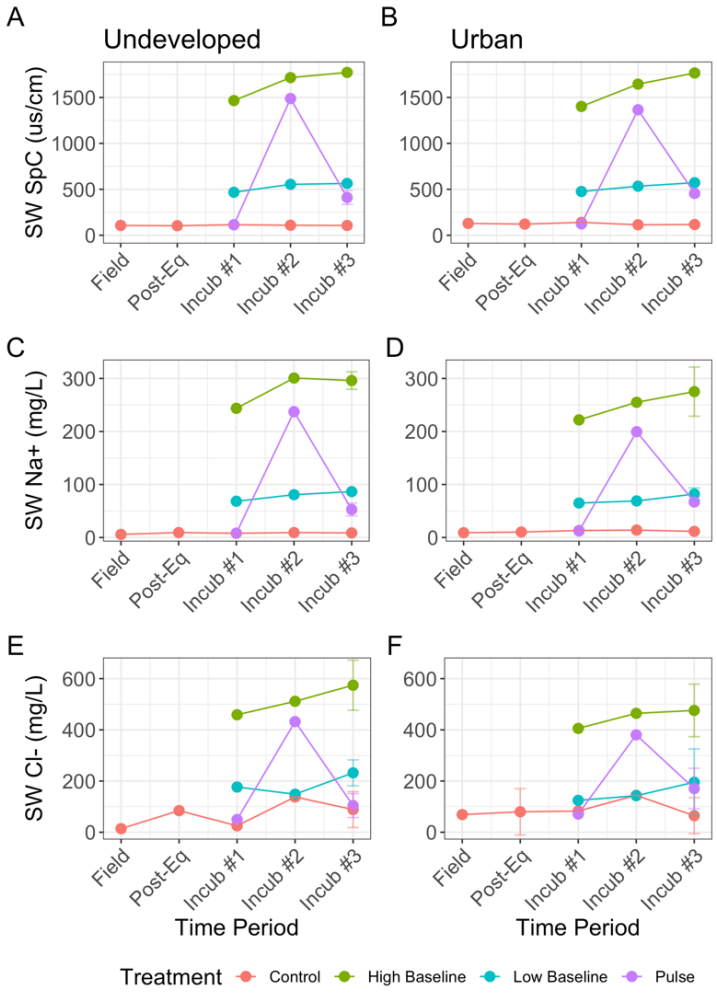

Figure 6. Surface water SpC (A, B), Na^+ (C, D), and Cl^- (E, F) concentrations in the undeveloped and urban experiments organized by time period and treatment.

2.3.2 Surface water and sediment changes from the field to mesocosm post-equilibration

The experiments caused surface water TSS to significantly increase from the field to post equilibration ($p < 0.05$; Figure 7). Surface water temperature increased from the field (undeveloped: 10.3°C; n = 2, urban: 16.7°C; n = 2) to post-equilibration (undeveloped: 24.2°C; n = 6, urban: 21.7°C; n = 6) and pH did not change between the field and post equilibration (Figure 7). Surface water DO decreased from the field to the post equilibration in both mesocosm experiments (Figure 7). Similarly, %OM significantly decreased from the field (1.68 ± 0.02; n = 6) to post-equilibration (1.16 ± 0.04; n = 5) in the undeveloped experiment; however, the decrease in the urban experiment was less pronounced (field: 4.28 ± 1.04; n = 6, post-equilibration: 3.96 ± 1.58; n = 6) and was not considered significant (Figure 8).

Although water temperature and DO changed from the field to post-equilibration, they stayed relatively consistent throughout the remainder of the experiment (Figure 7). Surface water pH and TSS in the high baseline were significantly lower than the control at the end of the urban experiment ($p < 0.05$), but not in the undeveloped experiment (Table 4). Unlike surface water pH, there were no significant differences in sediment pH between the control and salt treatments (Table 4). DO was not significantly different between the control and salt treatments at the end of the experiment (Table 4). In the undeveloped experiment, temperature ranged from 22.1 to 25.7°C; DO ranged from 4.28 to 6.21 mg/L; and pH from 7.11 to 7.84. In the urban experiment, temperature ranged from 19.5 to 21.7°C; DO ranged from 4.61 to 6.34 mg/L; and pH from 7.30 to 7.87. %OM at the end of

the experiment did not significantly differ between salt treatments in either experiment ($p > 0.05$).

Table 4. Measurements at the end of the experiment for surface water (SW) pH, TSS, sediment pH, and dissolved oxygen (DO) (n = 4). *Significantly different from the control ($p < 0.05$).

Experiment	Treatment	SW pH	TSS (mg/L)	Sediment pH	DO (mg/L)
Undeveloped	Control	7.45 ± 0.13	78 ± 8	6.17 ± 0.07	5.50 ± 0.55
	Low Baseline	7.48 ± 0.03	58 ± 11	6.21 ± 0.05	5.67 ± 0.18
	High Baseline	7.39 ± 0.05	63 ± 22	6.18 ± 0.15	5.42 ± 0.23
	Pulse	7.55 ± 0.04	66 ± 12	6.12 ± 0.12	5.50 ± 0.48
Urban	Control	7.68 ± 0.11	328 ± 205	5.87 ± 0.07	5.75 ± 0.41
	Low Baseline	7.55 ± 0.11	183 ± 114	5.90 ± 0.08	5.42 ± 0.21
	High Baseline	7.40 ± 0.08*	91 ± 35*	5.96 ± 0.05	5.36 ± 0.26
	Pulse	7.58 ± 0.09	143 ± 77	5.96 ± 0.09	5.51 ± 0.46

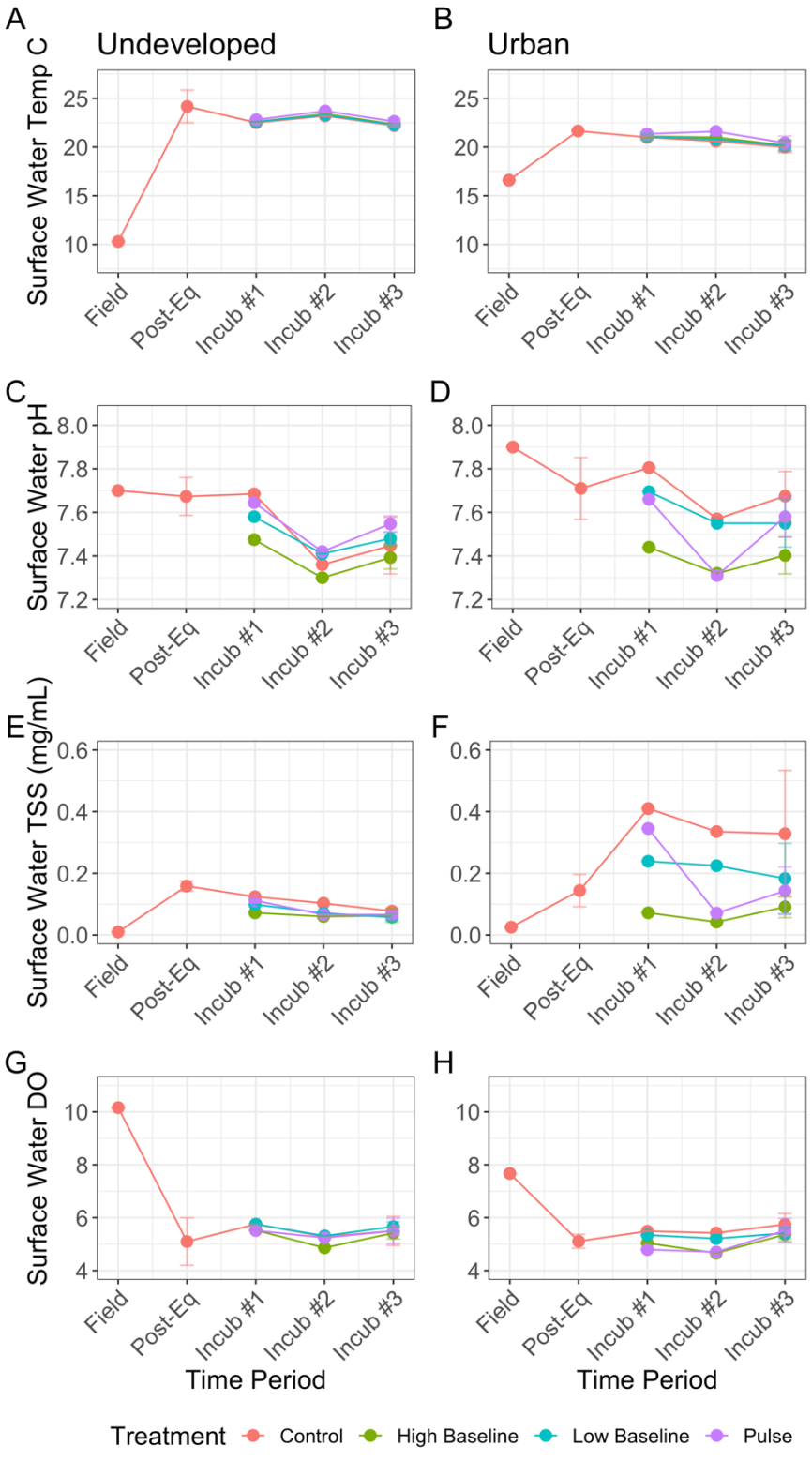

Figure 7. Surface water temperature (A, B), pH (C, D) total suspended solids (E, F), and dissolved oxygen (G, H) changes from the field samples to end of the experiment.

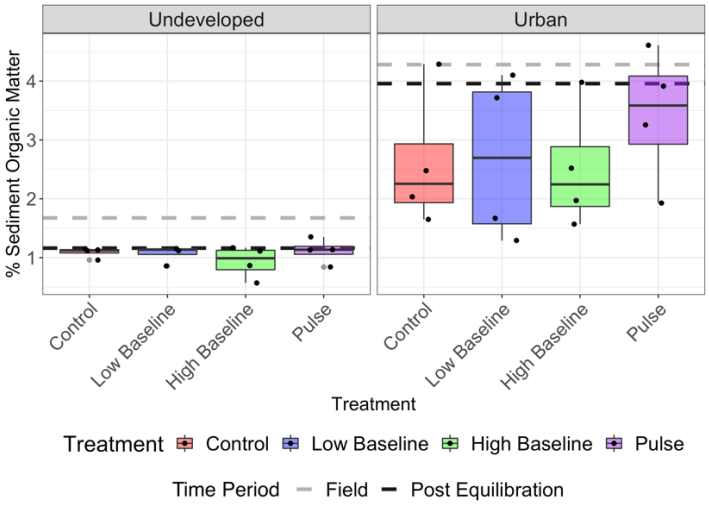

Figure 8. Comparisons of undeveloped and urban experiment sediment organic matter at the field (gray dashed line), post equilibration (black dashed line), and end of the experiment (colored boxes). Field and post equilibration measurements were each averaged to get mean values. Individual measurements at the end of the experiment are represented as black dots along their respective treatments.

2.3.3 Surface water temporal changes between salinity additions and the pulse

A spike of surface water nutrients, notably Ca^{2+}, K^{+}, and NH_4^{+} was observed in the pulsed treatments after the second incubation during which salinity concentrations were increased to the same magnitude as the high baseline (Figure 9). Prior to the second incubation period in the undeveloped experiment, pulse concentrations of Ca^{2+} (8.4 mg/L; n=2), K^{+} (4.2 mg/L; n=2), and NH_4^{+} (0.17 mg/L; n=2) were similar to the control concentrations (Ca^{2+}: 7.9 mg/L; n=2, K^{+}: 3.4 mg/L; n=2, NH_4^{+}: 0.16 mg/L; n=2) (Table 5a, b) . Ca^{2+} and K^{+} concentrations in the urban experiment had similar observations (Figure 9; Table 5a, b). After the second salt incubation, pulse Ca^{2+} and K^{+} concentrations increased and mimicked concentrations in the high baseline (HB) in both undeveloped (Ca^{2+} pulse: 17.9 mg/L; n=2, Ca^{2+} HB: 16.9 mg/L; n=2, K^{+} pulse: 9.3 mg/L; n=2, K^{+} HB: 10.0 mg/L; n=2) and urban (Ca^{2+} pulse: 19.0 mg/L; n=2, Ca^{2+} HB: 17.6 mg/L; n=2, K^{+} pulse: 8.2 mg/L; n=2, K^{+} HB: 9.9 mg/L; n=2) experiments (Table 5a), however NH_4^{+} did not follow this

pattern. After the second salt incubation in the undeveloped experiment, NH_4^+ in the pulse (0.28 mg/L; n=2) and high baseline (0.29 mg/L; n=2) increased 70 and 76 % from the control (0.17 mg/L; n=2), respectively, and were lower than the percent increases observed in the urban experiment (pulse: 185 %; 0.74 mg/L; n=2, HB: 177 %; 0.72 mg/L; n=2) above the control (0.26 mg/L; n=2) (Table 5b).

Decreases of surface water SRP in the salt treatments compared to the control were not consistent with results from other nutrients. After salt incubation #2 in the undeveloped experiment, SRP in the pulse (45.9 μg/L; n=2) and high baseline (43.6 μg/L; n=2) were 12 and 17% lower than the control (52.2 μg/L; n=2), respectively (Figure 9; Table 5b). The urban experiment had a greater magnitude SRP decrease post incubation 2 with the pulse (4.7 μg/L; n=2) and high baseline (4.8 μg/L; n=2) both being 62 % lower than the control (12.4 μg/L; n=2) (Figure 9; Table 5b).

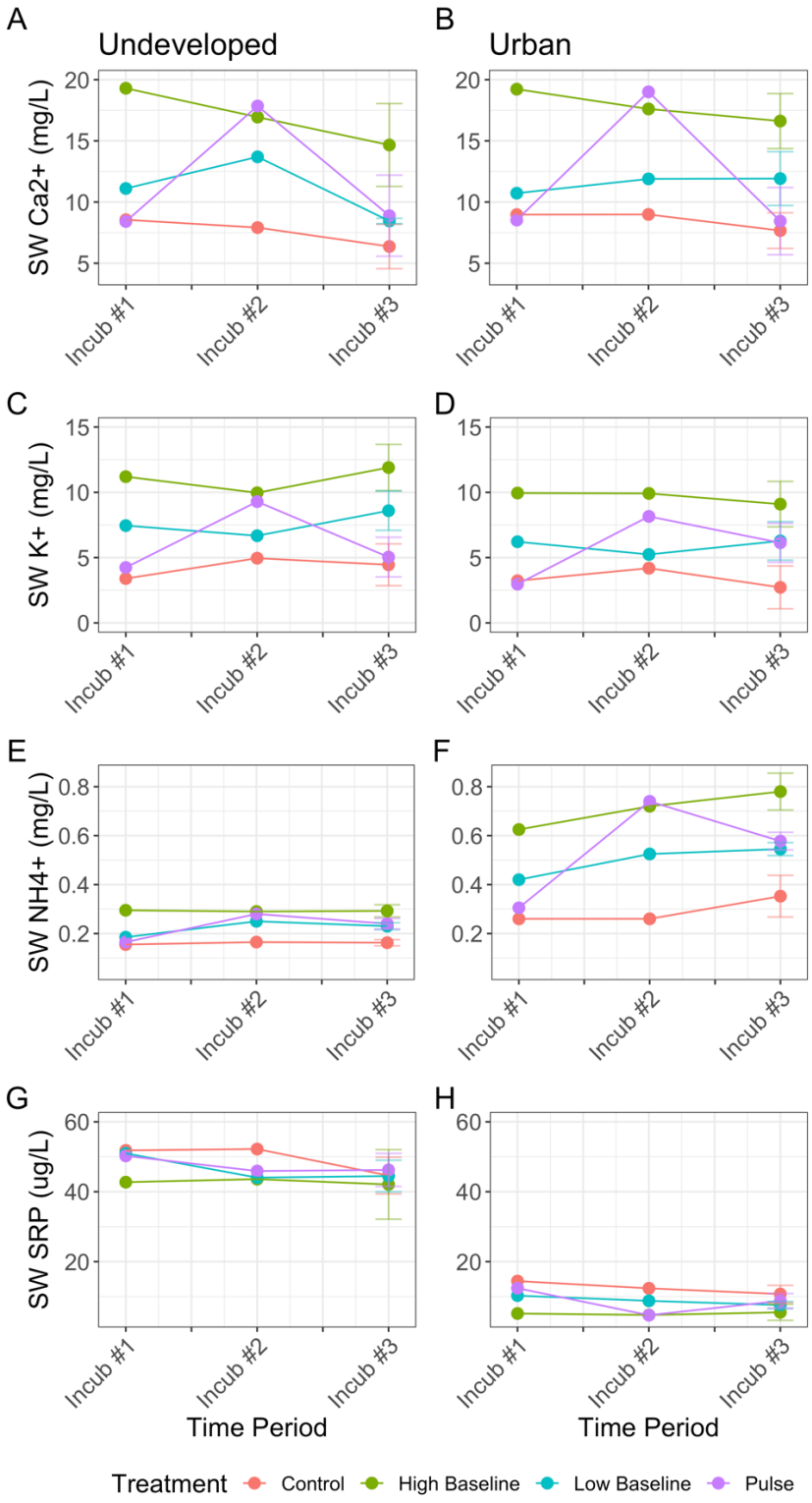

Figure 9. Surface water Ca^{2+} (A, B), K^{+} (C, D), NH_4^{+} (E, F) and SRP (G, H) concentrations changes from the first to last salt incubation in the undeveloped and urban experiments.

Table 5a. Calcium and potassium concentrations after each salt incubation organized by experiment and treatment type. Number of samples collected are given for each incubation period.

		Ca^{2+} (mg/L)			K^{+} (mg/L)		
Experiment	Treatment	Post-incub 1 (n=2)	Post-incub 2 (n=2)	Post-incub 3 (n=4)	Post-incub 1 (n=2)	Post-incub 2 (n=2)	Post-incub 3 (n=4)
Undeveloped	Control	8.6	7.9	6.4 ± 1.8	3.4	5.0	4.5 ± 1.6
	Low Baseline	11.1	13.7	8.5 ± 0.2	7.5	6.7	8.6 ± 1.5
	High Baseline	19.3	16.9	14.7 ± 3.4	11.2	10.0	11.9 ± 1.8
	Pulse	8.4	17.9	8.9 ± 3.3	4.2	9.3	5.0 ± 1.5
Urban	Control	9.0	9.0	7.7 ± 1.5	3.2	4.2	2.7 ± 1.6
	Low Baseline	10.7	11.9	11.9 ± 2.2	6.2	5.2	6.3 ± 1.5
	High Baseline	19.2	17.6	16.6 ± 2.3	9.9	9.9	9.1 ± 1.7
	Pulse	8.5	19.0	8.5 ± 2.8	3.0	8.2	6.1 ± 1.5

Table 5b. Ammonium and soluble reactive phosphorus concentrations after each salt incubation organized by experiment and treatment type. Number of samples collected are given for each incubation period.

		NH_4^{+} (mg/L)			SRP (μg/L)		
Experiment	Treatment	Post-incub 1 (n=2)	Post-incub 2 (n=2)	Post-incub 3 (n=4)	Post-incub 1 (n=2)	Post-incub 2 (n=2)	Post-incub 3 (n=4)
Undeveloped	Control	0.16	0.17	0.16 ± 0.01	51.8	52.2	44.6 ± 5.3
	Low Baseline	0.19	0.25	0.23 ± 0.01	51.0	44.0	44.5 ± 4.5
	High Baseline	0.30	0.29	0.29 ± 0.03	42.7	43.6	42.1 ± 9.9
	Pulse	0.17	0.28	0.27 ± 0.08	50.2	45.9	46.2 ± 4.7
Urban	Control	0.26	0.26	0.35 ± 0.09	14.4	12.4	10.7 ± 2.5
	Low Baseline	0.42	0.53	0.55 ± 0.03	10.3	8.8	7.58 ± 1.0
	High Baseline	0.63	0.72	0.78 ± 0.08	5.2	4.8	5.51 ± 2.3
	Pulse	0.31	0.74	0.58 ± 0.03	12.4	4.7	8.79 ± 2.1

2.3.4 Surface water and sediment water soluble fraction chemical responses

We observed uneven responses to different salinity regime treatments in the various chemical constituents and between the undeveloped and urban sediment experiments. At the end of both experiments with sediment from the undeveloped and urban reaches of Thomas Creek, the sediment WSF TDC, DOC, and SRP in the salt treatments were found to be significantly different from the control ($p < 0.05$; Table 6). Relative to the control, the high baseline treatments in the undeveloped experiment experienced the greatest increases in the sediment WSF TDC (69 ± 21 %; n = 4), DOC (86 ± 19 %; n = 4) and SRP (205 ± 11 %; n = 4) (Figure 10A, E). Similarly, sediment TDC and DOC in the urban experiment had the greatest increases in the high baseline (TDC: 64 ± 25 %; n = 4, DOC: 83 ± 29 %; n = 4) over the pulse (TDC: 51 ± 36 %; n = 4, DOC: 55 ± 24 %; n = 4) and low baseline treatments (29 ± 26 %; n = 4, DOC: 39 ± 25 %; n = 4) relative to the control. In the urban experiment, the high baseline sediment WSF SRP significantly increased from the control (97 ± 99 %; n = 4; $p < 0.05$) while the pulse and low baseline did not have detectable differences ($p > 0.1$). There were no corresponding significant surface water TDC or DOC changes in response to the different treatments in either experiment ($p > 0.1$; Table 6; Figure 10B). However, surface water SRP significantly declined ($p > 0.05$) at the end of the urban experiment in the high (-43 ± 19 %; n = 4) and low (-26 ± 8 %; n = 4) baseline treatments relative to the control concentrations (Table 6; Figure 10F). Similarly, there were significant increases in surface water NH_4^+ across all treatments in both experiments relative to the controls ($p > 0.05$), although the magnitudes of change were greatest in the high baseline treatment (Table 6; Figure 10D). There were no significant changes in the sediment WSF NH_4^+ (Table 6; Figure 10C).

Table 6. Surface water (SW) and sediment WSF TDC, NH_4^+, and SRP concentrations at the end of each experiment (n = 4). *Significantly different from the control ($p < 0.05$). Instrument level of detection (LOD) given for each analyte.

		TDC (mg/L): LOD 0.004 mg/L		NH_4^+ (mg/L): LOD 0.002 mg/L		SRP (μg/L): LOD 0.4 μg/L	
Experiment	Treatment	SW	WSF	SW	WSF	SW	WSF
Undeveloped	Control	12.2 ± 1.3	1.2 ± 0.1	0.16 ± 0.01	0.06 ± 0.04	44.6 ± 5.3	37.3 ± 2.5
	Low Baseline	11.2 ± 1.5	1.7 ± 0.3*	0.23 ± 0.01*	0.04 ± 0.02	44.5 ± 4.5	73.6 ± 3.0*
	High Baseline	11.8 ± 1.0	2.2 ± 0.2*	0.29 ± 0.03*	0.05 ± 0.04	42.1 ± 9.9	119 ± 4.5*
	Pulse	13.4 ± 1.2	2.1 ± 0.2*	0.27 ± 0.08*	0.04 ± 0.03	46.2 ± 4.7	91.2 ± 9.2*
Urban	Control	14.6 ± 1.4	2.3 ± 0.6	0.35 ± 0.09	0.06 ± 0.04	10.7 ± 2.5	4.6 ± 0.6
	Low Baseline	14.5 ± 1.1	3.1 ± 0.8	0.55 ± 0.03*	0.07 ± 0.05	7.6 ± 1.0*	6.4 ± 0.8
	High Baseline	14.2 ± 1.2	4.1 ± 0.7*	0.78 ± 0.08*	0.07 ± 0.02	5.5 ± 2.3*	10.3 ± 5.8*
	Pulse	15.3 ± 1.2	3.5 ± 0.7*	0.58 ± 0.03*	0.07 ± 0.04	8.8 ± 2.1	8.3 ± 3.9

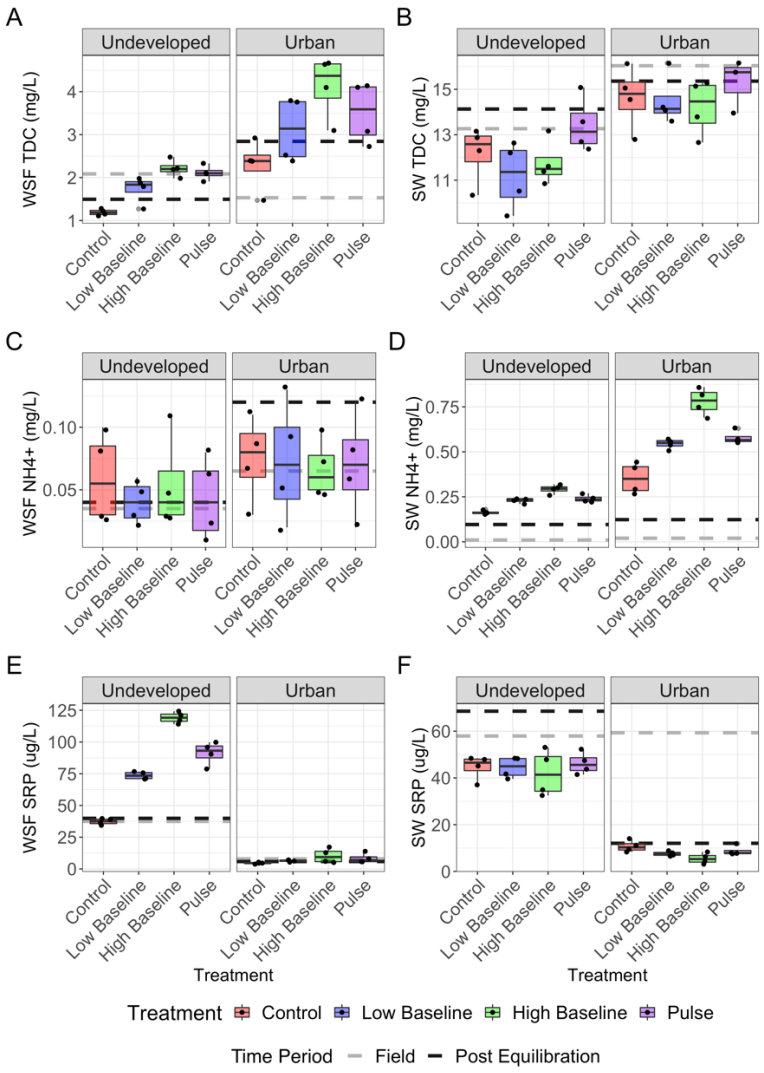

Figure 10. Comparisons of surface water and sediment WSF TDC (A, B), NH_4^+ (C, D), and SRP (E, F) at the field (gray dashed line), post-equilibration (black dashed line), and end of the experiment (colored boxes). Field and post equilibration measurements were each averaged to get mean values. Individual measurements at the end of the experiment are represented as black dots along their respective treatments.

The surface water K^+ at the end of the undeveloped mesocosm experiment significantly increased in the low and high baseline treatments ($p < 0.05$) compared to the control but were relatively unchanged in the pulse ($p > 0.1$; Table 7). At the end of the urban mesocosm experiment, the surface water K^+ was significantly different among treatments, with the high baseline treatment having the greatest increase relative to the

control (166 ± 40 %; n = 4) (Table 7; Figure 11B). Surface water Ca^{2+} increased by a similar magnitude as K^{+}, with the high baseline treatments having the greatest increase relative to the control (undeveloped: 114 ± 46 %; n = 4; $p < 0.05$, urban: 113 ± 28 %; n = 4; $p < 0.05$, Table 7; Figure 11A). Among treatments, only the high baseline surface water Ca^{2+} significantly increased in the undeveloped experiment, and the low and high baselines significantly increased in the urban experiment ($p < 0.05$; Table 7). The pulse surface water Ca^{2+} had no detectable differences from the control in either experiment ($p > 0.1$). The majority of sediment WSF Ca^{2+}, K^{+}, and Mg^{2+}, and surface water Mg^{2+} concentrations in the end of experiment controls were below detection and there were not enough above detection samples for these nutrients to be modeled ($n \leq 2$). No other surface water or WSF constituent nutrients had detectable changes from the controls.

Table 7. Surface water (SW) Ca^{2+} and K^{+} at the end of each experiment, organized by treatment (n = 4). Instrument level of detection (LOD) given for each nutrient. *Significantly different from the control ($p < 0.05$).

		Ca^{2+} (mg/L): LOD 0.28 mg/L	K^{+} (mg/L): LOD 0.016 mg/L
Experiment	Treatment	SW	SW
Undeveloped	Control	6.4 ± 1.8	4.5 ± 1.6
	Low Baseline	8.5 ± 0.2	8.6 ± 1.5*
	High Baseline	14.7 ± 3.4*	11.9 ± 1.8*
	Pulse	8.9 ± 3.3	5.0 ± 1.5
Urban	Control	7.7 ± 1.5	2.7 ± 1.6
	Low Baseline	11.9 ± 2.2*	6.3 ± 1.5*
	High Baseline	16.6 ± 2.3*	9.1 ± 1.7*
	Pulse	8.5 ± 2.8	6.1 ± 1.5*

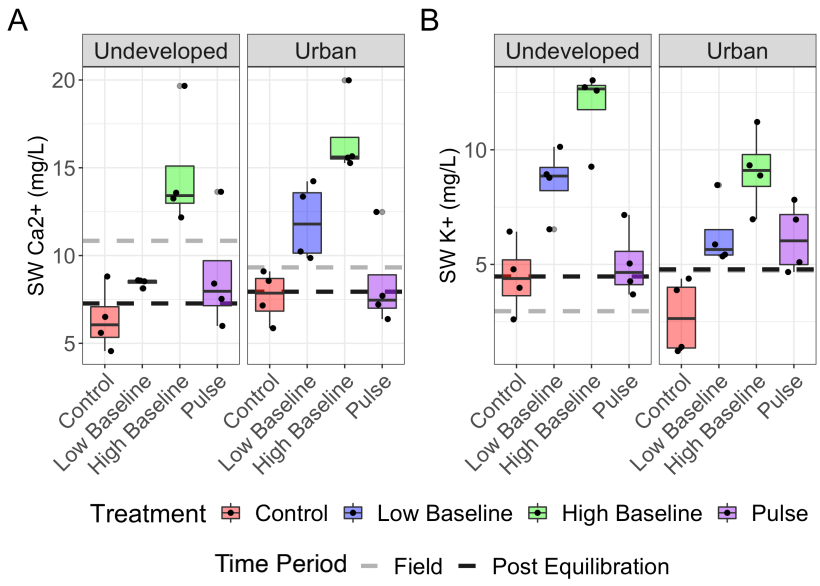

Figure 11. Comparisons of surface water Ca^{2+} (A) and K^{+} (B) at the field (gray dashed line), post-equilibration (black dashed line), and end of the experiment (colored boxes). Field and post equilibration measurements were each averaged to get mean values. Individual measurements at the end of the experiment are represented as black dots along their respective treatments.

2.3.5 Sediment chemical responses

Unlike the sediment WSF constituents and surface water solutes, no sediment metals (Al, Cd, Co, Cu, Pb, Zn) were found to have significant differences between the controls and salt treatments in either experiment ($p > 0.05$; Figure 12). However, sediment Na^{+} concentrations significantly increased from 1.0 ± 0.1 to 1.3 ± 0.2 mg/g (undeveloped) and 1.0 ± 0.4 to 1.8 ± 0.6 mg/g (urban) in the control to the high baseline treatment for both experiments, and from 1.0 ± 0.1 to 1.3 ± 0.1 mg/g in the control to the low baseline treatment in the undeveloped experiment ($p < 0.05$; Figure 12A). No other sediment nutrients (K^{+}, Mg^{2+}) had detectable changes from the controls ($p > 0.05$).

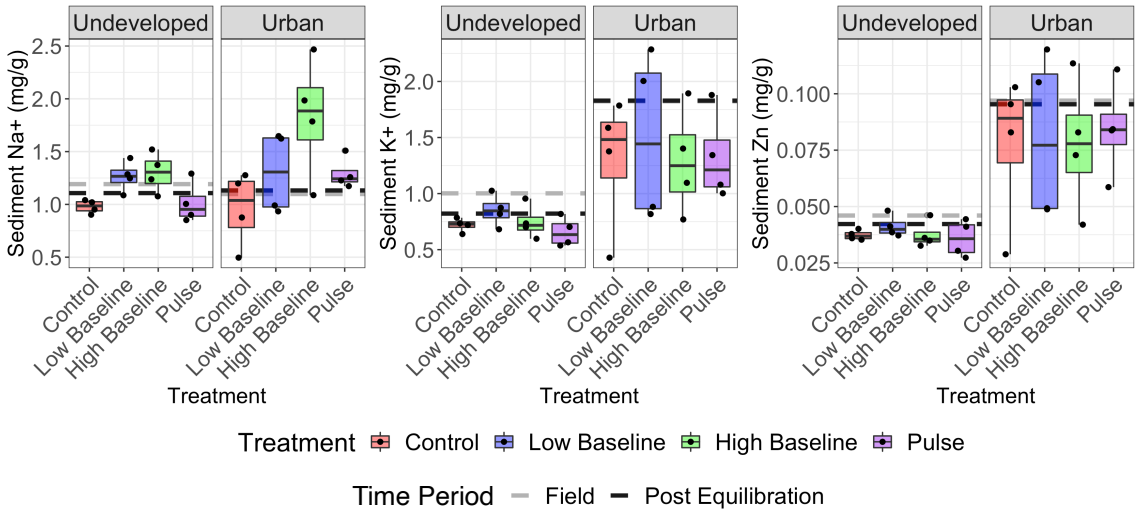

Figure 12. Concentrations of sediment Na^+ (A), K^+ (B), and Zn^{2+} (C) at the field (gray dashed line), post-equilibration (black dashed line) and end of the experiment (colored boxes). Field and post equilibration measurements were each averaged to get mean. Individual measurements at the end of the experiment are represented as black dots along their respective treatments.

2.3.6 Microbial responses to salinity regimes

Overall, salt treatments did not cause detectable changes in the sediment potential microbial respiration rate (MRR) or extracellular enzyme activity (EEA; Figure 13). At the end of the experiment, MRR and EEA were not significantly different from the control in any salt treatment (Table 8). In the undeveloped experiment, there was little variation from the post equilibration to the end of the experiment, but notably, EEA for nitrogen degrading enzymes (N EEA) increased in the high baseline (104 ± 246%; n = 4) and pulse (29 ± 197%; n = 4) relative to the control (Figure 13C), however there were no significant differences between the control and these two treatments ($p > 0.1$).

Table 8. MRR and EEA at the end of each experiment, grouped by treatment (n = 4).

			EEA (nmol/g/hr)			
Experiment	Treatment	MRR (μg.C/g/hr)	C	N	P	S
Undeveloped	Control	9.8 ± 0.6	43.8 ± 11.4	65.1 ± 37.0	53.4 ± 14.4	4.3 ± 1.1
	Low Baseline	9.8 ± 1.8	41.2 ± 7.2	51.2 ± 27.7	50.6 ± 12.2	4.4 ± 0.9
	High Baseline	9.4 ± 0.8	38.8 ± 8.4	99.7 ± 82.1	56.1 ± 14.5	4.2 ± 0.8
	Pulse	10.2 ± 0.8	36.4 ± 6.4	75.7 ± 65.7	43.6 ± 2.7	4.1 ± 0.5
Urban	Control	22.6 ± 10.6	152 ± 67.2	97.6 ± 26.7	156 ± 71.2	9.6 ± 1.8
	Low Baseline	21.1 ± 9.6	148 ± 75.5	90.5 ± 9.8	152 ± 76.4	10.6 ± 2.7
	High Baseline	20.8 ± 10.3	139 ± 80.2	99.2 ± 35.2	147 ± 80.8	9.8 ± 2.7
	Pulse	22.2 ± 9.0	151 ± 87.5	98.1 ± 18.8	146 ± 73.6	10.4 ± 2.7

When compared directly to the post-equilibration N EEA rates, the final high baseline N EEA rates in the undeveloped experiment increased significantly ($p < 0.05$), while MRR and the other EEA rates remained constant. In the urban experiment, the S EEA rates significantly decreased from the post equilibration to the end of experiment control, pulse, and high baseline treatments ($p < 0.05$) and weakly decreased in the low baseline treatment ($p < 0.1$). MRR and the C, N and P EEA rates at the end of the urban experiment were not significantly different from the post-equilibration period.

Correlation coefficients with %OM indicated overall strong positive relationships with potential microbial respiration rates and C, P, and S extracellular enzyme activity. Microbial respiration in all salt treatments was significantly correlated with % OM ($p < 0.05$). The low baseline had the strongest signal ($\tau = 0.98$), and the control had the weakest signal ($\tau = 0.71$; Figure 14). The low baseline had the weakest signal of all treatments in C ($\tau = 0.62$; $p < 0.05$), S ($\tau = 0.55$; $p > 0.05$), and P ($\tau = 0.47$; $p > 0.1$) enzyme activity; however, it had the strongest signal and was the only treatment to be significantly correlated in N enzyme activity ($\tau = 0.76$; $p < 0.05$; Table 14). Notably, N enzyme activity

in the pulse treatment showed the weakest signal and correlation out of all microbial groups we measured ($\tau = 0$; $p > 0.95$; Figure 14).

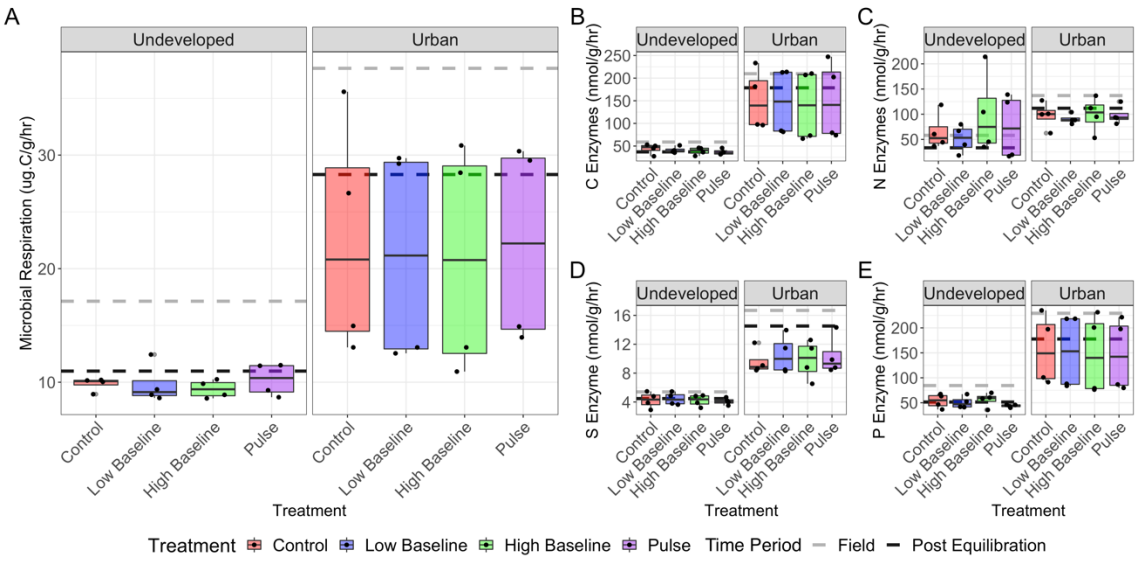

Figure 13. Microbial respiration (A) and C (B), N (C), S (D), and P (E) extracellular enzyme activity at the field (gray dashed line), post-equilibration (black dashed line), and end of the experiment (colored boxes). Field and post equilibration measurements were each averaged to get mean values. Individual measurements at the end of the experiment are represented as black dots along their respective treatments.

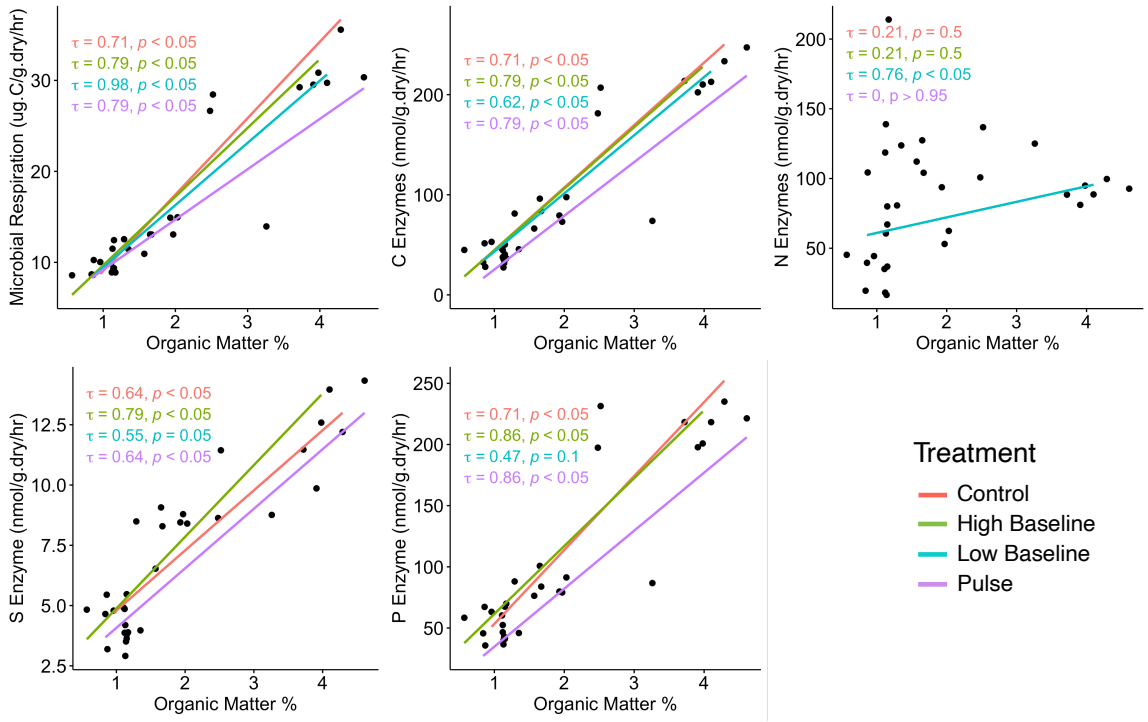

Figure 14. Sediment organic matter percent to microbial respiration and C, N, S, and P extracellular enzyme activity with Kendall rank correlation coefficients. Regression lines are given if the correlation was significant ($p < 0.05$).

2.4. Discussion

2.4.1 Overview

In agreement with previous studies on the effects of elevated salinity concentrations on stream sediment chemistry, increases in surface water salinity concentrations were found to change the flux of some nutrients, namely carbon, ammonium, potassium, calcium, and soluble reactive phosphorus, from sediments into the surface water of the experimental mesocosm chambers. The magnitude of these changes after the final incubation period were most often greatest in the high baseline treatment relative to the low baseline or pulse treatments. Potential microbial respiration and extracellular enzyme activity did not appear to be affected by any of the salinity treatments relative to the control. Low and high baseline treatment specific conductance in each corresponding treatment

chamber fell within the range of values historically observed in streams in the Great Basin, yet these concentrations may have been too low to induce a functional response in the sediment microbial community. In addition, there may have been a lag in the functional responses of the sediment microbial community that was longer than the duration of this mesocosm experiment. Despite these limitations in our ability to evaluate microbial responses to different salinity regimes, we did observe differences in the release and retention of different solutes from the sediments among salinity regimes, yet these effects of increased salinity exposure appeared to be more dependent on the magnitude of increased salinity than the duration of elevated salinity exposure.

2.4.2 Salinity-driven biogeochemical changes

High salinity exposure emerged as the driver of lower surface water pH and lower total suspended solids (TSS) in the water column of the experimental mesocosm chambers. At the end of the experiments, the high baseline treatments caused the greatest pH declines over the pulse and low baseline treatments, relative to the controls. This corroborates previous work that show higher salinity concentrations decrease pH (Kim & Koretsky, 2013) and subsequently increase sorption capacity on particulate surfaces (Green et al., 2009). Although we observed declines in surface water pH with greater salinity concentrations, sediment pH did not follow the same pattern. Similar to pH, water column TSS had the greatest declines in the high baseline over the other salt treatments at the end of the experiment and is most likely the result of increased flocculation (Sholkovitz 1976). Salts act as binding agents to suspended solids and as the particles bind, they increase in size and weight and eventually sink out of the water column into sediment. Water column

pH and TSS in the pulse and low baseline treatments had lower magnitude changes than the high baseline treatments, indicating that sustained high salinity is needed for decreases in pH and TSS to occur. These results suggest that sustained increases in salinity at baseflow may increase retention of particle-bound nutrients with limited ion exchange capacity that may settle at a faster rate compared to lower salinity streams.

2.4.3 Salinity drives varying nutrient and metal responses

Surface water and sediment chemistry responses varied among salinity regime treatments. Our hypothesis that flux rates of particular nutrients would be greatest in the high baseline treatment at the end of the experiment were validated for total dissolved carbon (TDC), dissolved organic carbon (DOC), ammonium (NH_4^+), soluble reactive phosphorus (SRP), calcium (Ca^{2+}), and potassium (K^+). Increases in surface water and the sediment water soluble fraction concentrations of TDC and DOC with increasing NaCl concentrations were also observed in salinity exposure experiments using sediments from Baltimore, Maryland, USA (Duan & Kaushal, 2015). The flux of ammonium (NH_4^+) is likely due to the positively charged NH_4^+ ions being adsorbed to newly introduced negative ions (i.e., Cl^-) (Nieder et al., 2011), however the signal differences observed in surface water and sediment WSF could be due to cation exchange interference from Na^+ ions or NH_4^+ uptake in the sediment by microbes. The high surface water NH_4^+ concentrations in the high baseline treatment at the end of both experiments could potentially be a result of salinity inhibiting the activity of stream nitrifier communities (Jeong et al., 2018). We did not observe any change in surface water nitrate concentrations for any treatment; this response was also observed in previous month-long salinity incubations (Compton &

Church, 2011) in which initial chloride additions had little effect on nitrate, whereas ammonium had a stronger immediate response to increased chloride.

In contrast to the changes in ammonium, TDC, and DOC, soluble reactive phosphorus (SRP) concentrations decreased in surface water while increasing in the sediment WSF. We hypothesize that the reason SRP declined in the water column was because of the potential sorption of SRP to particles that settled at a faster rate in the high baseline and pulse treatments because of enhanced flocculation with elevated salinity concentrations (McGechan & Lewis, 2002). There was a clear difference between the urban and undeveloped experiments, in which sediment WSF SRP increased on a greater magnitude in the undeveloped over urban experiment; however, this could have been a result of the undeveloped experiment having greater surface water SRP concentrations. The lack of a clear sulfate response to the salinity treatments was similarly found in sediment incubations from urban streams in Baltimore, Maryland (Duan & Kaushal, 2015).

The higher surface water cation (Ca^{2+}, K^{+}) concentrations observed in the high baseline treatment validate the results from previous work showing NaCl stimulates ion exchange (Bäckström et al., 2004; Kim & Koretsky, 2013; Lofgren, 2001; Norrström & Bergstedt, 2001). Increased cation fluxes occurred in the final incubation period in all three salt treatments, but the magnitude was the greatest in the high baseline. Although there were detectable amounts of Ca^{2+} in the salt used for the experiments, the observed fluxes in the experiment were several milligrams per liter higher than the corresponding concentrations in the mesocosm salt additions. Therefore, the elevated flux of cations into the surface water in the final incubation period in all of the salinity regime treatments most

likely occurred because of increased NaCl concentrations and not because of the background Ca^{2+} concentrations in the salt additions.

Other than sodium, we did not observe any sediment nutrient or metal differences between salinity treatments. It is possible that the NaCl concentrations were not high enough to cause changes to the sediment ion exchange capacity. Other road salts, such as MgCl and CaCl have a higher ion exchangeability rate than NaCl and are more likely to cause trace metal mobilization from sediment (Acosta et al., 2011).

This experiment was conducted over one summer month at urban and undeveloped stream reaches in Thomas Creek, Reno, NV. Potential seasonal changes in stream chemistry from road salt application, lawn fertilizer application, and hydrology (Fillo et al., 2021; Kaushal et al., 2005; Walsh et al., 2001) could have altered the chemical flux responses relative to what may have been observed if the experiment was carried out in another season. Lawn irrigation return flows in warm summer months can increase stream baseflow and dilute solute concentrations (Fillo et al., 2021; Manago & Hogue, 2017). Therefore, it is possible that the stream surface water and sediment used in this experiment could have had lower chemical concentrations than what may have been found in cold winter months when lawn irrigation decreases in Reno.

2.4.4 Microbial activity did not change between treatments

Contrary to our expectations, there were no clear impacts from the salinity treatments or legacies of salinity exposure on potential microbial respiration or extracellular enzyme activity (EEA). Previous work in terrestrial soils (Raiesi & Sadeghi, 2019) showed high salinity caused a decline in microbial respiration and EEA; however,

this experiment did not see a similar relationship. Microbial communities in sediments from streams draining undeveloped watersheds have been shown to be more functionally resilient to multiple stressors, including elevated salt concentrations, than those from urban stream sediments (Wang et al., 2014). The tight correlations of sediment organic matter with potential microbial respiration and extracellular enzyme activity were expected as microbes breakdown organic matter to access nutrients (Wilczek et al., 2005), but it was surprising that the salt treatments did not seem to cause most microbial activity to deviate from this correlation. The lack of correlation in nitrogen extracellular enzyme activity and sediment organic matter in the control, pulse, and high baseline treatments could be due to the experimental changes from the field inhibiting their activity, or the high magnitude salt treatments could have had a greater impact on enzyme activity than the low baseline treatment. While it is possible we may have observed functional differences if we had continued the experiment for longer, in the short-term, the sediment microbial communities from both reaches along Thomas Creek were functionally-resistant to additional stressors.

The temperature, light, and dissolved oxygen (DO) changes likely affected the response of the stream sediment microbes to the treatments relative to what we might expect from the field. Higher water temperatures in the lab could have favored certain microbial taxa and increased rates of biogeochemical cycling relative to field conditions. The lack of an artificial light to mimic natural patterns in sunlight also limited the scope of our inferences to the sediment below the streambed surface. While the predominantly dark conditions likely favored heterotrophs and caused a decline in autotrophs, we were intentionally targeting the sediment community both at and below the photic zone. There were lower DO concentrations in the experiment compared to the field which was likely a

result of the mesocosm glass cylinders being encased in plastic which limited surface water-air interaction. The increased water temperature also likely contributed to lower DO because oxygen is less soluble in warmer water. Although we stirred sediments between each incubation period, anaerobic conditions likely occurred in the mesocosm sediments. Anaerobic conditions are favorable for the mobilization of phosphorus which is released from bonds with cations under altered redox states which was observed with increased sediment WSF SRP concentrations in the high baseline treatments. Anaerobic conditions also increase rates of denitrification and reduce nitrification, which may explain why we did not observe changes in nitrate in the water column of the mesocosm chambers.

The similarities in specific conductance, sodium, and chloride in the controls of both experiments indicate that the microbial communities had similar exposure to baseline salinity. It is possible that microbial communities in Thomas Creek change throughout the year from stream chemistry changes; however, this experiment was conducted in the summer and not able to capture the potential variation. The urban site was located next to a commercial center and major highway where deicing salt application on roads and parking lots in the winter could have caused elevated stream salinity in the past and higher concentrations than what is observed in the summer. Elevated salinity relative to what was observed when this experiment took place could have changed the microbial community to be dominated by salt-tolerant species. Had this experiment taken place in the winter, it is possible that the microbial response would have been different.

Although the high and low baseline treatment salt concentrations were high enough to induce changes in the flux of a subset of elements, the regimes did not cause a clear microbial response. This apparent resistance of microbial activity indicates a stronger

tolerance to disturbance than was hypothesized. Furthermore, the similar responses of MRR and EEA in both experiments shows that the effects of legacy contaminant exposure may not always be retained throughout the year. This contradicts similar work in benthic communities from low contaminant concentration streams being highly sensitive to increases in salinity (Clements & Kotalik, 2016).

The three experimental 14-hour salt incubations did not cause a noticeable microbial response. Previous laboratory microcosm experiments with a 20-hour NaCl exposure caused decreased function in urban stream sediment denitrifier communities (Wang et al., 2014). A 72-hour NaCl incubation microcosm study found bacterial density of biofilm to decrease during salinity exposure, then recover after the salt was removed (Cochero et al., 2017). Microbes possess stressor tolerance mechanisms, including the accumulation of contaminants and alteration of cell membranes that in the face of disturbance can suppress the effects of stressors (Gadd & Griffiths, 1978). Disturbance length can result in immediate or delayed microbial responses (Hawkes et al., 2017) however MRR and EEA did not respond to elevated salinity in this experiment. It is possible that the salt incubations in this experiment were not long enough to cause a microbial response, or the microbes possessed tolerance mechanisms to withstand the salt stressor, or a combination of both.

2.5 Conclusion

Salinity regimes in streams are highly heterogeneous across the continental U.S. reflecting background catchment characteristics (e.g., climate, geology) and land use in the contributing watershed (Bolotin et al., 2022; Kaushal et al., 2019). Previous salinity

incubation experiments have shown that the flux of certain bioreactive elements increases with the concentration of salinity exposure (Duan & Kaushal, 2015), biofilms can be altered with salt exposure but recover quickly (Cochero et al., 2017), and that benthic communities in low specific conductance watersheds are sensitive to salinity exposure (Clements & Kotalik, 2016). Elevated salinity caused nutrient fluxes in sediment and surface water with the flux magnitude increasing with higher salt concentrations. The pulse treatment indicated nutrient fluxes decrease after a high salinity input is removed. Potential EEA rates and potential microbial respiration were found to be resistant to salt disturbance and legacies of high salinity exposure. These results show freshwater salinity causes secondary effects by changing concentrations of stream solutes with consequences for water quality. Future studies may take a seasonal approach to freshwater salinity and conduct experiments throughout the year as stream salinity concentrations and sediment microbial community composition may change. Incorporating light regimes and using a flow-through mesocosm design that continuously replaces water may better represent what may happen to microbial communities in the field when streams experience elevated freshwater salinity.

As stream salinity concentrations rise across the U.S. (Olson 2019; Kaushal et al., 2018a), it is important to understand the effects of the magnitude and duration of elevated salinity on stream ecosystem ecology and biogeochemistry. The observed resistance of stream sediment microbial communities to elevated salinity indicates that the ecosystem services they provide (e.g., water purification, organic matter decomposition) are more resistant in the short term to the concentrations we exposed them to. This experiment found elevated freshwater salinity releases carbon and nitrogen from sediment which can

contribute to alleviation of nutrient limitations on algal growth with negative implications for downstream water quality (Kaushal et al., 2021). The observed increases of surface water salt ions (i.e., calcium, potassium) can have negative implications for drinking water as salt can make water unpalatable, cause additional municipal processing that raises costs, and corrode infrastructure like lead water pipes (Braukmann & Böhme, 2011; Butler et al., 2016; Cañedo-Argüelles et al., 2013). Streams and rivers are often the most reliable sources of irrigation water for agriculture (Cañedo-Argüelles et al., 2013) and crop yields can be adversely affected by elevated potassium and calcium which induce metabolic impairment and oxidative stress in plants (Ullah et al., 2021). As urban areas expand and global stream salinity concurrently increases (Kaushal et al., 2021), understanding both the direct and indirect effects of salinity exposure for downstream ecosystem function will be critical for predicting ecosystem responses to freshwater salinization.

Chapter 3: Water and sediment chemistry, and microbial activity in streams draining the semi-arid city of Reno, NV

3.1 Introduction

Urbanization of landscapes has been increasing around the globe (Seto et al., 2012), which has introduced multiple stressors on freshwater ecosystems. Multiple stressors can limit the capacity of freshwater ecosystems to provide ecosystem services, such as recreation, nutrient retention, and wildlife habitat (Grimm et al., 2005; Meyer et al., 2005). The term 'urban stream syndrome' has been coined to describe how streams and rivers are degraded by the cities they drain (Meyer et al., 2005; Walsh et al., 2005). Symptoms include the intensification of storm flows because of increased overland flow from impervious surfaces and stormwater infrastructure, increased nutrient and contaminant concentrations, and a resulting decline in biotic richness (Meyer et al., 2005; Paul & Meyer, 2001; Walsh et al., 2005; Wise et al., 2019; Figure 2). Urban streams exhibit these changes in their physical, biological, and chemical conditions around the globe, but the degree of change can be dependent on climate (Hale et al., 2016) and underlying lithology (Blaszczak et al., 2019).

Streams in urban areas typically have higher stressor levels than non-urban streams (Booth et al., 2016; Paul & Meyer, 2001; Walsh et al., 2005). Urban stream temperature can be elevated compared to non-urban streams from the replacement of vegetation with roads and buildings that absorb and retain heat (urban heat island effect), and the removal of riparian vegetation which decreases stream shading and increases water heat absorption (Grimm et al., 2008; Paul & Meyer, 2001; Somers et al. 2013). Water quality in urban

streams can be degraded from non-point source loading of salts (road and parking lot deicing), nutrients (sewer leakage and fertilizer runoff), and metals (vehicle degradation) (Fillo et al., 2021; Kaushal et al., 2005; Paul & Meyer, 2001; Figure 2). High stressor levels may impact stream's ability to provide habitat for aquatic biota and for the retention of nutrients (Grimm et al., 2005).

Urban streams in arid and semi-arid climates are often non-perennial (López-López et al., 2019; Shanafield et al., 2021), but urbanization can increase baseflow and create perennial flows in otherwise non-perennial streams (Fillo et al., 2021; Solins et al., 2018; White & Greer, 2006; Figure 2). Baseflow in urban streams draining semi-arid cities and without upstream wastewater effluent inputs increases as a result of lawn irrigation return flows (Fillo et al., 2021) and leaking pipes (Bhaskar et al., 2016). Lower baseflow in urban streams can also occur because of impervious surface cover which reduces precipitation infiltration and groundwater recharge (Bhaskar et al., 2016; Paul & Meyer, 2001). This change in natural hydrology can dilute or concentrate contaminants in streams (Gallo et al., 2013; Walsh et al., 2005) with implications for sediment microbial communities (Allison & Vitousek, 2005; Martin et al., 2021; Figure 2).

Microbial activity in streams provides important ecosystem services, such as organic matter decomposition and nutrient uptake and transformation (Allison & Martiny, 2008), but these rates can change in response to alteration of in-stream hydrologic and chemical conditions as a result of upstream development (McDonald et al., 2011; Sheldon, 2005; Wang et al., 2014). Microbial activity can be sensitive to desiccation (Amalfitano et al., 2008) and increases in summer and fall seasonal baseflow in urban catchments as a result of lawn irrigation return flows (Fillo et al. 2021) might sustain more microbial

activity in an otherwise dry time of year. Elevated concentrations of salts and other chemical stressors may also reduce microbial activity (Wang et al., 2014; White & Greer, 2006), but whether these concentrations are diluted or concentrated downstream of development is unclear in semi-arid catchments. In both undisturbed and urban streams, microbial activity can also be nutrient limited, therefore microbes produce extracellular enzymes to access nutrients in the surrounding environment (Allison & Vitousek, 2005; Walsh et al., 2001, 2005). Conditions that are typically categorized as stressful, such as elevated salinity concentrations, may have indirect effects that alleviate nutrient limitation. Elevated stream salinity from sources like road salts can release moderate amounts of limiting nutrients (Duan & Kaushal, 2015) and have the potential indirect effect of increasing microbial activity; however, high chemical stressor concentrations can reduce the capacity of sediment microbial communities to transform nutrients and carbon (Rocca et al., 2019) (Figure 2). The combined legacy effects of changing hydrologic and chemical conditions on microbial activity in stream sediments are unclear.

In addition to land use, underlying lithology can influence urban stream hydrology and chemistry (Blaszczak et al., 2019; Hopkins et al., 2015; Utz et al., 2016). During low-precipitation periods, groundwater can be the primary driver of surface water flows (Nickolas et al., 2017). Certain lithologies discharge the majority of groundwater following precipitation (basalt) while others have a fractured geology which allows for slower water percolation and groundwater discharge to be sustained throughout dry months (sandstone) (Nickolas et al., 2017). Groundwater discharge to surface water during low flow periods can lead to increased salinity from naturally saline underlying lithology (Borrok & Engle, 2014), or in urban areas, the long subsurface residence time of road salts (Gabor et al.,

2017). To address the knowledge gap of microbial response to underlying lithology and multiple stressors, this field study investigated potential microbial respiration and extracellular enzyme activity in streams with varying underlying lithology, upstream urbanization, contaminant legacies, and streamflow classification.

In this study, we sampled a wide range of stream reaches to get a summer snapshot of 1) how stream chemistry and microbial activity change in streams as they move from undeveloped to urban environments and across varying underlying lithology types in the semi-arid city of Reno, Nevada, USA, and 2) how sediment microbial communities differ between wet and dry streams. To provide a better context to this summer snapshot, long-term water quality data and prior field sampling was used to measure temporal fluctuations in surface water quality. These long-term trends were compared to the summer field data to better understand how stream conditions may change throughout the year. We hypothesized that stream solute concentrations increase as a function of urban development in the contributing watershed, but that this pattern might be dependent on the lithology in the contributing watershed. We also hypothesized that microbial communities will have higher potential respiration rates and higher rates of extracellular enzyme activity in streams with flowing water which are more likely to be found downstream of development in the summer.

3.2 Methods

3.2.1 Site description

We sampled 13 sites across eight streams in the Reno-Sparks Metropolitan Statistical Area (MSA), Nevada, USA on July 21 and 22, 2021 (Figures 15, S1, and S3).

The Reno-Sparks MSA is in the northwestern part of the Great Basin and Nevada and lies in the rain shadow of the Sierra Nevada Mountains. The Reno-Sparks MSA is 1400 meters above sea level and has a semi-arid cold climate with most precipitation occurring in the winter and spring (Köppen-Geiger classification: BSk). In the 12 months preceding sampling, 7.7 cm of rain and 40.1 cm of snow fell in Reno-Sparks (Reno-Tahoe International Airport, National Weather Service). All sampled streams were within the Truckee River Basin, an endorheic river basin originating from Lake Tahoe, California and terminating 195 kilometers later in Pyramid Lake, Nevada.

Ten sites were chosen to span the widest gradient of wet and dry streams including various surface geology classifications and soil textures in a paired design above and below urban development (Tables 9 and 10). The remaining three sites were chosen as end members with either entirely undeveloped watersheds or highly urbanized watersheds (Table 9). The stream locations ranged from forested upland areas to valley urban areas (Figure S1). At the time of sampling, six sites were dry: Peavine Creek above (PEAV-ABOVE) and below (PEAV-BELOW), Steamboat Creek above (STM-ABOVE), Alum Creek above (ALUM-ABOVE), Evans Creek (EVAN) and Peavine Ponds Creek (PPC), and seven were wet: Hunter Creek (HUNT), Thomas Creek above (THOM-ABOVE) and below (THOM-BELOW), Steamboat Creek below (STM-BELOW), North Truckee Drain above (NTD-ABOVE) and below (NTD-BELOW), and Alum Creek below (ALUM-BELOW) (Table 9). Five streams (THOM, PEAV, STM, NTD and ALUM) had paired sites with one above and one below development (Table 9). Of the remaining three sites, two were above development (HUNT and PPC) and one was below (EVAN) (Table 9).

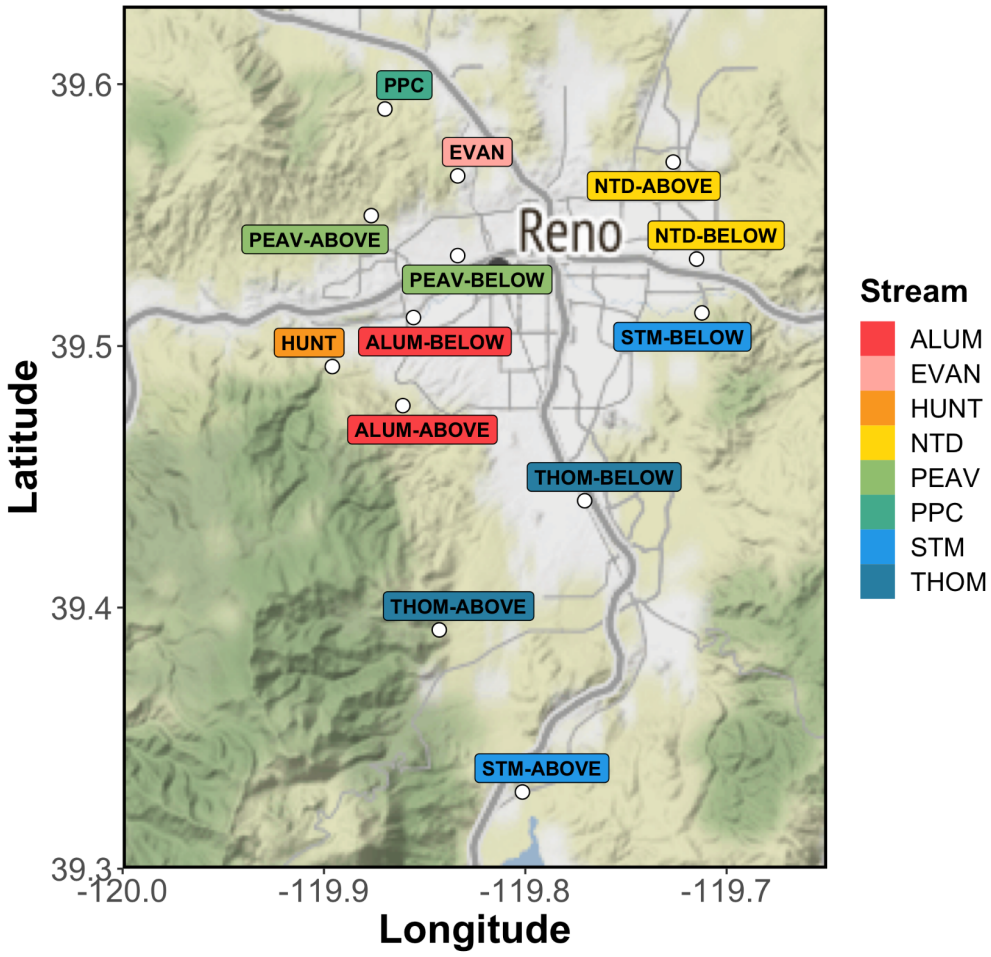

Figure 15. Map of the study area with a Google Maps 2022 land cover basemap. Paired sites are grouped by color. Urban development is indicated by gray shading.

Table 9. Watershed and stream characteristics of the study area (n = 13). Surface water presence refers to the presence of flowing surface water within the sampled reach on the date of sampling.

				Upstream watershed land cover type (%)			
Stream	Development location	Surface water presence	Upstream watershed area (km^2)	Urban	Agriculture	Undeveloped	Open water
ALUM	Above	Dry	5.0	0.4	0	99.6	0
ALUM	Below	Wet	16.1	35.4	0	64.3	0.3
THOM	Above	Wet	18.6	<0.1	0	99.7	0.3
THOM	Below	Wet	27.1	15.1	0.1	84.3	0.6
STM	Above	Dry	179	6.9	0	73.2	19.9
STM	Below	Wet	497	24.6	0.1	66.9	8.5
PEAV	Above	Dry	2.3	1.0	0	99.0	0
PEAV	Below	Dry	9.1	26.4	0	73.6	0
NTD	Above	Wet	151	25.0	0.2	73.1	1.9
NTD	Below	Wet	185	30.7	0.1	67.7	1.5
EVAN	Below	Dry	7.8	37.6	0	62.4	0
PPC	Above	Dry	5.8	1.9	0	98.2	0
HUNT	Above	Wet	29.8	<0.1	0	99.8	0.2

3.2.2 Watershed Characteristics

We delineated upstream watershed area in the NHDplusV2 Medium Resolution (1:100,000-scale) NHDFlowlines layer (Brakebill et al., 2019) and percent cover of different land cover types was estimated using the Model My Watershed tool Version 1.33.7 (Stroud Water Research Center, 2021). The 2019 National Land Cover Database (Dewitz & U.S. Geological Survey, 2021) was used to characterize the upland area of sites (Table 9). We grouped land use by four categories: urban, agriculture, undeveloped, and open water, as well as the total upland watershed area. To make the four categories, similar land classifications were grouped together: urban (developed open space + developed high intensity + developed low intensity + developed medium intensity), agriculture (cultivated crops), undeveloped (pasture hay + perennial ice snow + barren land + deciduous forest +

evergreen forest + mixed forest + shrub scrub + grassland herbaceous), and open water (open water + woody wetlands + emergent herb wetlands).

Total upstream watershed area at the above development sites was an average of 56 km^2 (range: 2.3 km^2 to 179 km^2; Table 9). The below development sites had an average watershed area of 124 km^2 (range: 7.8 km^2 to 497 km^2). Urban land cover in the above site's watersheds ranged from <0.1 to 25.0% (mean: 5.0%), with NTD-ABOVE (25.0%) and STM-ABOVE (6.9%) having the highest degrees of urban land cover (Table 9; Figure S2). Urbanization in the below development sites ranged from 15.1 to 37.6% (mean: 28.3%), with EVAN-BELOW having the highest urbanization percent in the contributing watershed (Table 9; Figure S2). Undeveloped land cover in the above site's watersheds (mean: 91.8%, range: 73.1% to 99.8%) was higher than the below sites (mean: 69.9%, range: 62.4% to 84.3%). Within the paired sites, all of the below development locations had a larger contributing watershed and greater urban percent than the above locations on the corresponding stream. Agriculture was <0.2% of land cover in all watersheds. Open water was <2% in all watersheds, with the exceptions of STM-ABOVE (19.9%) and STM-BELOW (8.5%); this was primarily due to two lakes (Washoe and Little Washoe) located in the Steamboat Creek watershed.

3.2.3 Watershed grain size distribution and surface geology

Soil textures were assessed using the 'XPolaris' package in R (Moro Rosso et al., 2021; R Core Team, 2021). The package uses 'POLARIS', a probabilistic soil series map based off the USDA NRCS Soil Survey Geographic (SSURGO) database (Chaney et al., 2016). 'POLARIS' has been previously used for estimating crop yields and nitrogen

fixation (Correndo et al., 2021; de Borja Reis et al., 2021). The map contains data for the probabilistic soil composition at 6 layers up to 200 cm in depth (30-meter spatial resolution). To calculate probabilistic soil composition and create a soil series map, unmapped SSURGO areas were gap-filled, political boundaries harmonized, and SSURGO coarse polygon data was spatially disaggregated using a machine-learning algorithm (Chaney et al., 2016). To measure the average watershed grain size distribution, we selected nine random points from each site's upper watershed. The points were grouped into three, evenly spaced transects above the sampling location running perpendicular to streamflow. Three points were measured on each transect: one at the valley floor and the other two on opposing hillsides. An additional point at the sampling location was also used. Sand and clay percentages at each of the 10 points were calculated from averaging the 0-5 and 5-15 cm layers. Data from the 10 points were then averaged to get upstream watershed sand and clay percentages for each site (Table 10).

Surface geology at all sites, except HUNT, was determined using the Preliminary revised geologic maps of the Reno urban area, Nevada (1:24,000-scale; Ramelli et al., 2011; Table 10). Data for these maps were collected during field surveys from 2000-2010. HUNT was located outside of the Ramelli et al., 2011 map boundary, so surface geology was determined using the Preliminary geologic map of the Mount Rose NW quadrangle, Washoe County, Nevada (1:24,000-scale; Hinz et al., 2018; Table 10). Field surveys from 2015-2018 collected data for this map.

Surface geology at the paired below development sites were either Truckee River deposits (ALUM, THOM, STM, NTD) or alluvial fan deposits (PEAV). The paired above development sites had four surface geology types: volcanic and sediment breccia

(THOM), Peavine sequence: metamorphosized volcanic rocks (PEAV), basin fill deposits (NTD), and alluvial fan deposits (ALUM, STM). The three non-paired streams had different surface geology types from each another: andesite lava of Peavine Mountain (EVAN), volcanic: granodiorite (PPC), and fluvial-lacustrine sediments (HUNT) (Table 10). Hydrothermal alteration (e.g., geothermal seep) was found in the contributing watersheds of all sites, except for Thomas Creek (above and below development) (Table 10).

Table 10. Site surface geology and watershed grain size for each sampling site. ^Hydrothermal alteration in contributing watershed. #Hydrothermal alteration at site.

	Surface geology			Watershed grain size 0-15 cm depth (n=10)	
Site	Code	Type	Age	Clay %	Sand %
ALUM-ABOVE	Qfo	Alluvial fan deposits^	Middle Pleistocene	17.8	44.0
ALUM-BELOW	Qrt	Truckee river deposits^	Late Pleistocene	20.5	42.1
THOM-ABOVE	Tub	Volcanic and sedimentary breccia	Oligocene	10.8	62.4
THOM-BELOW	Qay	Truckee river deposits	Holocene	12.2	62.6
STM-ABOVE	Qsu	Alluvial fan deposits^	Pleistocene/ Holocene	12.6	52.6
STM-BELOW	Qfl	Truckee river deposits^	Holocene	16.7	51.6
PEAV-ABOVE	Jv	Peavine sequence: metamorphosized volcanic rocks^	Middle Jurassic	19.6	45.0
PEAV-BELOW	Qfp	Alluvial fan deposits^	Middle Pleistocene	24.2	37.3
NTD-ABOVE	Qby	Basin fill deposits^	Holocene	16.1	43.0
NTD-BELOW	Qay	Truckee river deposits^	Holocene	19.6	40.8
EVAN	Tpa	Andesite lava of Peavine Mountain^#	Miocene	14.5	56.2
PPC	Kgd	Volcanic: Granodiorite^#	Cretaceous	15.8	55.0
HUNT	Ts	Fluvial-lacustrine sediments^	Miocene	16.8	45.7

3.2.4 Sediment and water collection

We collected sediment from all 13 sites and surface water from the seven sites that had flowing water. Water quality parameters (pH, dissolved oxygen (DO), temperature, and specific conductance) were measured at each site with surface water using a multiparameter sonde (YSI, Yellow Springs, OH, USA). The pH probe was calibrated within 24 hours before sampling. At each sampling location, four transects were established perpendicular to the flow of water and spaced 10 meters apart in the stream. A hand shovel was used to collect the top 5-10 cm of sediment at three locations on each transect (25%, 50%, and 75% of channel width). Before being transported back to the lab, large rocks and woody debris were removed and the sediment from all transects homogenized in a bucket. The composite samples were stored in plastic bags on ice until arrival in the lab where samples were stored at 4°C.

We collected water samples from each site with flowing surface water by filtering water through Whatman GF/F filters (Whatman, Piscataway, NJ, USA) using acid-washed syringes into acid-washed 60 mL HDPE bottles for dissolved nutrient, cation, and anion analysis. For dissolved metals analysis, water was filtered through Whatman 0.45 μm pore size PES membrane filters (Whatman, Piscataway, NJ, USA) into trace metal grade 15 mL polypropylene falcon tubes. One sample was collected in triplicate and two Type 1 water field blanks were taken. Dissolved nutrient, cation, and anion samples, and field blanks were held on ice for transport and frozen once returned to the lab. Dissolved metals samples were held at room temperature, in the dark, and preserved in 1% HNO_3 acid until analysis.

3.2.5 Sample processing

All sediment samples were sieved in the lab using a stainless steel #10 2 mm opening sieve and mixed to form a single composite sample from each site. Surface water and sediment water soluble fraction (WSF) constituents were analyzed for nutrients, anions, and cations. WSF constituents were extracted by vortexing 2.5 ± 0.25 g of wet sediment with 25 mL of deionized water at 3400 RPM for 10 seconds every 30 minutes over four hours. After settling overnight at 4°C, the samples were centrifuged at 3400 RPM for 15 minutes and the supernatant filtered through Whatman GF/F filters. A TOC analyzer with a TN module (TOC-V CPH; Shimadzu, Kyoto, Japan) was used to measure total dissolved carbon (TDC), dissolved organic carbon (DOC) and total dissolved nitrogen (TDN). Soluble reactive phosphorus (SRP) and ammonia (NH_3) were measured on an AQ400 discrete analyzer (SEAL Analytical, Mequon, WI, USA) based on US EPA methods 350.1 revision 2.0 and method 365.1 revision 2.0 (US EPA, 1993b, 1993a). Ammonium (NH_4^+) concentrations were calculated from NH_3 values, incorporating the influence of water pH and temperature (Emerson et al., 1975). Concentrations of anions: chloride (Cl^-), bromide (Br^-), nitrate (NO_3^-) and sulfate (SO_4^{2-}) and cations: sodium (Na^+), potassium (K^+), magnesium (Mg^{2+}) and calcium (Ca^{2+}) were measured on an ion chromatograph (ICS-2000) equipped with an AS18 anion column and KOH eluent generator (Dionex Corporation, Sunnyvale, CA, USA) at Duke University. Surface water trace metal (aluminum (Al), cadmium (Cd), cobalt (Co), copper (Cu), lead (Pb), nickel (Ni), and zinc (Zn)) concentrations were analyzed using inductively coupled plasma-mass spectrophotometry (ICPMS-2000, Shimazdu Corp, Kyoto, JP) at the UNR Analytical Core Lab. All instruments for water analysis used standard calibration methods with calibration

curves of $R^2 > 0.998$ (Table S3). Duplicate field and analytical samples were run on the AQ400, ICS-2000, and Shimadzu instruments with percent difference <10%. One triplicate sample was run on the ICPMS-2000 with a coefficient of variance of 11 ± 7%. Mid-analysis calibration checks were performed on each instrument with <5% deviation from the standard concentration.

Sediment was analyzed for organic matter content, pH, potential microbial respiration, EEA, trace metals, and bulk density. 3 ± 0.25 g of wet sediment was dried at 60°C for 48 hours, weighed, and then combusted at 500°C for 4 hours to determine dry weight and ash free dry mass (AFDM), respectively. We calculated the percent of organic matter in the sample using the equation: (dry weight – AFDM) / dry weight) x 100 = percent organic matter (% OM). Sediment pH was measured using 6g of air-dried sediment in 10 mL of 0.01 mol/L $CaCl_2$ (Carter & Gregorich, 1993). The sediment and solution were measured into an acid-washed falcon tube and vortexed for 30 seconds. After settling for 30 minutes, an Orion Star A211 pH meter (ThermoFisher Scientific, Waltham, MA, USA) was placed in the supernatant to get the pH reading. The pH meter was calibrated 30 minutes before use with a 3-point method of pH buffer solutions 4, 7, and 10. One sample was run in triplicate with a coefficient of variance of <1%. Sediment bulk density (g/mL) was determined by weighing 50 mL of homogenized wet sediment and was used to calculate the amount of organic matter in the sediment used for potential microbial respiration rates. Two samples were run in triplicate with an average coefficient of variance of 3 ± 1%.

To measure trace metal content, ~3g of wet sediment subsample was dried (48 hours at 60°C), ground using a porcelain mortar and pestle, and the aggregate passed

through a stainless steel #80 180 μm opening sieve (Method 3051A, US EPA 2007). A subsample of dried sediment (0.3 g) was measured into acid-washed glass scintillation vials and submitted for analysis to the UNR Analytical Core Lab. Samples were microwave digested using a Multiwave 5000 (Anton Parr, Graz, AT) at a ratio of 0.3 g of sieved aggregate to 9 mL omnitrace nitric acid (HNO_3) and 3 mL omnitrace hydrochloric acid (HCl). Trace metal concentrations of Al, Cd, Co, Cu, Pb, Ni, and Zn, and cation concentrations of Na^+, K^+, Mg^{2+}, and Ca^{2+} were analyzed using inductively coupled plasma-mass spectrophotometry (ICPMS-2000, Shimazdu Corp, Kyoto, JP). One sample was run in triplicate with an average coefficient of variance of 16 ± 7% (Table S4). Six method blanks and three Type 1 water blanks were analyzed during the sediment analyses. Three replicates of a fresh water sediment certified reference material (CRM016, Sigma Aldrich, St. Louis, MO, USA) were used to calibrate the instrument. Recovery rates of all CRM elements except Ca^{2+} and Ni ranged from 85 to 126% (100 ± 12%; Table S4). Sediment Ca^{2+} and Ni had high recovery rates at 240% and 483%, respectively, and were excluded from analysis (Table S4). Samples that had concentrations below detection were reported as below detection.

3.2.6 Potential microbial respiration and extracellular enzyme activity

Potential microbial respiration rates (MRR) were estimated using a modified version (Fierer et al., 2003b) of the substrate-induced respiration method (West & Sparling, 1986). Triplicate wet sediment samples (10 ± 0.25 g) were mixed with an autolyzed yeast extract solution (20 mL) and sealed in 125-mL acid-washed glass jars with septa. Rates of CO_2 production were measured over 4 hours using a 500 μl gas-tight syringe and needle

(7658-01, 7806-02; Hamilton Co, Reno, NV, USA) to extract gas (via the septa) and dispense into an infrared gas analyzer (LI-6265; LI-COR, Lincoln, Nebraska, USA) with N_2 as the carrier gas. The instrument was calibrated using a 6-point standard method with $r^2 > 0.995$ and CO_2 was measured as a proxy of microbial respiration at 2-hour intervals over 4 hours. In-between measurements, the glass jars were placed on a shaker table at low speed to prevent anoxic buildup in the sediment. Higher rates of CO_2 accumulation in each glass jar equated to higher potential rates of respiration.

Microbes produce extracellular enzymes that break down and make complex organic molecules bioavailable to microbes and plants (Allison & Vitousek, 2005). Potential extracellular enzyme activity (EEA) was measured using a modified version of the potential soil extracellular enzyme activity method (Bell et al., 2013). 91 mL of a Tris buffer solution, titrated to sample pH, was blended with 2.75 g of homogenized wet sediment. Triplicates of each sample slurry (800 μl) were placed into deep well plates and the slurry was inoculated with a fluorescence facilitating substrate (200 μl) for each enzyme measured. The activity of seven enzymes were measured: three carbon (α-D-glucopyranoside (AG_C), β-D-glucopyranoside (BG_C) and β-D-cellobioside (CB_C)), two nitrogen (L-Leucine-7-amido-4-methylcoumarin hydrochloride (LAP_N) and N-acetyl-β-D-glucosaminide (NAG_N)), one phosphorus (phosphate (PHOS_P)), and one sulfur (sulfate potassium salt (AS_S)) degrading enzymes. 4-Methylumbelliferone (MUB) was the standard measurement for all enzymes, except LAP_N. 7-amino-4-methylcoumarin (MUC) was the standard measurement for LAP_N. After incubating in the dark for three hours at 25°C, the deep well plates were centrifuged for three minutes then 250 μl of supernatant was transferred into black well plates and stabilized with 5 μl

of 10N NaOH. Sample fluorescence was read (365/450 nm) in analytical triplicate on an Infinite Pro 200 plate reader (Tecan Group, Männedorf, CH). The instrument was calibrated using a 7-point standard method with $R^2 > 0.995$. The samples were run at five below the optimal gain of the standards. This relationship was corrected in a second round of standards analysis using linear relationships with $R^2 > 0.999$ (Table S6a, b). EVAN was excluded from this analysis because of lab error.

3.2.7 Long-term monitoring and spring 2021 field collection of surface water quality data

The July 2021 sampling provided a snapshot of summer stream conditions. To contextualize this work with what is observed throughout the year, we used a long-term monitoring data and a spring 2021 field campaign. Data from the Water Quality Data Portal (Read et al., 2017) was used to gather surface water Ca^{2+}, Mg^{2+}, and Na^{2+} data in the North Truckee Drain from 2000-2014. This data was collected ~1 km downstream of NTD-LOW at 39.52489, -119.70570 and included more than 1,400 observations. The Truckee River Information Gateway was used to collect specific conductance data from Steamboat Creek (39.51268, -119.71226; same location as STM-BELOW in July 2021 sampling) and the North Truckee Drain (39.52489, -119.70570; same location as Water Quality Data Portal). This dataset included >143,000 hourly observations from 2001-2009. From February to April 2021, we collected filtered surface water samples every other week at Hunter Creek (39.49217, -119.89587; same location as HUNT in July 2021 sampling) and the North Truckee Drain (39.57029, -119.72652; same location as NTD-ABOVE in July 2021 sampling). These samples were analyzed using the same methods listed above for Cl^-, Na^+, and SO_4^{2-} concentrations.

3.2.8 Data analysis

Kendall rank correlation coefficient tests were used to assess the relationship between 1) upstream urban land cover with water quality and sediment parameters, 2) sediment pH and organic matter with MRR and EEA, 3) watershed clay and sand percent with water quality, sediment, and microbes, and 4) sediment WSF nutrients with EEA. If over 50% of samples across sites were below detection levels, the samples were excluded from analysis. We used a non-parametric test of correlation strength to allow for the natural skew of observed responses, as well as higher leverage points that could not be discounted as outliers.

To compare MRR and EEA with stream surface water presence type at the time of sampling (wet or dry), a one-tailed, two sample t-test was used because of the small sample size (n = 13), the data was independently collected, and log transformations allowed the data to meet the assumptions of normality and homogeneity. A t-test was also used to compare watershed sand and clay between the upper and lower paired sites. To test for normal distribution of data, a Shapiro-Wilk test (Shapiro & Wilk, 1965) was used and to test for homogeneity of variance, a Levene Test (Levene, 1960) was used. Data was log transformed only if it did not meet the significance test ($p > 0.05$) for normality and homogeneity. Sediment WSF constituent differences between above and below development paired sites were compared using the equation ((above-below)/ below) x 100.

In addition to t-tests, a generalized linear model with an effect of development (above or below) as a binary term was used to compare WSF constituents and their respective enzyme communities. For the model, C enzyme activity was compared with sediment WSF TDC and DOC; S enzyme activity with sediment WSF SO_4^{2-}; P enzyme

activity with sediment WSF SRP; and N enzyme activity with sediment WSF TDN, NO_3^- and NH_4^+. EEA and sediment WSF constituents were log transformed to fit the model. T-tests were also performed to assess the influence of site location (above or below development) on EEA. All models were analyzed using the 'lme4' package in R (Bates et al., 2015; R Core Team, 2021).

3.3 Results

3.3.1 Relationships between watershed urbanization with sediment and water chemistry

In general, watersheds with greater amounts of urban cover were associated with increased nutrient concentrations and water temperatures, as well as lower amounts of dissolved oxygen. Notably, urban development was positively correlated with surface water Co ($n = 7$, $\tau = 0.88$, $p < 0.01$) and SO_4^{2-} ($n = 7$, $\tau = 0.71$, $p < 0.05$), and sediment WSF NH_4^+ ($n = 13$, $\tau = 0.44$, $p < 0.05$) and SO_4^{2-} ($n = 13$, $\tau = 0.49$, $p < 0.05$) (Figure 16). Additionally, sediment WSF Cl^- ($n = 13$, $\tau = 0.37$), surface water Mg^{2+} ($n = 7$, $\tau = 0.62$), and sediment Mg^{2+} ($n = 13$, $\tau = 0.41$) were weakly positively correlated with percent watershed urban land cover ($p < 0.1$). Surface water dissolved oxygen ($n = 7$, $\tau = -0.62$) and pH ($n = 7$, $\tau = -0.62$) were weakly negatively correlated with percent watershed urban land cover ($p < 0.1$) and surface water temperature ($n = 7$, $\tau = 0.62$) had a weak positive correlation to urbanization ($p < 0.1$). No other solutes in surface water or sediment WSF nor specific conductance or sediment metals were correlated to percent urban land cover in the contributing watershed ($p > 0.1$). Sediment Al had the highest concentration of the

metals analyzed (mean = 14.9 mg/g; n=13) with PEAV-ABOVE having the highest concentration (26.2 mg/g).

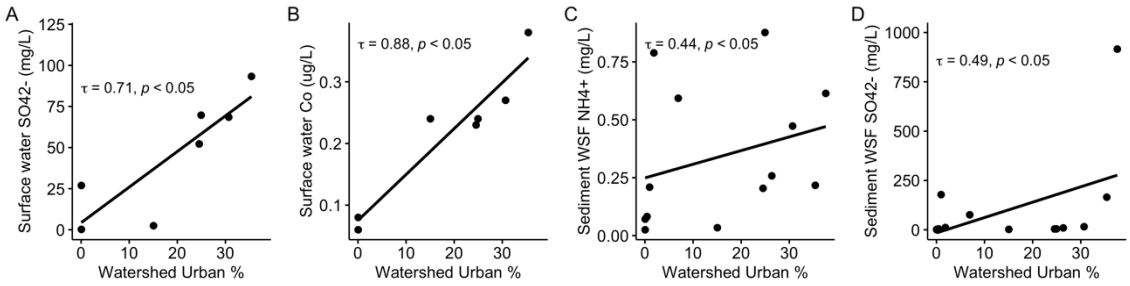

Figure 16. Watershed urban percent to surface water SO_4^{2-} (A) and Co (B) (n = 7), and sediment WSF NH_4^+ (C) and SO_4^{2-} (D) (n = 13) with Kendall rank correlation coefficients.

The sediment WSF concentrations between above and below development paired sites had variable percent changes (Figure 17). ALUM had the largest increases in all cations: Ca^{2+} (283%), Mg^{2+} (440%), K^+ (3071%), Na^+ (195%) and two anions: Br^- (1636%), SO_4^{2-} (3571%) from above to below development. PEAV had the largest increases in SRP (2310%), TDN (693%), DOC (521%), TDC (595%), and Cl^- (334%). NTD experienced increases in anions: Br^-, SO_4^{2-}, and Cl^-, and cations: Ca^{2+}, Mg^{2+}, K^+, and Na^+, decreases in carbon (TDC and DOC) and nitrogen (TDN and NH_4^+), and no change in NO_3^-. The highest magnitude change in THOM was SO_4^{2-}, which increased 1657%, whereas SRP, NH_4^+ and all cations decreased. STM had concentration decreases of more than 50% in all analytes except Br^-, which was below detection at both sites.

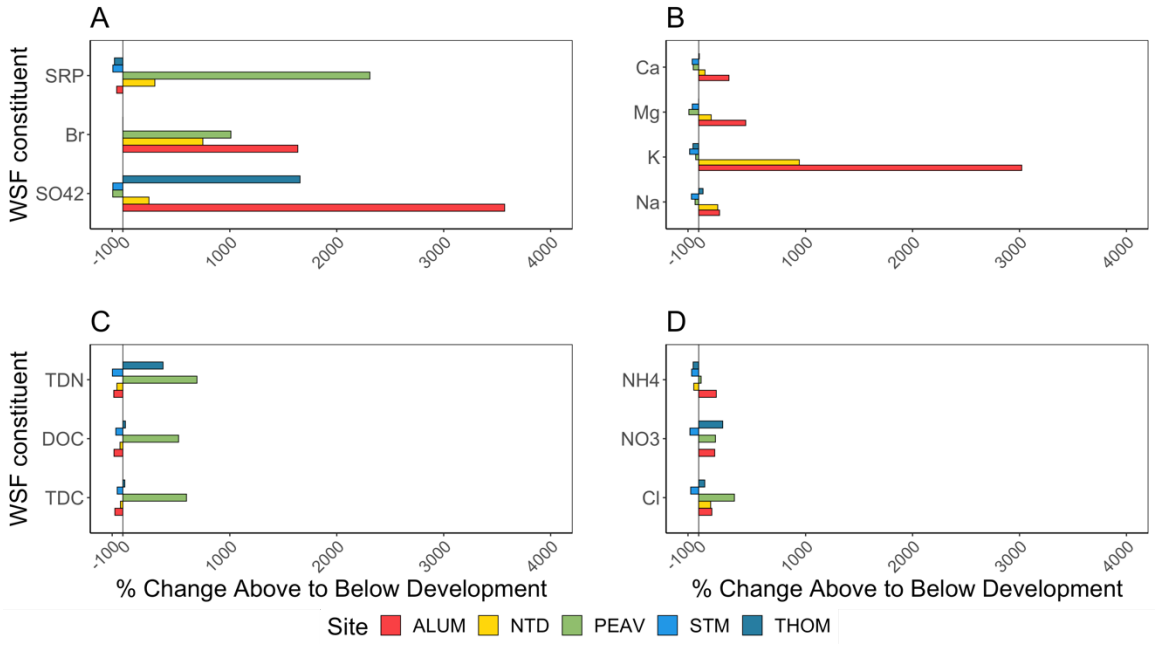

Figure 17. Sediment WSF constituent changes in paired sites from above to below development.

3.3.2 Relationships between watershed urbanization and chemistry with microbial activity

Overall, we observed similar rates of potential sediment extracellular enzyme activity (EEA) across all levels of urban development, regardless of site location (above or below development) (Table 11). Similarly, no EEA group (i.e., carbon, nitrogen, phosphorus, or sulfur degrading extracellular enzymes) or individual EEA were found to be significantly influenced by their respective sediment WSF nutrients or development location ($p > 0.1$; $n = 12$). Development location was removed from the model and a Kendall correlation was performed between EEA groups and sediment WSF nutrients, but there were no significant correlations ($p > 0.1$; Figure 18).

Table 11. T-test results for potential extracellular enzyme activity compared to development location (n = 12). Bolded EEA groups indicate log transformations to meet assumptions of normality.

EEA group	Development location	Mean ± SD (nmol/g.dry/hr)	p
C enzymes	Above	10.9 ± 7.57	0.61
C enzymes	Below	15.0 ± 15.9	-
N enzymes	Above	47.3 ± 32.9	0.8
N enzymes	Below	52.4 ± 48.8	-
P enzymes	Above	29.2 ± 22.7	0.53
P enzymes	Below	48.2 ± 59.5	-
S enzymes	Above	83.1 ± 54.9	0.95
S enzymes	Below	76.1 ± 59.3	-

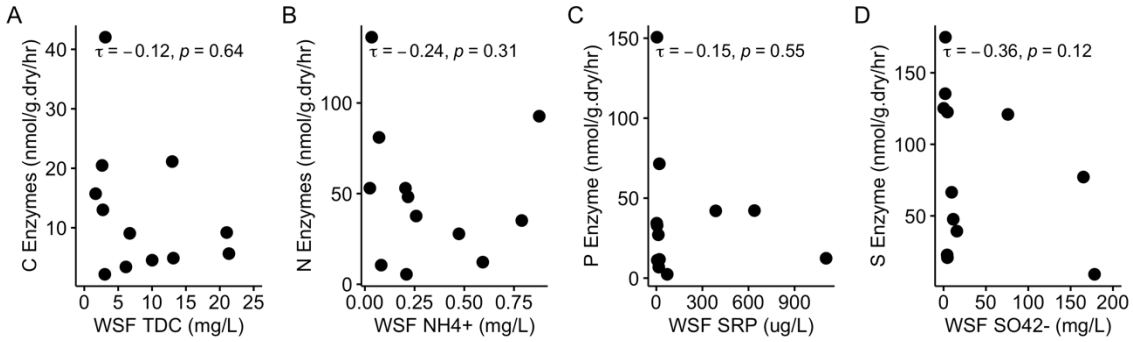

Figure 18. Sediment WSF TDC, NH_4^+, SRP, and SO_4^{2-} influence on C (A), N (B), P (C), and S (D) potential extracellular enzyme activity.

3.3.3 Microbial response to streamflow status

Potential microbial respiration rates (MRR; micrograms of C per gram of dry soil per hour (ug.C/g.dry/hr)) were similar across both wet and dry streams. Specifically, log transformed microbial respiration concentrations in wet streams (4.5 ± 4.9 ug.C/g.dry/hr) were not significantly different than dry streams (4.9 ± 3.4 ug.C/g.dry/hr; t(0.46) = 10.82, p = 0.66) (Figure 19A). EVAN (11.1 ug.C/g.dry/hr) and PEAV-BELOW (5.0 ug.C/g.dry/hr) had the highest amounts of microbial respiration in the dry sites while ALUM-ABOVE (3.1 ug.C/g.dry/hr) and PEAV-ABOVE (0.8 ug.C/g.dry/hr) had the

lowest rates. THOM-BELOW had the highest rates (15.3 ug.C/g.dry/hr) within wet sites, while ALUM-BELOW (2.24 ug.C/g.dry/hr) and NTD-BELOW (1.25 ug.C/g.dry/hr) had the lowest.

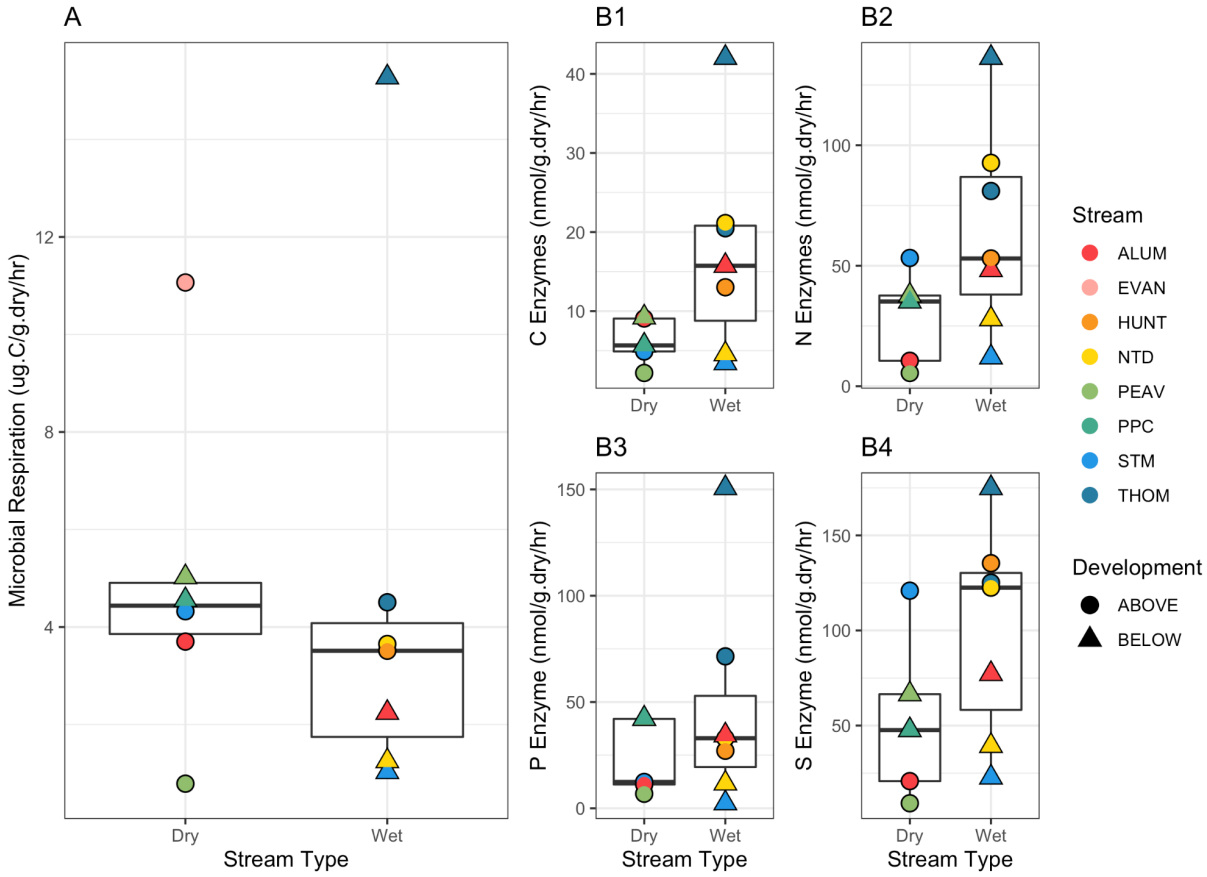

Figure 19. Microbial respiration (A) and N (B1), C (B2), P (B3), and S (B4) EEA grouped by stream type and development position. EVAN is present in panel A, but not in the B panels.

Similarly, there were no significant differences between stream surface water presence (dry or wet) and potential extracellular enzyme activity rates. Rates (nanomoles of activity per gram of dry soil per hour (nmol/g.dry/hr)) in wet streams of C (17.2 ± 13.0 nmol/g.dry/hr), N (64.4 ± 42.3 nmol/g.dry/hr), P (47.2 ± 50.5 nmol/g.dry/hr), and S (99.6 ± 55.0 nmol/g.dry/hr) EEA had no significant difference than in dry streams (C: 6.2 ± 3.0

nmol/g.dry/hr, N: 28.4 ± 19.9 nmol/g.dry/hr, P: 22.9 ± 17.6 nmol/g.dry/hr, S: 53.0 ± 44.1 nmol/g.dry/hr), however C enzymes were weakly greater in wet over dry streams ($p < 0.1$; Figure 19B). Of the three C enzymes, β-D-cellobioside EEA was significantly greater in wet (7.1 ± 4.8 nmol/g.dry/hr) than dry streams (2.0 ± 0.5 nmol/g.dry/hr; $p = 0.03$), whereas α-D-glucopyranoside; $p = 0.15$ and β-D-glucopyranoside; $p = 0.21$ were not significantly correlated with either surface water presence (wet or dry). Similarly, one N enzyme (L-Leucine-7-amido-4-methylcoumarin hydrochloride) was weakly greater in wet streams; $p = 0.08$, and the other (N-acetyl-β-D-glucosaminide) had no correlation; $p = 0.32$ (Table 12). THOM-BELOW had the highest amount of enzyme activity in all enzyme individuals and groups. PEAV-ABOVE had the lowest enzyme activity in all individuals and groups, except for the P enzyme, where STM-BELOW had the lowest activity.

Table 12. T-test results for comparisons of potential extracellular enzyme activity and microbial respiration with surface water presence (wet or dry). Bolded microbial groups and individuals indicate log-transformations to meet assumptions of normality. * $p < 0.05$, ^ $p < 0.1$

Microbial group	t	df	p
C enzymes^	-2.16	6.86	0.07
N enzymes	-1.66	7.77	0.14
P enzyme	-1.17	7.88	0.28
S enzyme	-1.47	7.02	0.18
Microbial respiration	-0.46	10.82	0.66
α-D-glucopyranoside	-1.57	9.65	0.15
β-D-cellobioside*	-2.81	6.2	0.03
β-D-glucopyranoside	-1.34	9.61	0.21
N-acetyl-β-D-glucosaminide	-1.06	8.90	0.32
L-Leucine-7-amido-4-methylcoumarin hydrochloride^	-2.00	9.27	0.08

3.3.4 Sediment organic matter and pH influences on microbial activity

Stream sediment organic matter was positively correlated with extracellular enzyme activity and microbial respiration; however, this was dependent on surface water presence (Figure 7). In wet streams, microbial respiration rates ($\tau = 0.71$, $p = 0.03$), and C EEA ($\tau = 0.9$, $p = 0.003$) and P EEA ($\tau = 0.71$, $p = 0.03$) were significantly correlated with organic matter ($p < 0.05$) while N EEA ($\tau = 0.62$, $p = 0.07$) was weakly correlated with sediment organic matter ($p < 0.1$). S EEA rates in wet streams were not correlated with organic matter ($p > 0.1$; $\tau = 0.52$, $p = 0.14$). MRR and EEA in dry streams were not correlated with organic matter ($p > 0.1$). Similarly, MRR and EEA were not correlated with sediment pH ($p > 0.1$; Table S8).

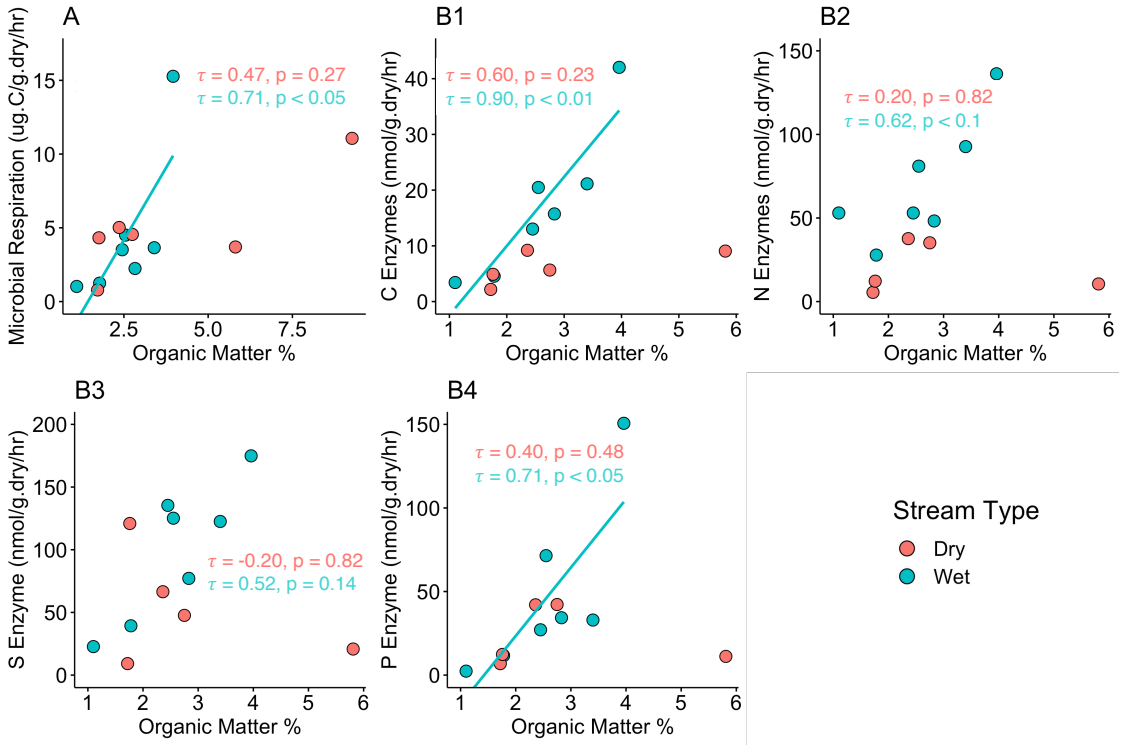

Figure 20. Correlations between organic matter percent and microbial respiration (A), and C (B1), N (B2), S (B3), and P enzymes (B4). EVAN was excluded from the EEA correlation but was included in microbial respiration. Regression lines are given if correlation was significant ($p < 0.05$).

3.3.5 Site surface geology and watershed grain size effects on water quality, baseflow, and microbial communities

There were weak, positive correlations between watershed clay and surface water SO_4^{2-} ($n = 7$, $\tau = 0.62$, $p < 0.1$) and Mg^{2+} ($n = 7$, $\tau = 0.62$, $p < 0.1$) (Figure 21A, B). The inverse was true for watershed sand, where there was a weak, negative relationship with surface water SO_4^{2-} ($n = 7$, $\tau = -0.62$, $p < 0.1$), but no correlation with surface water Mg^{2+} ($p > 0.1$). Microbial respiration had a weak, negative correlation with watershed clay ($n = 13$, $\tau = -0.38$, $p < 0.1$; Figure 21C) and a weak, positive correlation with watershed sand ($n = 13$, $\tau = 0.41$, $p < 0.1$). No other surface water or sediment WSF constituents nor sediment metals were correlated to percent clay or sand in the contributing watershed ($p > 0.1$). Within watersheds with paired sites, watershed clay or sand did not significantly differ between the above and below development locations ($p > 0.1$).

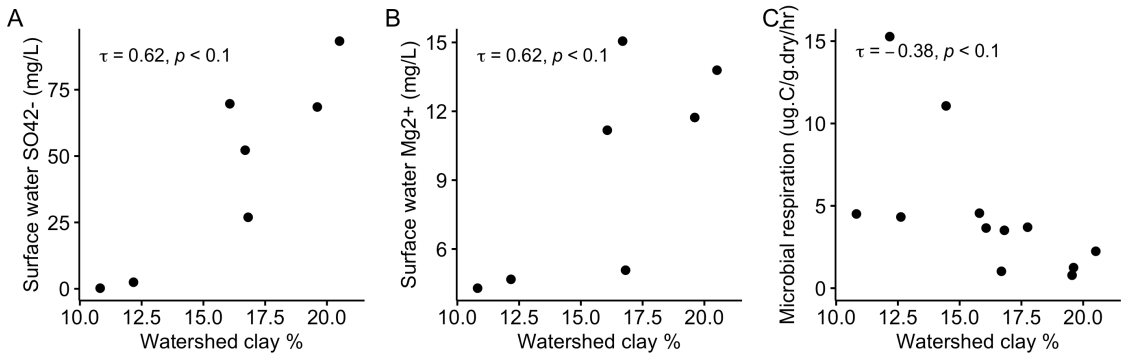

Figure 21. Watershed clay percentages compared to surface water SO_4^{2-} (A) and Mg^{2+} (B), and microbial respiration (C) with Kendall correlation coefficients.

Surface geology in Reno is highly heterogeneous (Ramelli et al., 2011), and this was reflected in the chemistry and watershed grain size differences among sites (Table 10). Hydrothermal alterations were found in the contributing watershed and directly at the Evans Creek site which had the highest concentrations of sediment WSF SO_4^{2-} (916 mg/L),

Na^+ (95.6 mg/L), Mg^{2+} (92.3 mg/L), and Ca^{2+} (294 mg/L) of site we measured. Peavine Ponds Creek was the only other site which had hydrothermal alteration in the contributing watershed and directly at the site however it had noticeably lower sediment WSF concentrations (SO_4^{2-}: 11.4 mg/L, Na^+: 4.9 mg/L, Mg^{2+}: 3.2 mg/L, Ca^{2+}: 17.1 mg/L) than Evans Creek. Within the five paired above/below development sites, only Steamboat Creek and Alum Creek were dry in the above development reach and wet in the below development reach at the time of sampling in July.

3.3.6 Temporal patterns of stream chemistry

From 2000-2014, summer and fall periods of lower surface water Ca^{2+} and Mg^{2+} concentrations were observed in the North Truckee Drain; however, Na^+ did not follow the same seasonal trend and had no clear temporal trend throughout the year (Figure 22). The July 2021 Ca^{2+} and Mg^{2+} field measurements at the North Truckee Drain were closer to the observed summer/fall concentrations than to the winter/spring concentrations (Figure 22). The July 2021 Na^+ field measurement coincided to what was observed throughout the year (Figure 22).

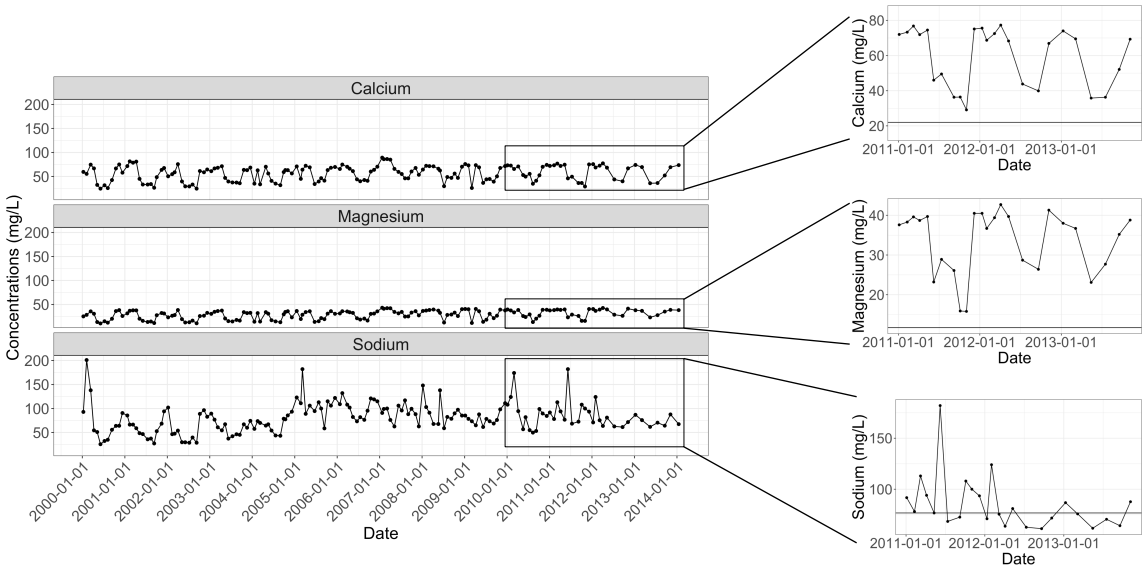

Figure 22. Calcium, magnesium, and sodium concentrations in the North Truckee Drain from 2000 to 2014. The zoomed images on the right are from 2011 to the end of 2013 and the solid horizontal lines are the July 2021 concentrations.

Specific conductance in Steamboat Creek and the North Truckee Drain were nearly identical to one another and both streams followed the same summer/fall dilution period as Ca^{2+} and Mg^{2+} (Figure 23). The July 2021 specific conductance data from both streams were nearly identical (STM-LOW: 823 μs/cm, NTD-LOW: 813 μs/cm) and overlapped the summer/fall concentrations (Figure 23).

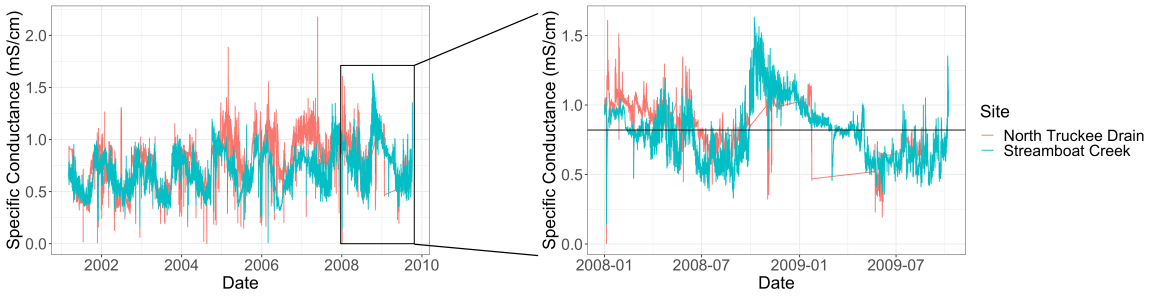

Figure 23. Specific conductance concentrations in the North Truckee Drain and Steamboat Creek from 2001 to 2009. The zoomed image on the right is data from 2008 to the end of 2009, and the solid horizontal line is the July 2021 concentration at both sites.

Chloride, sodium, and sulfate concentrations from February to the end of April in the North Truckee Drain were consistently higher than Hunter Creek (Figure 24; Table S9). The North Truckee Drain (NTD-ABOVE) has a high level of watershed urbanization (25%) compared to Hunter Creek (<0.1%; Table 9). Spring and July 2021 surface water concentrations in Hunter Creek were similar to one another, whereas July 2021 concentrations in the North Truckee Drain were noticeably lower than Spring 2021 (Figure 24; Table S9).

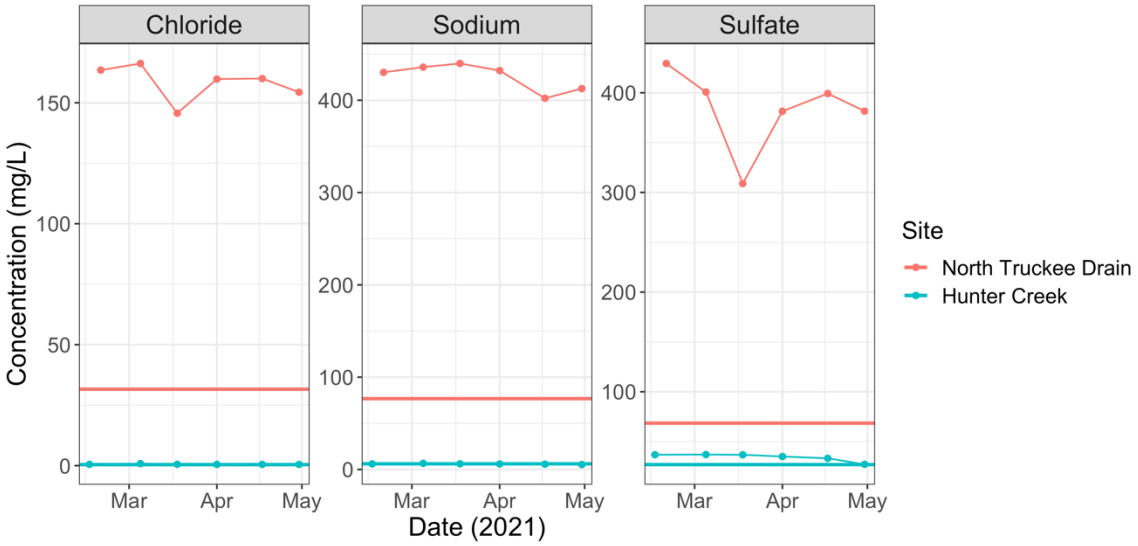

Figure 24. Chloride, sodium, and sulfate concentrations in the North Truckee Drain and Hunter Creek in Spring 2021. Solid red and blue horizontal lines indicate concentrations observed in July 2021.

3.4. Discussion

3.4.1 Overview

Watershed urbanization in arid environments can alter the perenniality of streams (Fillo et al., 2021) and the mobilization and transformations of solutes (Gabor et al., 2017; Hale et al., 2015) with unclear consequences for microbial activity. In this snapshot sampling of summer stream surface water and sediment chemistry in paired stream reaches

above and below urban development, we found no consistent patterns in urbanization effects on stream chemistry or microbial activity likely because of the highly heterogeneous geology in Reno, NV which imparts a stronger signal on among stream chemistry variation than longitudinal change as a result of urban development. From the single snapshot summer sampling event, our expectation that the presence of surface water affects microbial activity was partially met, with C and N degrading EEA being lower in dry streams than wet streams. Instead of the percent of urban development in the contributing catchment, stream sediment organic matter concentrations and the presence of surface water were the strongest predictors of sediment microbial activity. Although this sampling occurred once in the summer and is not representative of the range of conditions found throughout the year, the result of this study still provide insight into mid-summer variation in stream chemistry and microbial activity across a wide range in surface water conditions, percentages of development in the contributing watershed, and underlying watershed lithologies.

3.4.2 Stream chemistry responses to increasing watershed urbanization

We observed variation in both sediment and water chemistry among streams draining the Truckee River watershed. Most surface water solute and sediment water soluble fraction (WSF) concentrations did not significantly increase, and none significantly decreased with greater urban land cover in the contributing watershed. Stream solute concentrations (e.g., nitrate, chloride) in streams draining urban catchments in temperate climates tend to increase above a threshold of 5% impervious surface cover in the contributing watersheds (Booth & Jackson, 1997; Conway, 2007; Hatt et al., 2004; Meyer

et al., 2005). In contrast, urban streams in the arid southwest have been shown to have varying responses to urbanization due to dilution during summer months as a result of lawn irrigation return flows (Fillo et al. 2021) and in-stream nutrient uptake (Grimm et al., 2005).

Only sulfate and cobalt in surface water, and sulfate and ammonium in sediment WSF significantly increased with higher levels of watershed urbanization. High sulfate concentrations in our urban sites could be attributed to watershed hydrothermal alteration (Romero-Mujalli et al., 2022), leaking sewer pipes (Blaszczak et al., 2019), urine (Kirchmann & Pettersson, 1995), and construction materials (Moore et al., 2017). Throughout Reno, undeveloped and agricultural lands are being converted into residential housing, and this construction activity could be causing sulfate rich material to enter nearby streams via stormwater runoff or dust deposition. Concurrently, former livestock operations could be leaching legacy contaminants (e.g., NH_4^+) into groundwater that eventually reaches streams. High ammonium in urban streams could also be a result of sewer leakage, lawn fertilizer runoff, dog defecation, and changes to in-stream nutrient retention (Hale et al., 2015; Hobbie et al., 2017; Paul & Meyer, 2001; Walsh et al., 2005). The high amounts of cobalt were not surprising because vehicle use and degradation can contribute cobalt to the environment (Domingo, 1989); however, it was notable that other metals (Cd, Cu, Pb, Zn) which are found in car parts did not follow this trend (Paul & Meyer, 2001; Schuler & Relyea, 2018).

Surface water temperature and magnesium, sediment WSF chloride, and sediment magnesium weakly increased with urbanization while surface water pH and dissolved oxygen weakly decreased. Urban areas are known to have higher temperatures than surrounding non-urban areas (urban heat island effect) and combined with riparian

vegetation removal which decreases shade, it was not surprising that surface water temperature increased with urbanization (Grimm et al., 2008; Paul & Meyer, 2001; Somers et al. 2013). Urban streams are often associated with lower amounts of dissolved oxygen (Paul & Meyer, 2001, Blaszczak et al. 2019). Although we observed declines in dissolved oxygen with increasing urbanization, the steep slopes of the least developed stream reaches (i.e., THOM-ABOVE and HUNT) likely allow for turbulent mixing and greater dissolved oxygen inputs. As a result, it is difficult to determine if lower in-stream dissolved oxygen concentrations are the result of upstream urbanization. Magnesium chloride is a type of salt used on roads and the increased surface water magnesium concentrations could be attributed to remnants of deicing salt application from the winter seeping into streams (Schuler & Relyea, 2018). Since sampling took place in the summer, the increased chloride concentrations could be from saline groundwater inputs rather than from direct road salt application (Gabor et al., 2017).

We observed no consistent increase or decrease in specific surface water solute or sediment WSF among our paired upstream-downstream of development site comparisons. However, within particular streams, we observed consistent trends across all measured solutes or sediment WSF constituents. All sediment WSF constituents decreased in Steamboat Creek from above to below development. In the late 1800's, mining activity in the upper Steamboat Creek watershed created tailing piles adjacent to Washoe Lake which released contaminants into the watershed (Blum et al., 2001). Steamboat Creek drains Washoe Lake and the elevated contaminant concentrations could have been diluted as several streams (e.g., Galena Creek, Thomas Creek, and Dry Creek) enter Steamboat Creek

between our above and below development sites. No other stream had uniform solute increases from above to below development during our summer snapshot sampling.

3.4.3 Microbial activity relationships with stream chemistry, urban development, organic matter, and average watershed grain size

We did not observe a strong influence of stream sediment chemistry and urban development on in-stream microbial activity in this single summer sampling event. Catchment imperviousness (a measure of urbanization) has been shown to influence enzyme activity in Melbourne, Victoria, Australia (Harbott & Grace, 2005), but we did not see this relationship in our data. The wide range of sediment WSF nutrient concentrations in our sites, coupled with differences in watershed lithology, the presence of surface water, and urbanization could explain why we did not see nutrient availability having a significant influence on potential extracellular enzyme activity.

Sediment organic matter emerged as a primary driver of potential microbial respiration and extracellular enzyme activity, which is corroborated by previous work (Sinsabaugh et al., 2005). The weak positive correlation between watershed sand and microbial respiration could indicate a habitat preference for microbial communities. Since we did not see correlations between extracellular enzyme activity rates and watershed sand, it is possible that other factors are driving the lithology correlation with potential microbial respiration rates during the summer.

Our sites encompassed a wide range of sediment pH, however neither microbial respiration nor any extracellular enzyme was related to variation in pH. Certain microbial communities can show preferences to specific ranges of pH (Rocca et al., 2020; Wilczek et al., 2005), however, functional redundancies among different microbial taxa may explain

why even if microbial communities shift, the functional capacity of the community does not change (Wang et al. 2014). Although our results indicated that highly acidic (<5) sediment did not have a significant impact on microbial activity, the limited sampling period makes it difficult to determine if pH has a greater or weaker influence throughout the year with changing hydrology, organic matter, and nutrient availability.

3.4.4 Microbial activity across variation in stream dryness

The similarity of potential microbial respiration rates between wet and dry sites indicates perenniality is likely not a primary driver of spatial differences in microbial respiration during the summer dry season; however, hydrology changes throughout the year could yield varying results to what we observed. Although our expectations for microbial respiration were not met, all four enzyme groups had higher mean activity in wet streams than dry streams; however, the large variability in sample concentrations meant the activity differences were not statistically different. We observed the greatest difference in EEA rates within C and N enzyme groups, specifically β-D-cellobioside and L-Leucine-7-amido-4-methylcoumarin hydrochloride having strong and weak preferences, respectively, for wet over dry streams, showing they are reliant on water to sustain activity. This contrasts with α-D-glucopyranoside, β-D-glucopyranoside and N-acetyl-β-D-glucosaminide which showed no preference for surface water presence, indicating they have greater resiliency to changes in perenniality. Even though urbanization can change stream hydrology and turn non-perennial to perennial streams and vice versa, these results suggest that hydrologic variations did not impact the potential activity of most microbial

communities sampled. The microbial assays are potential measures of activity and do not capture the natural variation in activity that might occur under fluctuating wet or dry conditions in the sampled streams which vary in their degree of perenniality, but for which we do not have data.

3.4.5 Stream chemistry and hydrology responses to variation in geology

Surface geology varied among sites, making it difficult to discern if the observed stream chemistry and hydrology changes were primarily influenced by urbanization or geology. Steamboat Creek switched from dry at the above development site to wet at the below development site at the time of sampling, which was possibly due to new water sources from the streams that join the creek between our two sites. It is possible that geology played a role in the increased baseflow in Steamboat Creek, but it is difficult to disentangle if new water inputs or geology was the primary cause. Alum Creek also went from dry to wet between our two sites and had the greatest percent increase in urbanization from our above to below development sites. The new water sources in Alum Creek could be due to lawn irrigation return flows and leaking sewer pipes rather than changing surface geology, but this study was not able to capture what the primary cause of the increased baseflow was.

Hydrothermal alterations were found at the Evans Creek and Peavine Ponds Creek sampling locations, and in the contributing watersheds of all sites, except Thomas creek (above and below development). Hydrothermal alteration can result in cation fluxes and high sulfate content in streams (Romero-Mujalli et al., 2022), which could explain why Evans Creek had the highest sediment WSF concentrations of sulfate, sodium, magnesium,

and calcium. Peavine Ponds Creek also had hydrothermal alterations at the sampling site but had lower sediment WSF constituent concentrations than Evans Creek. This could be due to the magnitude of hydrothermal alterations, or the differing types of surface geology at the two sites. Hydrothermal alterations could also explain why Alum Creek had the highest sediment water-soluble fraction sulfate and cation increases from above to below development. Hydrothermal alterations are found throughout northwestern Nevada (Hinz et al., 2018; Kraal et al., 2021; Ramelli et al., 2011; Yang et al., 1999); however, hydrothermal fluids forming altered rock can have varying chemical compositions based on hydrology, lithology, and volcanic activity, which makes it difficult to quantify their impact to streams and rivers (Romero-Mujalli et al., 2022).

3.4.6 Seasonal dynamics of stream chemistry

Long-term monitoring of two urban streams in Reno identified seasonal chemistry patterns with a winter/spring concentration peak and a summer/fall dilution. This could be explained from elevated lawn irrigation return flows in warm months which increases baseflow and has the potential to dilute stream chemistry (Fillo et al., 2021). Spring and summer 2021 field work indicated that streams in urbanized watersheds potentially experience seasonal chemistry fluctuations at higher degrees than non-urban streams. This fits with data showing that lawn-watering restrictions in Los Angeles, CA decreased urban stream baseflow by 70% while baseflow in non-urban streams remained consistent in the same time period (Manago & Hogue, 2017). With lower baseflow, contaminants in urban streams can become concentrated. Lawn fertilizers have the potential to increase nutrient inputs to streams (Hobbie et al., 2017) but it appeared that the increase in summer/fall

baseflow had a diluting effect on stream chemistry. The small sampling period of this project limits our ability to predict annual stream chemistry dynamics in Reno; however, long-term monitoring data contextualized the work with seasonal trends which indicated diluted stream chemistry in the summer compared to the winter.

3.5 Conclusion

Across eight streams draining varying degrees of urbanized catchments and types of underlying lithology in the semi-arid city of Reno, NV, we found that potential sediment microbial activity responded more strongly to variation in stream sediment organic matter and hydrologic conditions over variation in stream chemistry. In urban areas with semi-arid climates, we expect that hydrologic regimes will be altered to turn non-perennial to perennial streams by wastewater treatment plant effluent, stormwater infrastructure, canal diversions, and lawn irrigation runoff (Fillo et al., 2021; Kaushal et al., 2019; Solins et al., 2018; White & Greer, 2006). Seasonal hydrologic trends were not captured in this field study and microbial community composition will likely change throughout the year with fluctuating hydrology, desiccation, and organic matter availability (Amalfitano et al., 2008; Febria et al., 2015).

The variation we observed in water and sediment chemistry might be due in part to increasing flow diluting solute concentrations. Long term data from two streams in Reno indicated seasonal trends of stream chemistry with concentrations becoming diluted during the summer and fall. Data from previous field surveys were combined with the July 2021 sampling and indicated stream chemistry in undeveloped watersheds can remain consistent throughout the year whereas stream chemistry in highly developed watersheds can have

strong seasonal dynamics. If sampling had occurred at multiple points throughout the year, it is possible that the undeveloped sites would have had more consistent stream chemistry compared to urban streams, which could have had higher stream solute concentrations in the winter as compared to the summer.

Variation among streams as a result of the heterogeneous underlying lithology of Reno imparted a strong signal on stream chemistry. Hydrothermal alterations were found in the majority of watersheds we surveyed and likely influenced stream chemistry in ways this project was not able to account for. Further work is needed to understand how heterogeneity in watershed geology influences stream chemistry in Reno.

Urbanization is increasing around the globe and causing changes to watershed hydrology and surface water quality (Booth et al., 2016). The findings from this single summer snapshot study suggest that natural variation in lithology may explain more of the spatial variation in summer stream chemistry in Reno, NV than the relative amount of urbanization in the contributing watershed. There were no consistent trends in the presence of surface water or stream solute concentrations above and below development, however, the stream reaches included in this study spanned watersheds of different sizes, aspects, and underlying lithology that may all affect the duration of surface water in streams during the summer months. Urban areas are exceptionally spatially heterogeneous (Pickett et al., 2017) and the results of this study demonstrate the complexities found in semi-arid cities which tend to have complicated and dynamic surface water flowpaths as a result of human use (e.g., irrigation canals). We were unable to disentangle the relative importance of watershed urbanization on stream microbial community functional capacity in this limited study, but these results highlight the exceptional heterogeneity found in the semi-arid city

of Reno, NV in stream chemistry, hydrology, and microbial activity even in a limited snapshot study. Future stream studies in Reno could focus on seasonal dynamics and how microbial activity changes throughout the year based on stream perenniality and chemistry.

Thesis Conclusion

This thesis explored the impacts of watershed urbanization, underlying lithology, and freshwater salinity on biogeochemical cycles. We conducted laboratory mesocosm experiments and a field survey to address the knowledge gaps of 1) how pulse versus press salinity regimes affect sediment chemistry flux rates and microbial activity, and 2) how stream chemistry changes with increasing watershed urbanization across several geologic contexts. Salinity regimes vary among streams and although we know that increasing salinity exposure affects microbial activity and the fluxes of elements from stream sediments, it was unclear how those microbes and fluxes might change between a press versus pulse regime. The area surrounding Reno has a highly heterogenous underlying lithology and we investigated how stream chemistry changes with increasing watershed urbanization across several different geologic contexts.

The second chapter focused on freshwater salinity regimes and used mesocosm experiments to measure sediment chemistry fluxes and microbial community response. In the pulse salinity treatment, the flux of carbon, phosphorus, ammonium, calcium, and potassium from the sediment into the water column decreased once the salinity exposure declined, whereas the high baseline press treatment resulted in elevated flux rates throughout the experiment. This indicated that the highest flux rates occur when salinity is consistently elevated. Microbial activity did not show a response to the different salinity regimes relative to the control. This indicated that the communities in the streams were resistant to press and pulse salt stressors at the concentrations of salts used in this study, or that the study did not occur over a long enough period for microbial activity to be impacted.

In the third chapter, we conducted a field study to get a snapshot on how urbanization and lithology influence stream chemistry and microbial activity. We also used long-term data in the Truckee River basin to examine seasonal trends in the concentrations of different solutes in two different streams in Reno, NV. In our snapshot summer study, sulfate, cobalt, and ammonium concentrations in the surface water and water leachable sediment ions increased with urban development in the contributing watershed, but among stream variation was greater than the influence of urban development because of the signal of the underlying lithology. Microbial activity did not change between undeveloped and developed stream reaches, but stream perenniality was found to strongly influence the activity of carbon extracellular enzymes.

The results of this work improve our understanding of how urbanization, underlying lithology, and changing salinity exposure affects stream water quality and microbial activity in Reno, NV. Water quality in the Truckee River basin is an important source of drinking and irrigation water, serves as habitat for fish, and provides a wide range of other ecosystem services for the northern Nevada community that resides in the basin (e.g., recreation). The Truckee River terminates in Pyramid Lake and adverse water quality from urban upstream sources (e.g., road salts, fertilizer, WWTP effluent, etc.) can impact the health of the lake, native trout species, and subsistence fishing (Dickerson & Vinyard, 1999; Galat, 1990; Wagner & Lebo, 1996). Therefore, understanding the impacts of expanding development, and point and non-point sources of pollution on stream chemistry and hydrology will be critical to maintaining and improving water quality in the basin.

References

Acosta, J. A., Jansen, B., Kalbitz, K., Faz, A., & Martínez-Martínez, S. (2011). Salinity increases mobility of heavy metals in soils. *Chemosphere*, *85*(8), 1318–1324. https://doi.org/10.1016/j.chemosphere.2011.07.046

Allison, S. D., & Martiny, J. B. H. (2008). Resistance, resilience, and redundancy in microbial communities. *Procedings of the National Academy of Sciences*, *105*, 11512–11519. https://doi.org/doi10.1073pnas.0801925105

Allison, S. D., & Vitousek, P. M. (2005). Responses of extracellular enzymes to simple and complex nutrient inputs. *Soil Biology and Biochemistry*, *37*(5), 937–944. https://doi.org/10.1016/j.soilbio.2004.09.014

Amalfitano, S., Fazi, S., Zoppini, A., Barra Caracciolo, A., Grenni, P., & Puddu, A. (2008). Responses of benthic bacteria to experimental drying in sediments from Mediterranean temporary rivers. *Microbial Ecology*, *55*(2), 270–279. https://doi.org/10.1007/s00248-007-9274-6

Bäckström, M., Karlsson, S., Bäckman, L., Folkeson, L., & Lind, B. (2004). Mobilisation of heavy metals by deicing salts in a roadside environment. *Water Research*, *38*(3), 720–732. https://doi.org/10.1016/j.watres.2003.11.006

Baker, M. E., Schley, M. L., & Sexton, J. O. (2019). Impacts of Expanding Impervious Surface on Specific Conductance in Urbanizing Streams. *Water Resources Research*, *55*(8), 6482–6498. https://doi.org/10.1029/2019WR025014

Bates, D., Mächler, M., Bolker, B., & Walker, S. (2015). Fitting Linear Mixed-Effects Models Using lme4. *Journal of Statistical Software*, *67*(1). https://doi.org/10.18637/jss.v067.i01

Bell, C. W., Fricks, B. E., Rocca, J. D., Steinweg, J. M., McMahon, S. K., & Wallenstein, M. D. (2013). High-throughput fluorometric measurement of potential soil extracellular enzyme activities. *Journal of Visualized Experiments : JoVE*, *81*. https://doi.org/10.3791/50961

Bhaskar, A. S., Beesley, L., Burns, M. J., Fletcher, T. D., Hamel, P., Oldham, C. E., & Roy, A. H. (2016). Will it rise or will it fall? Managing the complex effects of urbanization on base flow. *Freshwater Science*, *35*(1), 293–310. https://doi.org/10.1086/685084

Bird, D. L., Groffman, P. M., Salice, C. J., & Moore, J. (2018). Steady-State Land Cover but Non-Steady-State Major Ion Chemistry in Urban Streams. *Environmental Science and Technology*, *52*(22), 13015–13026. https://doi.org/10.1021/acs.est.8b03587

Blanck, H., & Wängberg, S.-Å. (1988). Induced Community Tolerance in Marine Periphyton established under Arsenate Stress. *Canadian Journal of Fisheries and Aquatic Sciences*, *45*(10), 1816–1819. https://doi.org/10.1139/f88-213

Blanck, H., Wängberg, S.-A., & Molander, S. (1988). Pollution-Induced Community Tolerance—A New Ecotoxicological Tool. In *Functional Testing of Aquatic Biota for Estimating Hazards of Chemicals* (pp. 212–219). ASTM International. https://doi.org/10.1520/STP26265S

Blaszczak, J. R., Delesantro, J. M., Zhong, Y., Urban, D. L., & Bernhardt, E. S. (2019). Watershed urban development controls on urban streamwater chemistry variability. *Biogeochemistry*, *144*(1), 61–84. https://doi.org/10.1007/s10533-019-00572-7

Blodgett, D., & Johnson, J. M. (2022). *nhdplusTools: Tools for Accessing and Working with the NHDPlus*.

Blum, M., Sexauer Gustin, M., Swanson, S., & Donaldson, S. G. (2001). Mercury in water and sediment of Steamboat Creek, Nevada: Implications for stream restoration. *Journal of the American Water Resources Association*, *37*(4), 795–804. https://doi.org/https://doi.org/10.1111/j.1752-1688.2001.tb05512.x

Bolen, W. P. (2014). Salt. *US Geological Survey Minerals Yearbook*.

Bolotin, L. A., Summers, B. M., Savoy, P., & Blaszczak, J. R. (2022). Classifying freshwater salinity regimes in central and western U.S. streams and rivers. In *Limnology And Oceanography Letters*. John Wiley and Sons Inc. https://doi.org/10.1002/lol2.10251

Booth, D. B., & Jackson, C. R. (1997). Urbanization of aquatic systems: degredation thresholds, stormwater detection, and the limits of mitigation. *Journal of the American Water Resources Association*, *33*(5), 1077–1090. https://doi.org/https://doi.org/10.1111/j.1752-1688.1997.tb04126.x

Booth, D. B., Roy, A. H., Smith, B., & Capps, K. A. (2016). Global perspectives on the urban stream syndrome. *Freshwater Science*, *35*(1), 412–420. https://doi.org/10.1086/684940

Bormann, F. H., & Likens, G. E. (1967). Nutrient Cycling. *Science*, *155*(3761), 424–429.

Borrok, D. M., & Engle, M. A. (2014). The role of climate in increasing salt loads in dryland rivers. *Journal of Arid Environments*, *111*, 7–13. https://doi.org/10.1016/j.jaridenv.2014.07.001

Brakebill, J. W., Schwarz, G. E., & Wieczorek, M. E. (2019). *National Water Quality Program An Enhanced Hydrologic Stream Network Based on the NHDPlus Medium Resolution Dataset*.

Braukmann, U., & Böhme, D. (2011). Salt pollution of the middle and lower sections of the river Werra (Germany) and its impact on benthic macroinvertebrates. *Limnologica*, *41*(2), 113–124. https://doi.org/10.1016/j.limno.2010.09.003

Bureau of Reclamation. (2006). *Central Arizona Salinity Study Phase II-Salinity Control in Waste Water Treatment Plants*.

Butler, L., Scammell, M., & Benson, E. (2016). The Flint, Michigan, Water Crisis: A Case Study in Regulatory Failure and Environmental Injustice. *Environmental Justice*, 93–97. https://doi.org/https://doi.org/10.1089/env.2016.0014

Cañedo-Argüelles, M., Grantham, T. E., Perrée, I., Rieradevall, M., Céspedes-Sánchez, R., & Prat, N. (2012). Response of stream invertebrates to short-term salinization: A mesocosm approach. *Environmental Pollution*, *166*, 144–151. https://doi.org/10.1016/j.envpol.2012.03.027

Cañedo-Argüelles, M., Hawkins, C. P., Kefford, B. J., Schäfer, R. B., Dyack, B. J., Brucet, S., Buchwalter, D., Dunlop, J., Frör, O., Lazorchak, J., Coring, E., Fernandez, H. R., Goodfellow, W., González Achem, A. L., Hatfield-Dodds, S., Karimov, B. K., Mensah, P., Olson, J. R., Piscart, C., … Timpano, A. J. (2016). Saving freshwater from salts. *Science*, *351*(6276), 914–916. https://doi.org/DOI: 10.1126/science.aad3488

Cañedo-Argüelles, M., Kefford, B. J., Piscart, C., Prat, N., Schäfer, R. B., & Schulz, C. J. (2013). Salinisation of rivers: An urgent ecological issue. *Environmental Pollution*, *173*, 157–167. https://doi.org/10.1016/j.envpol.2012.10.011

Carter, M. R., & Gregorich, E. G. (1993). *Soil Sampling and Methods of Analysis Second Edition*.

Chaney, N. W., Wood, E. F., McBratney, A. B., Hempel, J. W., Nauman, T. W., Brungard, C. W., & Odgers, N. P. (2016). POLARIS: A 30-meter probabilistic soil series map of the contiguous United States. *Geoderma*, *274*, 54–67. https://doi.org/10.1016/j.geoderma.2016.03.025

Chowdhury, N., Marschner, P., & Burns, R. G. (2011). Soil microbial activity and community composition: Impact of changes in matric and osmotic potential. *Soil Biology and Biochemistry*, *43*(6), 1229–1236. https://doi.org/10.1016/j.soilbio.2011.02.012

Clements, W. H., & Kotalik, C. (2016). Effects of major ions on natural benthic communities: An experimental assessment of the US Environmental Protection Agency aquatic life benchmark for conductivity. *Freshwater Science*, *35*(1), 126–138. https://doi.org/10.1086/685085

Cochero, J., Licursi, M., & Gómez, N. (2017). Effects of pulse and press additions of salt on biofilms of nutrient-rich streams. *Science of the Total Environment*, *579*, 1496–1503. https://doi.org/10.1016/j.scitotenv.2016.11.152

Compton, J. E., & Church, M. R. (2011). Salt Additions Alter Short-term Nitrogen and Carbon Mobilization in a Coastal Oregon Andisol. *Journal of Environmental Quality*, *40*(5), 1601–1606. https://doi.org/10.2134/jeq2011.0013

Conway, T. M. (2007). Impervious surface as an indicator of pH and specific conductance in the urbanizing coastal zone of New Jersey, USA. *Journal of Environmental Management*, *85*(2), 308–316. https://doi.org/10.1016/j.jenvman.2006.09.023

Correndo, A. A., Rotundo, J. L., Tremblay, N., Archontoulis, S., Coulter, J. A., Ruiz-Diaz, D., Franzen, D., Franzluebbers, A. J., Nafziger, E., Schwalbert, R., Steinke, K., Williams, J., Messina, C. D., & Ciampitti, I. A. (2021). Assessing the uncertainty of maize yield without nitrogen fertilization. *Field Crops Research*, *260*. https://doi.org/10.1016/j.fcr.2020.107985

Corsi, S. R., Graczyk, D. J., Geis, S. W., Booth, N. L., & Richards, K. D. (2010). A fresh look at road salt: Aquatic toxicity and water-quality impacts on local, regional, and national scales. *Environmental Science and Technology*, *44*(19), 7376–7382. https://doi.org/10.1021/es101333u

de Borja Reis, A. F., Moro Rosso, L., Purcell, L. C., Naeve, S., Casteel, S. N., Kovács, P., Archontoulis, S., Davidson, D., & Ciampitti, I. A. (2021). Environmental Factors Associated With Nitrogen Fixation Prediction in Soybean. *Frontiers in Plant Science*, *12*. https://doi.org/10.3389/fpls.2021.675410

Dennehy, K. F., Litke, D. W., Tate, C. M., Qi, S. L., Mcmahon, P. B., Bruce, B. W., Kimbrough, R. A., & Heiny, J. S. (1998). *Water Quality in the South Platte River Basin, Colorado, Nebraska, and Wyoming, 1992-95*. https://doi.org/10.3133/cir1167

DeVilbiss, S. E., Steele, M. K., Brown, B. L., & Badgley, B. D. (2022). Stream bacterial diversity peaks at intermediate freshwater salinity and varies by salt type. *Science of the Total Environment*, *840*. https://doi.org/10.1016/j.scitotenv.2022.156690

Dewitz, J., & U.S. Geological Survey. (2021). *National Land Cover Database (NLCD) 2019 Products (ver. 2.0, June 2021): U.S. Geological Survey data release*.

Dickerson, B. R., & Vinyard, G. L. (1999). Effects of High Chronic Temperatures and Diel Temperature Cycles on the Survival and Growth of Lahontan Cutthroat Trout. *Transactions of the American Fisheries Society*, *128*, 516–521. https://doi.org/10.1577/1548-8659(1999)128<0516:EOHCTA>2.0.CO;2

Domingo, J. L. (1989). Cobalt in the Environment and Its Toxicological Implications. In *Reviews of Environmental Contamination and Toxicology* (pp. 105–132). https://doi.org/10.1007/978-1-4613-8850-0_3

Duan, S., & Kaushal, S. S. (2015). Salinization alters fluxes of bioreactive elements from stream ecosystems across land use. *Biogeosciences*, *12*(23), 7331–7347. https://doi.org/10.5194/bg-12-7331-2015

Duncan, J. M., Welty, C., Kemper, J. T., Groffman, P. M., & Band, L. E. (2017). Dynamics of nitrate concentration-discharge patterns in an urban watershed. *Water Resources Research*, *53*(8), 7349–7365. https://doi.org/10.1002/2017WR020500

Elphick, J. R. F., Bergh, K. D., & Bailey, H. C. (2011). Chronic toxicity of chloride to freshwater species: Effects of hardness and implications for water quality guidelines. *Environmental Toxicology and Chemistry*, *30*(1), 239–246. https://doi.org/10.1002/etc.365

Emerson, K., Russo, R. E., Lund, R. E., & Thurston, R. v. (1975). Aqueous ammonia equilibrium calculations: Effect of pH and temperature. *Journal of the Fisheries Board of Canada*, *32*, 2379–2383. https://doi.org/https://doi.org/10.1139/f75-274

Febria, C. M., Hosen, J. D., Crump, B. C., Palmer, M. A., & Williams, D. D. (2015). Microbial responses to changes in flow status in temporary headwater streams: A cross-system comparison. *Frontiers in Microbiology*, *6*(JUN). https://doi.org/10.3389/fmicb.2015.00522

Fierer, N., Schimel, J. P., & Holden, P. A. (2003a). Influence of drying-rewetting frequency on soil bacterial community structure. *Microbial Ecology*, *45*(1), 63–71. https://doi.org/10.1007/s00248-002-1007-2

Fierer, N., Schimel, J. P., & Holden, P. A. (2003b). Variations in microbial community composition through two soil depth profiles. *Soil Biology and Biochemistry*, *31*(1), 167–176. https://doi.org/https://doi.org/10.1016/S0038-0717(02)00251-1

Fillo, N. K., Bhaskar, A. S., & Jefferson, A. J. (2021). Lawn Irrigation Contributions to Semi-Arid Urban Baseflow Based on Water-Stable Isotopes. *Water Resources Research*, *57*(8). https://doi.org/10.1029/2020WR028777

Gabor, R. S., Hall, S. J., Eiriksson, D. P., Jameel, Y., Millington, M., Stout, T., Barnes, M. L., Gelderloos, A., Tennant, H., Bowen, G. J., Neilson, B. T., & Brooks, P. D. (2017). Persistent Urban Influence on Surface Water Quality via Impacted Groundwater. *Environmental Science and Technology*, *51*(17), 9477–9487. https://doi.org/10.1021/acs.est.7b00271

Gadd, G. M., & Griffiths, A. J. (1978). Microorganisms and Heavy Metal Toxicity. *Microbial Ecology*, *4*, 303–317. https://doi.org/10.1007/BF02013274

Galat, D. L. (1990). Seasonal and long-term trends in truckee river nutrient concentrations and loadings to pyramid lake: a terminal saline lake. *Water Research*, *24*(8), 1031–1040. https://doi.org/https://doi.org/10.1016/0043-1354(90)90126-Q

Gallo, E. L., Brooks, P. D., Lohse, K. A., & McLain, J. E. T. (2013). Land cover controls on summer discharge and runoff solution chemistry of semi-arid urban catchments. *Journal of Hydrology*, *485*, 37–53. https://doi.org/10.1016/j.jhydrol.2012.11.054

Green, S. M., Machin, R., & Cresser, M. S. (2009). Does road salting induce or ameliorate DOC mobilisation from roadside soils to surface waters in the long term? *Environmental Monitoring and Assessment*, *153*(1–4), 435–448. https://doi.org/10.1007/s10661-008-0369-4

Grimm, N. B., Faeth, S. H., Golubiewski, N. E., Redman, C. L., Wu, J., Bai, X., & Briggs, J. M. (2008). Global Change and the Ecology of Cities. *Science*, *319*(5864), 756–760. https://doi.org/10.1126/science.1150195

Grimm, N. B., Pickett, S. T., Redman, C. L., & Grove Grove, J. (2000). Integrated approaches to long-term studies of urban ecological systems. *BioScience*, *50*(7), 571–584. https://doi.org/https://doi.org/10.1641/0006-3568(2000)050[0571:IATLTO]2.0.CO;2

Grimm, N. B., Sheibley, R. W., Crenshaw, C. L., Dahm, C. N., Roach, W. J., & Zeglin, L. H. (2005). N retention and transformation in urban streams. *Journal of the North American Benthological Society*, *24*(3), 626–642. https://doi.org/https://doi.org/10.1899/04-027.1

Groffman, P. M., Bain, D. J., Band, L. E., Belt, K. T., Brush, G. S., Morgan Grove, J., Pouyat, R. v, Yesilonis, I. C., & Zipperer, W. C. (2003). Down by the riverside: urban riparian ecology. *Frontiers in Ecology and the Environment*, *1*(6), 315–321. https://doi.org/https://doi.org/10.1890/1540-9295(2003)001[0315:DBTRUR]2.0.CO;2

Hale, R. L., Scoggins, M., Smucker, N. J., & Suchy, A. (2016). Effects of climate on the expression of the urban stream syndrome. *Freshwater Science*, *35*(1), 421–428. https://doi.org/10.1086/684594

Hale, R. L., Turnbull, L., Earl, S. R., Childers, D. L., & Grimm, N. B. (2015). Stormwater Infrastructure Controls Runoff and Dissolved Material Export from Arid Urban Watersheds. *Ecosystems*, *18*(1), 62–75. https://doi.org/10.1007/s10021-014-9812-2

Harbott, E. L., & Grace, M. R. (2005). Extracellular enzyme response to bioavailability of dissolved organic C in streams of varying catchment urbanization. *Journal of the North American Benthological Society*, *24*(3), 588–601. https://doi.org/https://doi.org/10.1899/04-023.1

Hatt, B. E., Fletcher, T. D., Walsh, C. J., & Taylor, S. L. (2004). The influence of urban density and drainage infrastructure on the concentrations and loads of pollutants in small streams. *Environmental Management*, *34*(1), 112–124. https://doi.org/10.1007/s00267-004-0221-8

Hawkes, C. v., Waring, B. G., Rocca, J. D., & Kivlin, S. N. (2017). Historical climate controls soil respiration responses to current soil moisture. *Proceedings of the National Academy of Sciences of the United States of America*, *114*(24), 6322–6327. https://doi.org/10.1073/pnas.1620811114

Hinz, N. H., Ramelli, A. R., & Henry, C. D. (2018). *Preliminary geologic map of the Mount Rose NW quadrangle, Washoe County, Nevada* (No. 18–3; Open File Report).

Hobbie, S. E., Finlay, J. C., Janke, B. D., Nidzgorski, D. A., Millet, D. B., & Baker, L. A. (2017). Contrasting nitrogen and phosphorus budgets in urban watersheds and implications for managing urban water pollution. *Proceedings of the National Academy of Sciences of the United States of America*, *114*(16), 4177–4182. https://doi.org/10.1073/pnas.1618536114

Hopkins, K. G., Morse, N. B., Bain, D. J., Bettez, N. D., Grimm, N. B., Morse, J. L., Palta, M. M., Shuster, W. D., Bratt, A. R., & Suchy, A. K. (2015). Assessment of regional variation in streamflow responses to urbanization and the persistence of physiography. *Environmental Science and Technology*, *49*(5), 2724–2732. https://doi.org/10.1021/es505389y

Jacobson, C. R. (2011). Identification and quantification of the hydrological impacts of imperviousness in urban catchments: A review. *Journal of Environmental Management*, *92*(6), 1438–1448. https://doi.org/10.1016/j.jenvman.2011.01.018

Jeong, D., Cho, K., Lee, C.-H., Lee, S., & Bae, H. (2018). Effects of salinity on nitrification efficiency and bacterial community structure in a nitrifying osmotic membrane bioreactor. *Process Biochemistry*, *73*, 132–141. https://doi.org/10.1016/j.procbio.2018.08.008

Kaushal, S. S., & Belt, K. T. (2012). The urban watershed continuum: Evolving spatial and temporal dimensions. *Urban Ecosystems*, *15*(2), 409–435. https://doi.org/10.1007/s11252-012-0226-7

Kaushal, S. S., Duan, S., Doody, T. R., Haq, S., Smith, R. M., Newcomer Johnson, T. A., Newcomb, K. D., Gorman, J., Bowman, N., Mayer, P. M., Wood, K. L., Belt, K. T., & Stack, W. P. (2017). Human-accelerated weathering increases salinization, major ions, and alkalinization in fresh water across land use. *Applied Geochemistry*, *83*, 121–135. https://doi.org/10.1016/j.apgeochem.2017.02.006

Kaushal, S. S., Gold, A. J., Bernal, S., Johnson, T. A. N., Addy, K., Burgin, A., Burns, D. A., Coble, A. A., Hood, E., Lu, Y. H., Mayer, P., Minor, E. C., Schroth, A. W., Vidon, P., Wilson, H., Xenopoulos, M. A., Doody, T., Galella, J. G., Goodling, P., … Belt, K. T. (2018b). Watershed 'chemical cocktails': forming novel elemental combinations in Anthropocene fresh waters. *Biogeochemistry*, *141*(3), 281–305. https://doi.org/10.1007/s10533-018-0502-6

Kaushal, S. S., Groffman, P. M., Likens, G. E., Belt, K. T., Stack, W. P., Kelly, V. R., Band, L. E., & Fisher, G. T. (2005). Increased salinization of fresh water in the northeastern United States. *Proceedings of the National Academy of Sciences of the United States of America*, *102*(38), 13517–13520. https://doi.org/https://doi.org/10.1073/pnas.0506414102

Kaushal, S. S., Likens, G. E., Pace, M. L., Haq, S., Wood, K. L., Galella, J. G., Morel, C., Doody, T. R., Wessel, B., Kortelainen, P., Räike, A., Skinner, V., & Utz, R. (2019). Novel 'chemical cocktails' in inland waters are a consequence of the freshwater salinization syndrome. *Philosophical Transactions of the Royal Society B*, *374*, 20180017. https://doi.org/10.1098/rstb.2018.0017

Kaushal, S. S., Likens, G. E., Pace, M. L., Reimer, J. E., Maas, C. M., Galella, J. G., Utz, R. M., Duan, S., Kryger, J. R., Yaculak, A. M., Boger, W. L., Bailey, N. W., Haq, S., Wood, K. L., Wessel, B. M., Park, C. E., Collison, D. C., Aisin, B. Y. 'aaqob I., Gedeon, T. M., … Woglo, S. A. (2021). Freshwater salinization syndrome: from emerging global problem to managing risks. *Biogeochemistry*, *154*(2), 255–292. https://doi.org/10.1007/s10533-021-00784-w

Kaushal, S. S., Likens, G. E., Pace, M. L., Utz, R. M., Haq, S., Gorman, J., & Grese, M. (2018a). Freshwater salinization syndrome on a continental scale. *Proceedings of the National Academy of Sciences of the United States of America*, *115*(4), E574–E583. https://doi.org/10.1073/pnas.1711234115

Kim, S. Y., & Koretsky, C. (2013). Effects of road salt deicers on sediment biogeochemistry. *Biogeochemistry*, *112*(1–3), 343–358. https://doi.org/10.1007/s10533-012-9728-x

Kirchmann, H., & Pettersson, S. (1995). Human urine - Chemical composition and fertilizer use efficiency. *Fertilizer Research*, *40*, 149–154. https://doi.org/https://doi.org/10.1007/BF00750100

Kraal, K. O., Ayling, B. F., Blake, K., Hackett, L., Perdana, T. S. P., & Stacey, R. (2021). Linkages between hydrothermal alteration, natural fractures, and permeability: Integration of borehole data for reservoir characterization at the Fallon FORGE EGS site, Nevada, USA. *Geothermics*, *89*, 101946. https://doi.org/10.1016/j.geothermics.2020.101946

Lake, P. S. (2000). Disturbance, patchiness, and diversity in streams. *Am. Benthol. Soc*, *19*(4), 573–592. https://doi.org/https://doi.org/10.2307/1468118

Levene, H. (1960). Robust Tests for Equality of Variances. *Stanford University Press*, 278–292.

Lind, L., Schuler, M. S., Hintz, W. D., Stoler, A. B., Jones, D. K., Mattes, B. M., & Relyea, R. A. (2018). Salty fertile lakes: how salinization and eutrophication alter the structure of freshwater communities. *Ecosphere*, *9*(9). https://doi.org/10.1002/ecs2.2383

Lofgren, S. (2001). The chemical effects of deicing salt on soil and stream water of five catchments in southeast Sweden. *Water Air and Soil Pollution*, *130*(1), 863–868. https://doi.org/10.1023/A:1013895215558

López-López, E., Sedeño-Díaz, J. E., Mendoza-Martínez, E., Gómez-Ruiz, A., & Ramírez, E. M. (2019). Water quality and macroinvertebrate community in dryland streams: The case of the Tehuacán-Cuicatlán Biosphere Reserve (México) facing climate change. *Water*, *11*(7). https://doi.org/10.3390/w11071376

Manago, K. F., & Hogue, T. S. (2017). Urban Streamflow Response to Imported Water and Water Conservation Policies in Los Angeles, California. *JAWRA Journal of the American Water Resources Association*, *53*(3), 626–640. https://doi.org/10.1111/1752-1688.12515

Martin, G., Dang, C., Morrissey, E., Hubbart, J., Kellner, E., Kelly, C., Stephan, K., & Freedman, Z. (2021). Stream sediment bacterial communities exhibit temporally-consistent and distinct thresholds to land use change in a mixed-use watershed. *FEMS Microbiology Ecology*, *97*(2). https://doi.org/10.1093/femsec/fiaa256

McCann, K. S. (2000). The diversity–stability debate. *Nature*, *405*(6783), 228–233. https://doi.org/10.1038/35012234

McDonald, R. I., Douglas, I., Revenga, C., Hale, R., Grimm, N., Grönwall, J., & Fekete, B. (2011). Global urban growth and the geography of water availability, quality, and delivery. *Ambio*, *40*(5), 437–446. https://doi.org/10.1007/s13280-011-0152-6

McGechan, M. B., & Lewis, D. R. (2002). Sorption of phosphorus by soil, part 1: Principles, equations and models. *Biosystems Engineering*, *82*(1), 1–24. https://doi.org/10.1006/bioe.2002.0054

Meyer, J. L., Paul, M. J., & Taulbee, W. K. (2005). Stream ecosystem function in urbanizing landscapes. *Journal of the North American Benthological Society*, *24*(3), 602–612. https://doi.org/https://doi.org/10.1899/04-021.1

Moore, J., Bird, D. L., Dobbis, S. K., & Woodward, G. (2017). Nonpoint Source Contributions Drive Elevated Major Ion and Dissolved Inorganic Carbon

Concentrations in Urban Watersheds. *Environmental Science and Technology Letters*, *4*(6), 198–204. https://doi.org/10.1021/acs.estlett.7b00096

Moro Rosso, L. H., de Borja Reis, A. F., Correndo, A. A., & Ciampitti, I. A. (2021). XPolaris: an R-package to retrieve United States soil data at 30-meter resolution. *BMC Research Notes*, *14*(1), 327. https://doi.org/10.1186/s13104-021-05729-y

Nickolas, L. B., Segura, C., & Brooks, J. R. (2017). The influence of lithology on surface water sources. *Hydrological Processes*, *31*(10), 1913–1925. https://doi.org/10.1002/hyp.11156

Nieder, R., Benbi, D. K., & Scherer, H. W. (2011). Fixation and defixation of ammonium in soils: A review. *Biology and Fertility of Soils*, *47*(1), 1–14. https://doi.org/10.1007/s00374-010-0506-4

Norrström, A.-C., & Bergstedt, E. (2001). The impact of road de-icing salt (NaCl_ on colloid dispersion and base cation pools in roadside soils. *Water, Air, and Soil Pollution*, *127*, 281–299. https://doi.org/10.1023/A:1005221314856

Paul, M. J., & Meyer, J. L. (2001). Streams in the urban landscape. *Annual Review of Ecology and Systematics*, *32*(1), 207–231. https://doi.org/10.1007/978-0-387-73412-5_12

Pickett, S. T. A., Cadenasso, M. L., Rosi-Marshall, E. J., Belt, K. T., Groffman, P. M., Grove, J. M., Irwin, E. G., Kaushal, S. S., LaDeau, S. L., Nilon, C. H., Swan, C. M., & Warren, P. S. (2017). Dynamic heterogeneity: a framework to promote ecological integration and hypothesis generation in urban systems. *Urban Ecosystems*, *20*(1), 1–14. https://doi.org/10.1007/s11252-016-0574-9

Pillsbury, A. F. (1981). The Salinity of Rivers. *Scientific American*, *245*(1), 54–65. https://doi.org/10.2307/24964504

R Core Team. (2021). R: A Language and Environment for Statistical Computing. *R Foundation for Statistical Computing, Vienna, Austria*. https://www.R-project.org/

Raiesi, F., & Sadeghi, E. (2019). Interactive effect of salinity and cadmium toxicity on soil microbial properties and enzyme activities. *Ecotoxicology and Environmental Safety*, *168*, 221–229. https://doi.org/10.1016/j.ecoenv.2018.10.079

Ramelli, A. R., Henry, C. D., Walker, J. P., & with contributions by John W. Bell, P. H. C. C. M. dePolo, L. J. G. P. K. H. J. H. T. and M. C. W. (2011). Preliminary revised geologic maps of the Reno urban area, Nevada. In *Nevada Bureau of Mines and Geology* (No. 2011–07; Open File Report).

Read, E. K., Carr, L., de Cicco, L., Dugan, H. A., Hanson, P. C., Hart, J. A., Kreft, J., Read, J. S., & Winslow, L. A. (2017). Water quality data for national-scale aquatic

research: The Water Quality Portal. *Water Resources Research*, *53*(2), 1735–1745. https://doi.org/10.1002/2016WR019993

Rocca, J. D., Simonin, M., Bernhardt, E. S., Washburne, A. D., & Wright, J. P. (2020). Rare microbial taxa emerge when communities collide: freshwater and marine microbiome responses to experimental mixing. *Ecology*, *101*(3). https://doi.org/10.1002/ecy.2956

Rocca, J. D., Simonin, M., Blaszczak, J. R., Ernakovich, J. G., Gibbons, S. M., Midani, F. S., & Washburne, A. D. (2019). The Microbiome Stress Project: Toward a global meta-analysis of environmental stressors and their effects on microbial communities. *Frontiers in Microbiology*, *9*(3272). https://doi.org/10.3389/fmicb.2018.03272

Romero-Mujalli, G., Hartmann, J., Hosono, T., Louvat, P., Okamura, K., Delmelle, P., Amann, T., & Böttcher, M. E. (2022). Hydrothermal and magmatic contributions to surface waters in the Aso caldera, southern Japan: Implications for weathering processes in volcanic areas. *Chemical Geology*, *588*, 120612. https://doi.org/10.1016/j.chemgeo.2021.120612

Schimel, J. P. (2018). Life in Dry Soils: Effects of Drought on Soil Microbial Communities and Processes. *Annual Review of Ecology, Evolution, and Systematics*, *49*, 409–432. https://doi.org/10.1146/annurev-ecolsys-110617

Schuler, M. S., & Relyea, R. A. (2018). A Review of the Combined Threats of Road Salts and Heavy Metals to Freshwater Systems. *BioScience*, *68*(5), 327–335. https://doi.org/10.1093/biosci/biy018

Seto, K. C., Güneralp, B., & Hutyra, L. R. (2012). Global forecasts of urban expansion to 2030 and direct impacts on biodiversity and carbon pools. *Proceedings of the National Academy of Sciences*, *109*(40), 16083–16088. https://doi.org/10.1073/pnas.1211658109

Shanafield, M., Bourke, S. A., Zimmer, M. A., & Costigan, K. H. (2021). An overview of the hydrology of non-perennial rivers and streams. *Wiley Interdisciplinary Reviews: Water*, *8*(2). https://doi.org/10.1002/wat2.1504

Shapiro, S. S., & Wilk, M. B. (1965). An Analysis of Variance Test for Normality (Complete Samples). *Oxford University Press*, *52*(3), 591–611. https://www.jstor.org/stable/2333709

Sheldon, F. (2005). Incorporating natural variability into the assessment of ecological health in Australian dryland rivers. *Hydrobiologia*, *552*(1), 45–56. https://doi.org/10.1007/s10750-005-1504-7

Sholkovitz, E. R. (1976). Flocculation of dissolved organic and inorganic matter during the mixing of river water and seawater. *Geochimica et Cosmochimica Acta*, *40*(7), 831–845. https://doi.org/https://doi.org/10.1016/0016-7037(76)90035-1

Sinsabaugh, R. L., Gallo, M. E., Lauber, C., Waldrop, M. P., & Zak, D. R. (2005). Extracellular enzyme activities and soil organic matter dynamics for northern hardwood forests receiving simulated nitrogen deposition. *Biogeochemistry*, *75*(2), 201–215. https://doi.org/10.1007/s10533-004-7112-1

Sklar, L. S., & Dietrich, W. E. (2001). Sediment and rock strength controls on river incision into bedrock. *Geological Society of America*, *29*(12), 1087–1090. https://doi.org/10.1130/0091-7613(2001)029<1087:SARSCO>2.0.CO;2

Snodgrass, J. W., Moore, J., Lev, S. M., Casey, R. E., Ownby, D. R., Flora, R. F., & Izzo, G. (2017). Influence of Modern Stormwater Management Practices on Transport of Road Salt to Surface Waters. *Environmental Science and Technology*, *51*(8), 4165–4172. https://doi.org/10.1021/acs.est.6b03107

Solins, J. P., Thorne, J. H., & Cadenasso, M. L. (2018). Riparian canopy expansion in an urban landscape: Multiple drivers of vegetation change along headwater streams near Sacramento, California. *Landscape and Urban Planning*, *172*, 37–46. https://doi.org/10.1016/j.landurbplan.2017.12.005

Stets, E. G., Lee, C. J., Lytle, D. A., & Schock, M. R. (2018). Increasing chloride in rivers of the conterminous U.S. and linkages to potential corrosivity and lead action level exceedances in drinking water. *Science of the Total Environment*, *613–614*, 1498–1509. https://doi.org/10.1016/j.scitotenv.2017.07.119

Stroud Water Research Center. (2021). *Model My Watershed 1.33.7.* https://wikiwatershed.org

Ullah, A., Bano, A., & Khan, N. (2021). Climate Change and Salinity Effects on Crops and Chemical Communication Between Plants and Plant Growth-Promoting Microorganisms Under Stress. *Frontiers in Sustainable Food Systems*, *5*(618092). https://doi.org/10.3389/fsufs.2021.618092

US EPA. (1993a). Method 350.1 Determination of ammonia nitrogen by semi-automated colorimetry. In *OHIO* (Vol. 45268).

US EPA. (1993b). *Method 365.1, Revision 2.0: Determination of Phosphorus by Semi-Automated Colorimetry*. www.epa.gov

Utz, R. M., Hopkins, K. G., Beesley, L., Booth, D. B., Hawley, R. J., Baker, M. E., Freeman, M. C., & Jones, K. L. (2016). Ecological resistance in urban streams: The role of natural and legacy attributes. *Freshwater Science*, *35*(1), 380–397. https://doi.org/10.1086/684839

Vengosh, A. (2013). Salinization and Saline Environments. In *Treatise on Geochemistry: Second Edition* (Vol. 11, pp. 325–378).

Wagner, P., & Lebo, M. (1996). Managing the resources of Pyramid Lake, Nevada, amidst competing interests. *Journal of Soil and Water Conservation*, *51*(2), 108.

Walsh, C. J., Roy, A. H., Feminella, J. W., Cottingham, P. D., Groffman, P. M., & Ii, R. P. M. (2005). The urban stream syndrome: current knowledge and the search for a cure. *Journal of the North American Benthological Society*, *24*(3), 706–723. https://doi.org/https://doi.org/10.1899/04-028.1

Walsh, C. J., Sharpe, A. K., Breen, P. F., & Neman, J. A. S. (2001). Effects of urbanization on streams of the Melbourne region, Victoria, Australia. I. Benthic macroinvertebrate communities. *Freshwater Biology*, *46*(4), 535–551. https://doi.org/10.1046/j.1365-2427.2001.00690.x

Wang, S. Y., Bernhardt, E. S., & Wright, J. P. (2014). Urban stream denitrifier communities are linked to lower functional resistance to multiple stressors associated with urbanization. *Hydrobiologia*, *726*(1), 13–23. https://doi.org/10.1007/s10750-013-1747-7

Wang, S. Y., Sudduth, E. B., Wallenstein, M. D., Wright, J. P., & Bernhardt, E. S. (2011). Watershed urbanization alters the composition and function of stream bacterial communities. *PLoS ONE*, *6*(8). https://doi.org/10.1371/journal.pone.0022972

West, A. W., & Sparling, G. P. (1986). Modifications to the substrate-induced respiration method to permit measurement of microbial biomass in soils of differing water contents. *Journal of Microbiological Methods*, *5*(3), 177–189. https://doi.org/https://doi.org/10.1016/0167-7012(86)90012-6

White, M. D., & Greer, K. A. (2006). The effects of watershed urbanization on the stream hydrology and riparian vegetation of Los Peñasquitos Creek, California. *Landscape and Urban Planning*, *74*(2), 125–138. https://doi.org/10.1016/j.landurbplan.2004.11.015

Wilczek, S., Fischer, H., & Pusch, M. T. (2005). Regulation and seasonal dynamics of extracellular enzyme activities in the sediments of a large lowland river. *Microbial Ecology*, *50*(2), 253–267. https://doi.org/10.1007/s00248-004-0119-2

Williams, W. D. (2001). Salinization: unplumbed salt in a parched landscape. *Water and Science Technology*, *43*(4), 85–91. https://doi.org/https://doi.org/10.2166/wst.2001.0186

Wise, J. L., van Horn, D. J., Diefendorf, A. F., Regier, P. J., Lowell, T. v., & Dahm, C. N. (2019). Dissolved organic matter dynamics in storm water runoff in a dryland urban

region. *Journal of Arid Environments*, *165*, 55–63. https://doi.org/10.1016/j.jaridenv.2019.03.003

Yachi, S., & Loreau, M. (1999). Biodiversity and ecosystem productivity in a fluctuating environment: The insurance hypothesis. *Ecology*, *96*(4), 1463–1468. https://doi.org/10.1073/pnas.96.4.1463

Yang, K., Huntington, J. F., Boardman, J. W., & Mason, P. (1999). Mapping hydrothermal alteration in the Comstock mining district, Nevada, using simulated satellite-borne hyperspectral data. *Australian Journal of Earth Sciences*, *46*(6), 915–922. https://doi.org/10.1046/j.1440-0952.1999.00754.x

Supplemental material

Figures

Figure 25. Site conditions at the time of sampling in July 2021

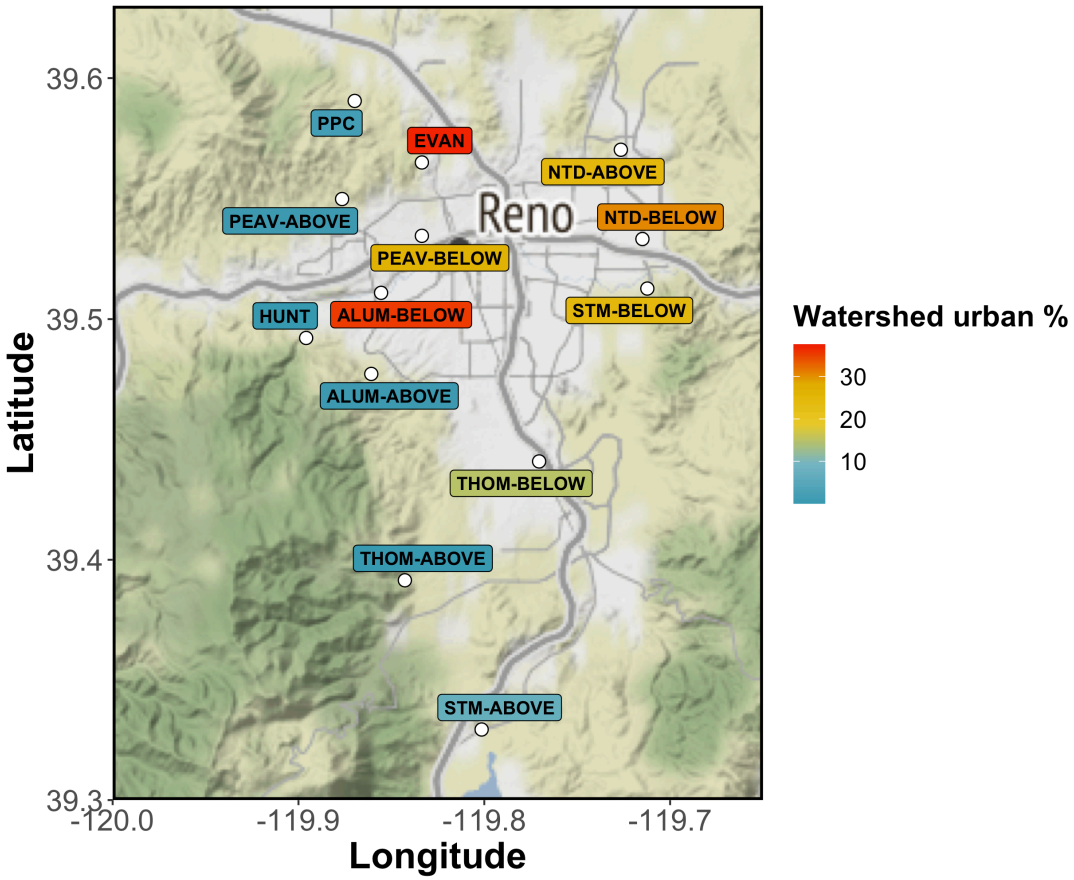

Figure 26. Map of the study area with a Google Maps 2022 land cover basemap. Urban development is indicated by gray shading. The red to blue label color indicates upstream watershed urbanization percent at each site.

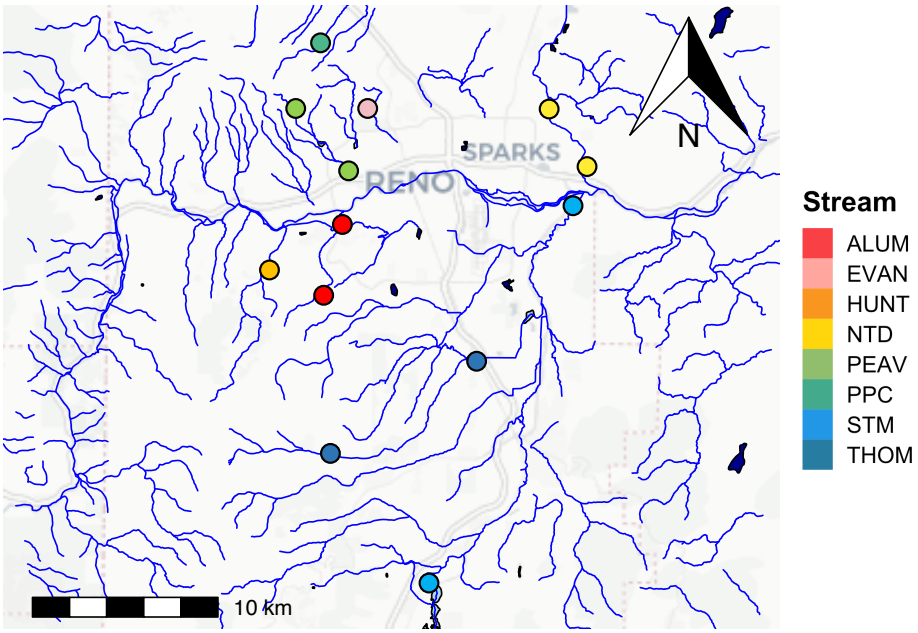

Figure 27. Map of the study area with a National Hydrography Dataset layer. Streams are grouped by color. The map was created using the 'nhdplusTools' package in R (Blodgett & Johnson, 2022; R Core Team, 2021).

Tables

Table 13. Thomas Creek upstream watershed and site characteristics.

		Upstream watershed cover (%)								
Thomas Creek locations	Upstream watershed area (km^2)	Urban	Undeveloped	Agriculture	Open water	SW pH	Sediment pH	DO	Temp (°C)	OM (%)
Undeveloped	18.6	<0.1	99.7	0	0.3	7.69	6.25	10.20	10.3	1.68
Urban	27.1	15.1	84.3	<0.1	0.6	7.97	5.80	7.67	16.7	4.28

Table 14. Surface water, sediment WSF, sediment, and microbial activity replicates per experiment (undeveloped or urban). Number of samples in the field and post-equilibration columns indicate samples taken prior to the salt incubations. Surface water samples were not collected in every mesocosm chamber after the post-incubation 1 and 2, and are reflected in those columns. Surface water and sediment samples were collected in every chamber after the post-incubation 3.

			Time periods				
			Total number of samples		Number of samples per salt treatment		
Sample type		Constituent	Field	Post-eq	Post-incub 1	Post-incub 2	Post-incub 3
Surface water	-	TDC, DOC, TDN, Cl^-, SO_4^{2-}, Br^-, NO_3^-, Na^+, K^+, Mg^{2+}, Ca^{2+}, SRP, NH_4^+, pH, DO, SpC, Temp	2	6	2	2	4
	-	TSS	6	6	2	2	4
Sediment WSF	-	TDC, DOC, TDN, Cl^-, SO_4^{2-}, Br^-, NO_3^-, Na^+, K^+, Mg^{2+}, Ca^{2+}, SRP, NH_4^+	2	6	-	-	4
Sediment	-	Al, Cd, Co, Cu, Pb, Ni, Zn, Na^+, K^+, Mg^{2+}, Ca^{2+}, pH, bulk density	2	6	-	-	4
	-	Organic matter	6	6	-	-	4
Microbial activity	-	MRR, EEA	2	6	-	-	4

Table 15. Analytical chemistry instrument calibration information.

	Instrument			
	ICS-2000	Shimadzu TOC/TN	AQ400	ICPMS-2000
Number of calibration points	6	4-6	8	6-7
R^2	>0.998	>0.998	>0.998	>0.999

Table 16. Sediment trace metal and nutrient certified reference material (CRM) observed and certified value mean and standard deviation (SD), and triplicate samples coefficient of variation (CV) mean. % Recovery was calculated using the equation (observed value – certified value) * 100 = % recover rate. **Bolded** elements (Ca^{2+} and Ni) were excluded from analysis in both chapters. Cd was excluded from analysis in Ch.2.

Element	CRM			Sample CV	
	Observed ± SD (mg/kg)	Cert. Val. ± SD (mg/kg)	Recovery %	Ch.2 Mean %	Ch.3 Mean %
Al	8729 ± 144	8920 ± 657	98	2.5	7.6
Ca^{2+}	**54319 ± 11164**	**22600 ± 532**	**240**	**-**	**-**
Cd	0.4 ± 0.0	0.5 ± 0.1	89	**-**	29.6
Co	6.6 ± 0.6	6.0 ± 0.2	110	3.9	10.2
Cu	14.8 ± 1.2	15.5 ± 0.4	96	5.1	12.2
K	2478 ± 312	1960 ± 141	126	3.8	19.2
Mg^{2+}	13609 ± 81.0	13200 ± 332	103	4.2	15.0
Na^{+}	289 ± 19.7	292 ± 16	99	2.0	20.3
Ni	**80.6 ± 7.2**	**16.7 ± 0.2**	**483**	**-**	**-**
Pb	12 ± 0.7	14.1 ± 0.7	85	1.6	23.8
Zn	67.1 ± 5.5	69.7 ± 2.1	96	3.7	9.8

Table 17. Chemical concentrations in the salt used for the mesocosm experiment. BDL = Below instrument detection limit.

	Chemical concentrations in the low and high press salt solutions (mg/L)		
Solute	Low press (230 mg/L NaCl)	High press (860 mg/L NaCl)	Detection Limit (mg/L)
TDC	BDL	BDL	0.004
DOC	BDL	BDL	0.004
TDN	BDL	BDL	0.1
Cl^-	148	556	0.1
SO_4^{2-}	BDL	BDL	0.1
Br^-	1.07	1.04	0.1
Na^+	89.4	339	1.0
Mg^{2+}	0.06	0.26	0.03
K^+	BDL	BDL	0.4
Ca^{2+}	BDL	0.28	0.08
Al	BDL	BDL	0.01
Cd	BDL	BDL	0.0001
Co	BDL	BDL	0.0004
Cu	BDL	BDL	0.002
Ni	BDL	BDL	0.0008
Pb	BDL	BDL	0.0002
Zn	BDL	BDL	0.003

Table 18a. MUB site-specific conversion relationships between optimal and 5 below gain.

Site	Slope	R^2
STM-BELOW	1.9755x + 182.39	0.999
PPC	1.9788x + 74.22	0.999
HUNT	1.9701x + 152.47	0.999
PEAV-BELOW	1.9584x + 144.51	0.999
STM-ABOVE	1.9584x + 144.51	1
NTD-ABOVE	1.9845x + 91.35	0.999
ALUM-BELOW	1.9505x + 227.38	0.999
NTD-BELOW	1.9907x + 52.96	0.999
PEAV-ABOVE	1.9449x + 148.21	0.999
ALUM-ABOVE	1.9687x + 121.27	0.999
THOM-BELOW	1.9931x + 183.78	0.999
THOM-ABOVE	1.9322x + 175.13	0.999

Table S6b. MUC site-specific conversion relationships between optimal and 5 below gain.

Site	Slope	R^2
STM-BELOW	1.8496x + 156.45	0.999
PPC	1.8656x + 69.89	0.999
HUNT	1.8527x + 121.22	0.999
PEAV-BELOW	1.8658x + 72.09	1
STM-ABOVE	1.8658x + 72.09	1
NTD-ABOVE	1.8848x + 68.71	0.999
ALUM-BELOW	1.8715x + 141.41	0.999
NTD-BELOW	1.9273x – 10.33	1
PEAV-ABOVE	1.8797x + 79.54	1
ALUM-ABOVE	1.8797x + 79.54	0.999
THOM-BELOW	1.8458x + 180.32	0.999
THOM-ABOVE	1.8291x + 123.21	0.999

Table 19a. Sodium (Na^+) concentrations in each time period organized by experiment and treatment type. Standard deviation given when n > 2.

		Time periods: Na^+ (mg/L)				
Experiment	Treatment	Field	Post-eq	Post-incub 1	Post-incub 2	Post-incub 3
Undeveloped	Control	5.8	9.3 ± 3.1	7.9	9.3	8.7 ± 2.8
	Low Baseline	-	-	68.4	80.7	86.5 ± 0.6
	High Baseline	-	-	243	300	296 ± 16.6
	Pulse	-	-	8.2	237	52.8 ± 12.0
Urban	Control	8.9	10.3 ± 3.1	13.1	13.9	11.5 ± 2.3
	Low Baseline	-	-	65.1	68.9	81.9 ± 11.4
	High Baseline	-	-	222	255	275 ± 46.4
	Pulse	-	-	12.3	200	66.9 ± 3.6

Table S7b. Chloride (Cl^-) concentrations in each time period organized by experiment and treatment type. Standard deviation given when n > 2.

		Time periods: Cl^- (mg/L)				
Experiment	Treatment	Field	Post-eq	Post-incub 1	Post-incub 2	Post-incub 3
Undeveloped	Control	13.6	84.5 ± 93.2	25.2	138	88.7 ± 70.3
	Low Baseline	-	-	176	149	232 ± 50.6
	High Baseline	-	-	459	511	574 ± 97.9
	Pulse	-	-	49.6	432	104 ± 46.9
Urban	Control	68.4	79.9 ± 90.4	82.8	144	64.6 ± 70.3
	Low Baseline	-	-	125	143	195 ± 130
	High Baseline	-	-	406	464	476 ± 103
	Pulse	-	-	71.0	380	171 ± 79.2

Table 20. Sediment pH, potential microbial respiration rate (MRR), and potential extracellular enzyme activity (EEA) at each site.

			EEA (nmol/g.dry/hr)			
Site	Sediment pH	MRR (ug.C/g.dry/hr)	C	N	P	S
THOM-LOW	5.64	15.3	42.0	136	151	175
THOM-UP	6.3	4.5	20.5	81.0	71.5	125
STM-LOW	7.38	1.0	3.4	53.0	2.4	22.7
NTD-LOW	7.5	1.3	4.6	27.8	11.7	39.3
NTD-UP	7.13	3.7	21.1	92.7	32.9	123
ALUM-LOW	5.87	2.2	15.7	48.2	34.3	77.1
HUNT	6.94	3.5	13.0	53.0	27.1	135
PEAV-UP	4.07	0.8	2.2	5.5	6.9	9.2
STM-UP	4.97	4.3	4.9	12.2	12.4	121
ALUM-UP	3.49	3.7	9.1	10.5	11.2	20.8
PEAV-LOW	7.15	5.0	9.2	37.6	42.0	66.5
EVAN	6.97	11.1	-	-	-	-
PPC	7.16	4.6	5.7	35.1	42.2	47.6

Table 21. Surface water chloride, sodium, and sulfate concentrations in Hunter Creek and the North Truckee Drain from spring and July 2021.

	Surface water (mg/L)		
Site	Cl^-	Na^+	SO_4^{2-}
Hunter Creek (Spring 2021)	0.56 ± 0.13	6.0 ± 0.4	34.3 ± 3.8
Hunter Creek (July 2021)	0.44	6.1	26.9
North Truckee Drain (Spring 2021)	158 ± 7.4	425 ± 14.8	383 ± 40.6
North Truckee Drain (July 2021)	29.2	72.5	69.7